République Algérienne Démocratique et Populaire

Ministère de l'Enseignement Supérieur et de la Recherche Scientifique

Université de Batna

Faculté de Technologie

MAGISTER En ELECTROTECHNIQUE

Option de Commande Electrique

Préparé au

Laboratoire des Systèmes Propulsion-Induction Electromagnétiques
LSP-IE'2000 Batna

Présenté par

Salim ATALLAH

(Ingénieur en Electrotechnique de l'Université de Batna, Promo'2008)

MODÉLISATION ET COMMANDE D'UNE BDFM (BRUSHLESS DOUBLY FED MACHINE)

In English, « ***Modeling and Control of the BDFM*** »

Soutenu le **24/11/2011**.

Devant le Jury composé de :

A. Makouf	*Professeur,*	*Univ. Batna,*	Président
M.-S. Naït–Saïd	*Professeur,*	*Univ. Batna*	Rapporteur
D. Benattous	*Maître de Conf. A,*	*C. Univ.Oued Souf*	Examinateur
S. Drid	*Maître de Conf. A,*	*Univ. Batna*	Examinateur
B. Abdelhadi	*Maître de Conf. A,*	*Univ. Batna*	Examinateur

ABSTRACT

The intermittent nature of the wind has made it more unique and yet challenging in comparison with most of other sources of energy. Wind speed might have not been a matter of concern in the old days when stone windmills were used for grinding wheat or other agricultural crops. But as far as producing electricity is concerned, fixed frequency and stable output voltage are the two major grid requirements and can neither be deviated from nor compromised. The most common approach to bridge between a variable speed source and fixed frequency/voltage in wind energy systems is a doubly fed induction generator (DFIG), which has the disadvantage of using brushes and slip rings, and hence, elevating the maintenance costs.

This dissertation presents an advanced solution to the above problem by designing the Brushless Doubly Fed Induction generator (BDFIG) system for the wind energy conversion to reduce the maintenance cost and to improve the system reliability of the wind turbine system. The proposed BDFIG employs two three-phase windings in the stator to eliminate the brushes and copper rings in DFIG. The unified dq dynamic reference frame model of BDFIG is developed and implemented using MATLAB/SIMULINK. Based on the model, the control scheme for flexible power flow control in BDFIG is developed. The independent control of the active and reactive powers flow is achieved under the closed loop stator flux oriented control scheme.

Keywords: *Brushless Doubly Fed Machine (BDFM), Power Winding (PW), Control Winding (CW), Variable Speed Generation, Unified Reference Frame Model, Cross Coupling, Vector Control.*

Dedications & Acknowledgments

*First of all, Praise be to **GOD** for the Islam blessing and for giving me bravery and patience during all these years of study.*

This study was carried out in the Laboratory of Induction Propulsion Electromagnetic Systems LSP-IE at Batna University. In this regard, I wish to express my sincere thanks to everyone who contributed to the progress of this work which was headed by the Laboratory Director Prof A. MAKOUF.

*I would like to thank my supervisor **Prof M.S. Nait-Said** for his help, inspiration, and encouragement.*

I am grateful to Prof. A. MAKOUF from Batna University, M.C. S. DRID from Batna University, M.C. B. ABDELHADI from BATNA University and M.C D. BENATTOUS From EL-Oued University Center for their interest in this work and holding the post of referee.

I would like to express my gratitude to the people of the Electrical Engineering Department from Batna University.

Finally, I would also like to thank my whole family, particularly my parents for their care over the years.

I would like to dedicate this work:

To my dear parents

To my brothers

To my colleagues and friends

To all the family

ATALLAH SALIM

TABLE OF CONTENTS

MOTIVATION AND OBJECTIVS 1

I. STATE OF THE ART OF VARIABLE SPEED ENERGY GENERATION DRIVE SYSTEMS 3

I.1 BACKGROUND 4

I.2 EVOLUTION OF THE WIND SYSTEM AT VARIABLE SPEED GENERATION 5

I.2.1 Squirrel Cage Induction Generator (SQIG) 6
I.2.2 Doubly Fed Induction Generator (DFIG) 6
I.2.3 Brushless Doubly Fed Induction Generator (BDFIG) 7

I.3 GENERATOR COMPARISONS 8

I.4 STATE OF THE ART 9

I.4.1 BDFM (Brushless Doubly Fed Machine) 11
I.4.2 BDFRM (Brushless Doubly Fed Reluctance Machine) 11
- Advantages of brushless doubly-fed reluctance machine 11
- Disadvantages of brushless doubly-fed reluctance machine 11

I.4.3 Research groups 12
I.4.4 BDFM Control Strategies 12
- ✓ Feedback linearization 13
- ✓ Control winding phase angle control 13
- ✓ Speed and power factor control 14
- ✓ Vector control 15
- ✓ Direct torque control 17

I.4.5 Main applications of the BDFM 18

II. PRINCIPLE OF OPERATION AND DYNAMIC MODELE ANALYSIS OF THE BDFM 19

II.I PRINCIPLE OPERATION OF THE BDFM 20

II.1.1 Topology of the Machine 20
II.I.2 Operation modes of the BDFM 21
a) Induction mode 22
b) Synchronous mode 22

II.I.3 Magnetic Couplings 23
II.2 DYNAMIC MODEL OF THE BDFM 25
II.2.1 General electrical m achine coupled-circuit model 26
II.2.1.1 Stator voltage equation 26
II.2.1.2 Rotor voltage equation: 29
II.2.2 Variables expressed in space vector 31
II.2.2.1 Voltage equations for the BDFM expressed in space vectors 31
II.2.3 Unified reference frame model of the BDFM 37
II.2.4 Torque Calculation 38
II.3 DYNAMIC MODEL SIMULATIONS RESULTS 40
II.3.1 Singly fed induction mode operation 41
II.3.2 Doubly-fed synchronous operation mode 43
II.4 CONCLUSION 44

III. STEADY STATE ANALYSIS OF THE BDFM 45

III.1 STEADY STATE MODEL OF THE MACHINE 46
III.1.1 Machine model according to PW variables 46
III.1.2 Simplified model 48
III.1.3 Equivalent circuit model 50
III.2 SIMULATION RESULTS 51
III.3. CONCLUSION 54

VI. VECTOR CONTROL ALGORITHM FOR THE BDFM 55

VI.I: CONTROL STRATEGY 56
IV.I.1: Control Principle 56
IV.2: PW FLUX REFERENCE FRAME MACHINE MODEL 57
IV.3: DYNAMIC CONTROL FUNCTIONS 58
IV.3.1: Control of power winding current 58
IV.3.2: Control of control winding current 59
IV.3.4: Speed control 62
IV.3.5: PW power control 63
IV.4: CONTROL SCHEME 64
IV.4.1: PW flux estimator 65
IV.4.2: Torque Estimator 65
IV.5: SIMULATION RESULTS 66
IV.5.1: CW current control results 66
IV.5.2: Electromagnetic torque regulation results 67

IV.5.3 Dynamic of the speed control loop 68
IV.5.4 Load torque perturbation 68
IV.5.6 Active and reactive power control 69
IV.6) CONCLUSIONS 72

GENERAL CONCLUSION AND RECOMMANDATIONS 73

APPENDICES 75

A. COORDINATE TRANSFORMATION 76
B. TRANSFORMATION BETWEEN DIFFERENT REFERENCE FRAMES 78
C. BDFM ELECTRICAL PARAMETER FOR SIMULATION 81
D. DIFIRENTS ROTORS CONFIGURATION 82

REFERENCES 83

LIST OF FIGURES

Fig. I.1: Ideal wind generator at variable speed generation 5
Fig. I.2: Wind variable speed generator with gearbox 5
Fig I.3: First generation of the system at VSG 6
Fig. I.4: Second generation of the VSGs 7
Fig I.5: Third generation of the VSG 8
Fig1.6: BDFTSIG for wind power generation 9
Fig 1.7: Cascade machine in a casing and squirrel cage rotor 10
Fig I.8: Brushless doubly-fed machine with cage rotor or reluctance rotor 10
Fig I.9: Block diagram of the feedback linearization 13
Fig I.10: Block diagram of the control winding phase angle control 14
Fig I.11: Speed and power factor control, ... 15
Fig I.12: Block diagram of the rotor flux orientation control 16
Fig I.13: Block diagram of the vector control with PW flux orientation 17
Fig I.14: Direct torque control 17
Fig II.1: BDFM system. 20
Fig II.2: Nested loop rotor cage of cambridge prototype. 20
Fig II.3: BDFM coupling mechanism schematic 21
Fig II.4: Schematic of the two sets stator winding & n rotor nest of the BDFM 26
FigII.5: Open loop speed scalar control scheme. 41
Fig II.6: Rotor speed and CW frequency responses in time 41
Fig II.7: PW and CW responses-time currents 42
FigII.8: Electromagnetic torque-rotor speed characteristics 42
Fig. II.9: Rotor speed and electromagnetic torque 43
Fig. II.10: speed and electromagnetic torque time response under load torque 43
Fig.III.1: Referred per-phase equivalent circuit for the BDFM 50
Fig.III.2: Referred per-phase equivalent circuit for the BDFM with only power supply. 51
Fig.III.3: Electrical variables of the stator windings (RMS value). 52
Fig.III.4: Active and reactive power of the stator windings. 53
Fig.III.5: Apparent power and electromagnetic torque of the BDFM 53
Fig.IV.1: vector control scheme of BDFM 57

Fig IV.2: Implemented PW current control 59
Fig IV.3: CW current control loop 61
Fig IV.4: Speed control loop 62
Fig IV.5: Powers control loop 63
Fig IV.6: General vector control schema 64
Fig IV.7: CW current dynamic response 66
Fig IV.8: Torque control response 67
Fig IV.9: Control responses with steps of the rotor speed reference 68
Fig IV.10: Control responses with a load perturbation 68
Fig IV.11: Reactive power control response 69
Fig IV.12: Active power control response 69
Fig IV.13: Speed, CW current and CW frequency 70
Fig IV.14: Speed, CW current , CW frequency PW active and reactive power 72

LIST OF TABLES

Table. I.1: Comparison of variable speed generation techniques 8
Table. I.2: Research groups 12
Table. II.1: Different operation modes of the BDFM in steady state conditions 21
Table. II.2: Magnetic coupling conditions 24

NOMENCLATURE

LIST OF SYMBOLS

f_p (f_c): PW (CW) frequency.
f_{rp} (f_{rc}): Rotor voltage frequency induced by PW (CW).
$\vec{\imath}_p(\vec{\imath}_c)$: Stator PW (CW) current vector.
$\vec{\imath}_r$: Rotor current vector.
$L_p(L_c)$: Stator PW (CW) self-inductance.
L_r: Rotor self-inductance.
$M_p(M_c)$: Unified frame stator PW (CW) to rotor coupling inductance.
N_r: Number of rotor nests.
P_c: CW active power.
P_p: PW active power.
$p_p(p_c)$: Power (control) winding pole pairs Number.
Q_c: CW reactive power.
Q_p: PW reactive power.
$\mathcal{R}_e\{\dots\}$: Real part.
$R_p(R_c)$: Stator PW (CW) resistance.
R_r: Rotor resistance.
$s_p(s_c)$: Slips for the power and control winding.
T_L: Load torque.
$T_{em_p}(T_{em_c})$: PW (CW) electromagnetic torque.
T_{em}: Total electromagnetic torque.
$\vec{V}_p(\vec{V}_c)$: Stator PW (CW) fed voltage vector.
$\mathfrak{I}_m\{\dots\}$: Imaginary part.
θ_{obs_p} (θ_{obs_c}): Angle between the PW (CW) and the generic reference frame.
θ_r : Rotor shaft displacement between the rotor and the PW reference axis.
ω_p (ω_c): Synchronous angular frequency of the PW (CW).
ω_{rp}: Angular slip speed of the PW.
δ: Initial angle between the rotor and the PW references axis.
$\vec{\varphi}_p(\vec{\varphi}_c)$: Stator PW (CW) flux linkage vector.
$\vec{\varphi}_r$: Rotor flux linkage vector.
$\sigma_p(\sigma_c)$: PW (CW) inductance leakage coefficient.
Ω: Rotor's mechanical angular speed.
Ω_n: Natural speed.
γ: Angle between the PW and the CW references axis.

SUBSCRIPTS

p, c, r:	Power winding, control winding, rotor.
$S_p\,(S_c)$:	Stator power (control) winding phase.

SUPERSCRIPTS

$*$:	Complex conjugate.
dq:	The direct and quadrant component on the power winding flux frame.
dq_p:	Generic reference frame of P_p-pole pairs.
dq_c:	Generic reference frame of P_c-pole pairs.
xy_p:	Rotor reference frame.
$\alpha\beta_c$:	Control winding reference frame.
$\alpha\beta_p$:	Power winding reference frame.

ACRONYMS

BDFM:	Brushless Doubly Fed Machine.
BDFRM:	Brushless Doubly Fed Reluctance Machine.
BDFTSIG:	Brushless Doubly Fed Twin Stator Induction Generator.
CW:	Control winding
DFIG:	Doubly-fed induction generator.
FSG:	Fixed speed generation.
PMSG:	Permanent magnet synchronous generators.
PW:	Power winding.
SQIG:	Squirrel Cage Induction Generator.
VSCF:	Variable-speed constant-frequency.
VSG:	Variable speed generation.
WRIM:	Wound Rotor Induction Machine.

MOTIVATION AND OBJECTIVE

When wind power generator is connected to the power grid, the output frequency should be identical with the frequency of the power grid. Wind energy capturing and conversion efficiency can be improved by taking advantage of variable-speed constant-frequency (VSCF) method which uses the Wound Rotor Induction Machine (WRIM, old material).

But the main problem is that the slip rings and wound rotor arrangement which limit its application in harsh environment. Among the possible solutions for these shortcomings is the introduction of the so-called Brushless Doubly Fed Machine (BDFM), which can be seen as an advanced version of the (WRIM), because it is based on the same principle of the slip energy recovery used for the output control.

The BDFM (which is also known as a self-cascaded machine) is a kind of AC excited machine with special structure is composed of two three-phase windings in the stator [called power winding (PW) and control winding (CW)] and a special rotor cage that have a similar performance to a synchronous machine [Qi-06]. The BDFM then has some very attractive features: it is brushless in operation, offers high power factor operation when operating as variable speed drive, and can achieve variable speed operation with a fractionally rated inverter. The fractional rating of the inverter will lead to significant economic benefits, as typically the cost of a variable speed drive is dominated by the cost of the inverter [ROB-05].

But the existence of multiple reference frames related to the two stator windings and the rotor makes it difficult to exploit the well known standard induction machine control strategies.

OBJECTIVES

The main objectives of this dissertation which deals with the study of the vector control for the BDFM in variable speed energy generation are:

1) Develop a mathematical dynamic model for the BDFM based on the complex space vector notation, leading to a unified *dq* reference frame model.
2) Apply a vector control algorithm to drive a brushless doubly fed machine (BDFM).

OUTLINE OF THE DISSERTATION:

The structure of the dissertation document will be continued according to the following chapters:

In chapter 1 the evolution of the System at variable speed energy generation for renewable energy systems will be described. Then, a comparison of different principle generation wind turbines technologies will be made, focusing on the brushless doubly fed machine with its advantages. This chapter will continue with a description of the research groups and the control strategies state of the art.

Chapter 2, the operation principle of the BDFM will be analyzed. The machine topology will be described and different operation modes will be presented. Also a detail discussion of the BDFM modeling will be made. Firstly we shall develop a mathematical model for the BDFM based on coupled magnetic circuit theory and complex space vector notation; secondly a unified dq reference frame model will be treated. Finally to validate the proposed model some simulation results will be carried out.

Chapter 3: This chapter presents a steady state model and performance study of a BDFM. Firstly, the steady state model of the machine will be developed, then the mathematical relation between different electrical variables of the two stator windings at different rotor speeds will be presented. After there, the equivalent circuit of the machine will be given. Lastly, simulation results will be carried out to achieve the principles feature of the machine at steady state operation.

Chapter 4: in this chapter vector control algorithm for the BDFM will be developed. The goal of BDFM control is to achieve a similar dynamic performance to that of classical doubly fed induction machine, exploiting the well-known induction motor vector control philosophy.

Finally the main results and the future works will be presented in the general conclusion and recommendations.

Chapter One:

STATE OF THE ART OF VARIABLE SPEED ENERGY GENERATION DRIVE SYSTEMS

In this introductory chapter firstly background of the dissertation will be described the study and the evolution of the System at variable speed energy generation for renewable energy systems.

Next, a comparison of different principle generation wind turbines technologies from the point of view of the electrical generator will be made, focusing on the brushless doubly fed machine with its advantages.

This chapter will continue with a description of the research groups and the control strategies´ state of the art.

I.1 BACKGROUND:

The present study is focused on the field of the use of electrical machines in medium and high power energy systems.

Nowadays, energy is generated in two ways: fixed speed generation (FSG) and variable speed generation (VSG), In the case of the wind generation, the fixed speed wind turbine is simple, robust, and reliable it uses low cost electrical components. But it has some drawbacks, like uncontrollable reactive power consumption, mechanical stress and limited power quality control, [AKE-00].

On the other hand, the variable speed wind turbine has reduced mechanical stress, increased power capture, and reduced acoustical noise and increased control capability.

But it also has some drawbacks: additional losses due to the power electronics, more components and increased capital costs due to the power electronics, but the electronic over cost of the systems of VSG is not considerable compared to its advantages on the level of the mechanical system, in term of maintenance, and lifetime [POZ-03].

Besides, the machine design characteristics are different in fixed and variable speed wind turbines. The fixed speed wind turbines are designed to obtain maximum efficiency at one wind speed and the variable speed wind turbines are designed to achieve the maximum efficiency over a wide range of wind speed.

Therefore, in power energy generations, the variable speed generations systems allows for variable energetic resources to be exploited better. When the application requires variable speed, two main technologies are used individually or combined:

- ✓ Mechanically, by means of pitch controlled blades.
- ✓ Electrically by using the “electrical drive” concept that consists of the use of an electrical machine, power electronics and the associated control system.

The technology of the classic electrical machines (DC, asynchronous, synchronous…) is widely developed. Traditionally, in high performance applications, DC motors were used, nevertheless the fast development produced in the field of power electronics, as well as the existence of powerful microprocessors has allowed the introduction of the AC machines for almost all type of applications.

Thus, since 1990s, high performance vector controls to AC machine systems have been implemented successfully.

The present research proposes a new alternative concerning a new type of electrical machine for wind energy systems.

I.2 EVOLUTION OF THE WIND SYSTEM AT VARIABLE SPEED GENERATION:

Until the mid 1990s, most of the installed wind turbines were based on squirrel cage induction machines directly connected to the grid and the generation was always done at fixed speed.

Nowadays, most of the installed wind turbines are based in a doubly-fed induction generator (DFIG) sharing the market with the wound rotor synchronous generators (WRSG) and the new arrivals permanent magnet synchronous generators (PMSG). All of them allow variable speed generation.

The wind system of (VSG) must be composed of a minimum: turbine, an axis of transmission, an electronic converter and an electric generator drive Fig I.1.

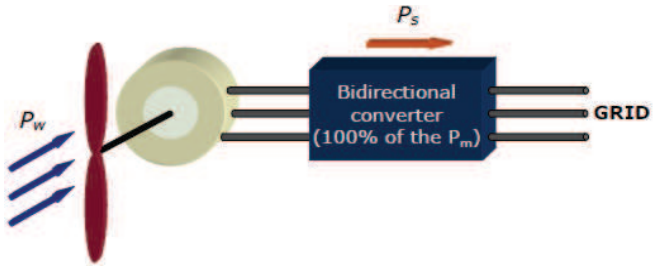

Fig I.1 Ideal wind generator at variable speed generation

The current optimum speed turbine is a few dozen of turns per minute, which requires:

- ✓ Insertion of a gearbox between the turbine and the electric machine (Fig.I.2), or
- ✓ Design a multipole generator adapted to the optimal speeds

The first solution is used by most manufacturers of wind turbines and is currently the only approach competitive commercial on the machine. The second one is an expensive and very cumbersome because it relies on the permanent magnet being the optimum technological choice for this approach and presents a line search of some manufacturers, but so far there is no significant implementation.

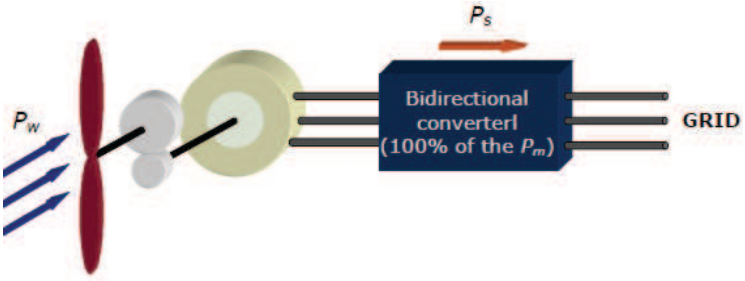

Fig I.2 Wind variable speed generator with gearbox

The turbine and the gearbox represent the necessary mechanical set for providing the wind energy as the magnitudes of torque and speed to the generator machine; there are different approaches to realize the VSG:

I.2.1 Squirrel Cage Induction Generator (SQIG)

To assure energy generation at nominal grid frequency and nominal grid voltage at any rotor speed, using vector control techniques with converter, this approach is known as the first generation system of VSG (*Fig I.3*).

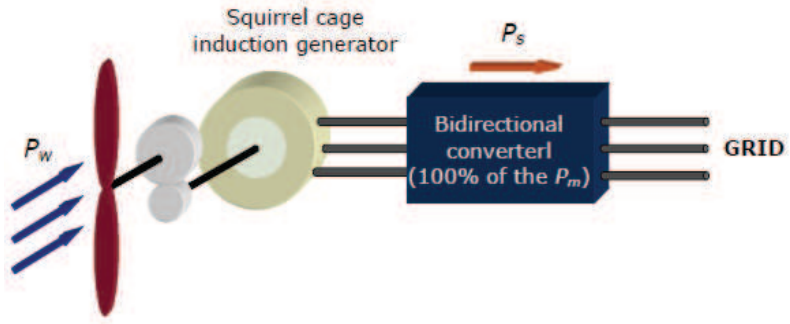

Fig I.3 First generation system of VSG

The advantages of this technique are:

- ✓ Capacity to generate at any speed of the rotor.
- ✓ Less stress on drive train.
- ✓ Mechanical simplicity which leads to an inexpensive design and low maintenance.

The main disadvantage of this technique is:

- ✓ The size of the converter which must be of the same power level as that of the generator.
- ✓ The harmonic distortion generated by the converter needs to be eliminated by a nominal power filters system [SIM-97].
- ✓ Limited power quality control.

I.2.2 Doubly Fed Induction Generator (DFIG)

Doubly fed induction generators (DFIG) with a wounded rotor have been used as variable speed electric generator especially in wind power generators systems. In this case the stator is connected directly to the grid and the rotor is fed by a bidirectional converter that in its turn is connected to the grid (*Fig1.4*).

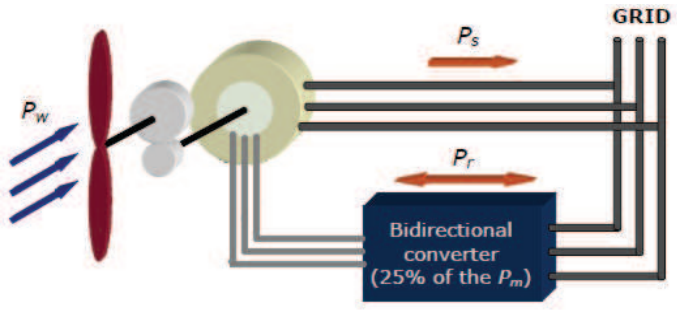

Fig I.4 Second generation of the VSGs

Using vector control techniques, a bidirectional converter assures energy generation at rated grid frequency and rated grid voltage independently of the rotor speed.

The converter main aims to compensate the difference between the speed of the rotor and the synchronous speed. The size of the converter will depend on the desired speed range. The bigger speed range, the more power compensation via rotor is needed. The variation of the speed in the variable speed generation systems is 25% to 50% of the rated speed.

Therefore, the advantages of this BDFM drive with respect to that of SQIG are:

- ✓ Smaller size of the converter.
- ✓ Less cost and bigger system reliability.
- ✓ Full variable speed rang.
- ✓ Less stress on drive train.

The disadvantages of this BDFM drive are:

- ✓ The presence of slip rings reduces the lifetime of the machine and increases the maintenance costs.
- ✓ Losses in converter.

An alternative to overcome this drawback is the so called Brushless Doubly Fed Machine (BDFM).

I.2.3: Brushless Doubly Fed Induction Generator (BDFIG)

The BDFIG or BDFM has its origins from the cascade technology induction machines and consists of two sets of three-phase windings with different number of pole pairs in the stator and a special rotor cage as shown in *Fig I.5*.

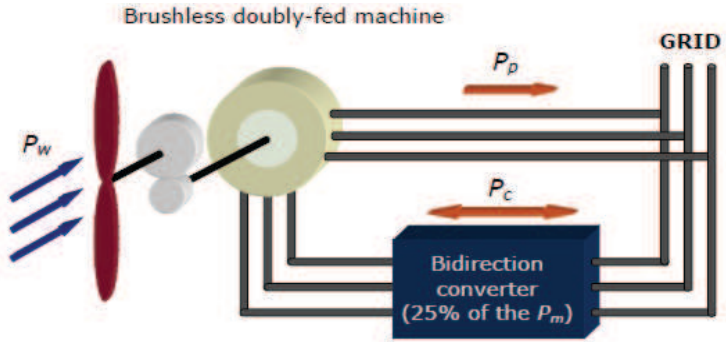

Fig I.5 Third generation of the VSG

The potential advantages of this structure are:

- ✓ The rated power of the converter is lower than the nominal power of the generator (advantage similar to that of the DFIG).
- ✓ The gearbox could be done with one stage of reduction.
- ✓ Robust machine with a great overload capacity and easy installation in hostile atmospheres (advantage similar to that of the SQIG).
- ✓ The cost of the BDFM is between 10% over the cost of the SQIG and 20% below that of the DFIG. The price of the converter is the same as that of the DFIG converter (50 to 70% cheaper than the SQIG converter).

I.3 GENERATOR COMPARISONS:

The following table summarizes the basic characteristics of each conversion type.

	First generation (SQIG)	*Second generation (DFIG)*	*Present generation (BDFM)*
Speed limitation	**No**	Yes	Yes
Converter power	100% of the *Pm*	**25% of the Pm**	**25% of the Pm**
Harmonic distortion	High	**Low**	**Low**
Cost of the Maintenance	**Low**	Medium/High	**Low**
System (Machine+ converter) cost	Medium/High	Medium	**Medium/Low**
Robustness & Reliability	**High**	Medium	**High**

Table I.1. Comparison of variable speed generation techniques [POZ-03]

The wind energy industry has evolved from the classical constant speed generation to the variable speed generation based on DFIG structure. Nowadays, most of the wind farms are based on variable speed generation and they use DFIG. Indeed these electrical machines have been widely used in other types of applications for many years.

In this research work, the BDFM has been chosen initially in the study of the doubly-fed stator machines. This decision is made because the BDFM is a special case of the induction machine. It still that the choice of the BDFM, mainly developed in the research laboratories, by the industrial ones is related to the questions of cost and reliability.

Considering the BDFM advantages, which is so called to be the 3rd generation of wind turbines with the variable speed generation, should present the best part relatively to DFIG in its own area applications.

The present wind and hydraulic context can also support the use of the BDFM which is able to provide a power given with an obstruction equal or inferior that has the DFIG equivalent [POZ-03]. This situation justifies the lot of research in the laboratories for this new type of machine (BDFM), from where the recourse toward to its mathematical model and then to its control.

I.4 STATE OF THE ART OF BDFM:

To combine the advantages of doubly fed generators with high reliability and low maintenance requirements by avoiding the use of the slip rings and brushes a renewed research effort has been made to develop alternatives for classical slip-ring doubly-fed induction machines. For example, the use of two cascaded induction machines which so called Brushless Doubly Fed Twin Stator Induction Generator (BDFTSIG) and associated control strategies was investigated by ***Hopfensperger***, as shown in Fig I.6. In this configuration, the rotor energy is transferred by using a second fractional induction machine (auxiliary machine), which is directly coupled to the main generator (main machine) through the back-to-back connection of rotor circuit.

In a special operation mode (synchronous mode) the rotor current frequency in the both machines is the same so that the main machine (power) can be controlled through the rotors from the auxiliary machine (control).

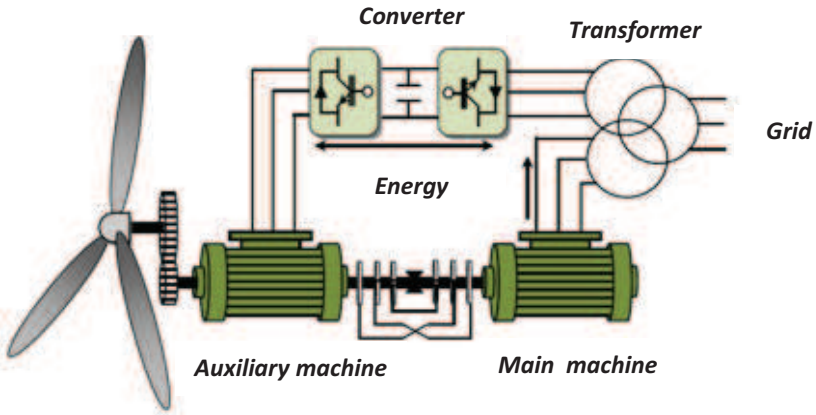

Fig1.6. BDFTSIG for wind power generation

Cascade machines have been improved, including both magnetic cores in the same casing. So, robust rotor squirrel cage could be obtained as illustrated in *Fig 1.7*.

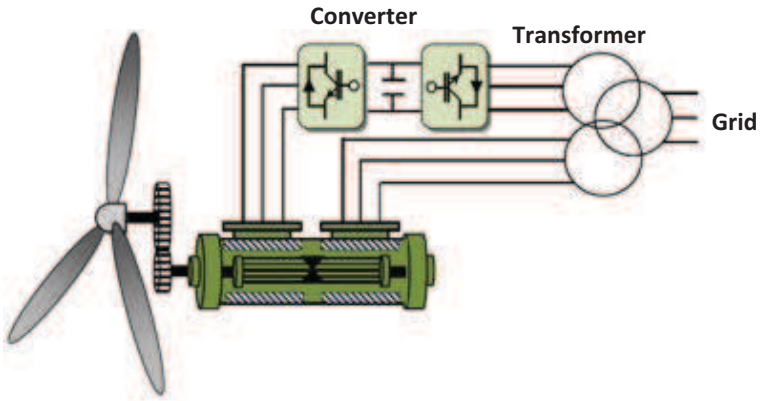

Fig 1.7 Cascade machine in a casing and squirrel cage rotor

The last evolution consisted in the integration of both stator windings in a same magnetic core, as depicted in Fig.1.8. These machines would maintain the principle of cascade operation. But, for the magnetic couplings to take place in the desired way, the windings of the stator and the rotor will have to fulfill some specifications as follows.

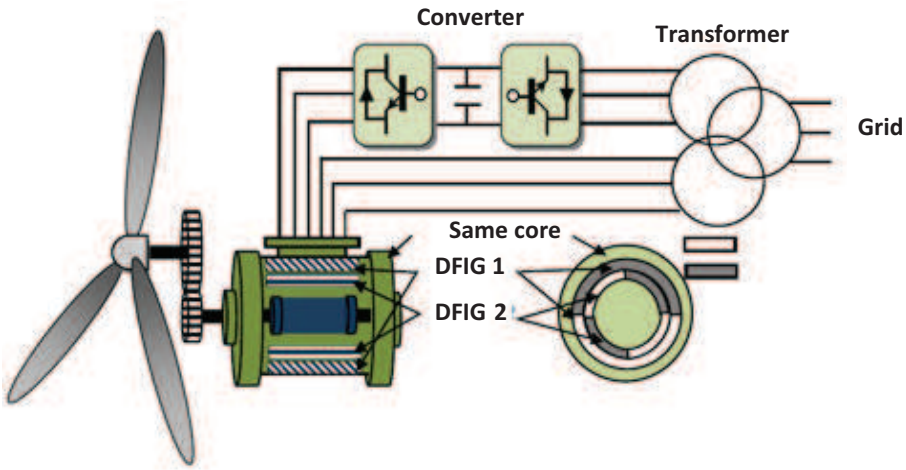

Fig I.8 Brushless doubly-fed machine with cage rotor or reluctance rotor

To maintain the principle operation of the cascade structure, certain conditions should be respected:

- Direct coupling phenomena between the two stator winding must be prevented.
- Electromagnetic coupling between the rotor and each stator windings must be optimized.

Two rotors types can be used, as cage type (BDFM) or as reluctance type Brushless Doubly Fed Reluctance Machine (BDFRM).

I.4.1 BDFM (Brushless Doubly Fed Machine):

This type of machine was developed by René Spée and Alan Wallace, of Oregon State University (USA). They patented the design of the machine and the steady-state analysis was based on the first results of their research. Also, throughout the decade of the 1990s, they published studies about the design, modeling [LI-91] and control [ZHO-97]. Currently R.A Mc Mahon of the University of Cambridge (UK) and P.C Roberts of Scientific Generics Ltd (UK) work on the analysis of the machine operation and the design of the different rotor structures [ROB-05a, McM-06].

I.4.2 BDFRM (Brushless Doubly Fed Reluctance Machine):

This type of machine was developed in its different aspects at the Ohio State University (USA) by Longya Xu, [FEN-91]. More recently, R.E. Betz of the University of Newcastle (Australia) and M.G. Jovanovic of the University of Northumbria (UK) have continued the study of the BDFRM, giving a special attention to control techniques optimization [BET-00].

It has been possible to compare the advantages of each type of machine through a bibliographical analysis:

- *Advantages of BDFRM:*

1. Simple machine model and its control.
2. High efficiency due to the fact that there are no copper losses in the rotor.

- *Disadvantages of BDFRM:*

1. The high space harmonic rates cause:
   - Greater nonlinearities.
   - Higher harmonic distortion.
2. Few practical experiences of the reluctance rotor machines with respect to the induction machines.
3. The volumetric efficiency for the torque generation in the machine is not proved.

I.4.3 Research groups

In the past few years, some research groups have worked on the BDFM, mainly in three different areas: design, modeling and control of the machine.

Table I-2 resumes the different areas of the work of each research group. The research groups are currently working on BDFM.

	DESIGNE	MODELING	CONTROL
Oregon State University (United States)	X	X	X
Cambridge University (England)	X	X	X
Universidad Federal de Santa Catarina (Brazil)	X	X	
Universidad Politécnica de Madrid (Spain)	X		
Mondragon Unibertsitatea (Spain)	X	X	X
Shenyang University of Technology (China)	X	X	
Hunan University (China)			X
Zhejiang University (China)	X	X	X
Harbin Institute of Technology (China)			X
South Chine University of Technology (China)		X	

Table I.2: Research groups [IZA-08]

Most of the research groups have worked in the design and modelling of the machine. The objective of the investements is to build an efficient machine for a possible future implementation in wind generation. However, the electromagnetic behavior of this type of machines is complex and so the control is not simpler. For example, the stability of the machine is limited with the open loop scalar voltage control [SAR-06].

Therefore, it is necessary to improve the control strategies to guarantee the stability of the machine at all speed range.

I.4.4 BDFM Control Strategies:

In the BDFM, different control strategies have been implemented. Since the machine has stability problems with open loop scalar voltage control, all of the control strategies that have been implemented in the BDFM are closed loop strategies. In the state of the art, different control strategies that have been implemented in the BDFM like [IZA-08]:

- ✓ Feedback linearization
- ✓ Control winding phase angle control

- ✓ Speed and power factor control
- ✓ Vector control
- ✓ Direct torque control

The different control strategies are described.

- *Feedback linearization:*

This technique allows the inherently non-linear, time-varying BDFM state-space system to be controlled in such a way that it will behave identically to a very simple linear time-invariant system. Standard linear control theory can then be applied to the resulting linear system. This has the advantage that an optimal controller can be designed much more easily than would be possible for a non-linear system [ROB-02]. The block diagram of this strategy is given in Fig 1.9:

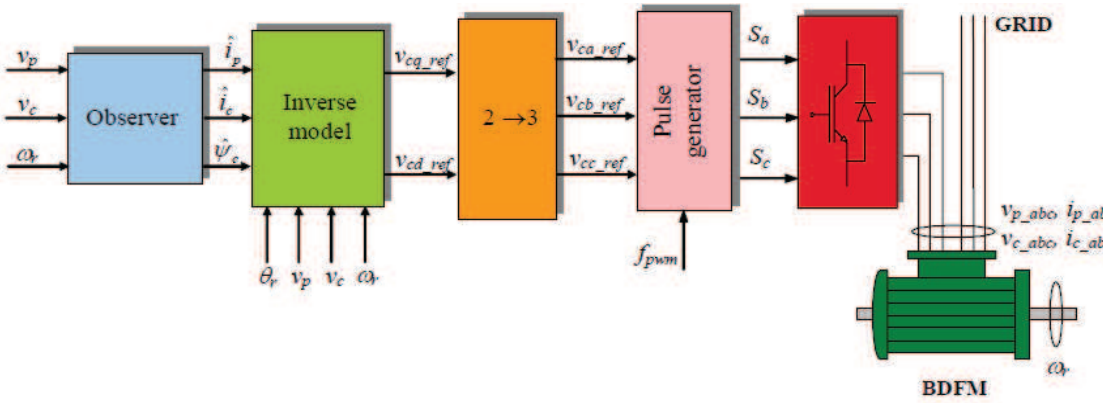

Fig I.9 Block diagram of the feedback linearization

- *Control winding phase angle control:*

The control strategy involves directly by controlling the phase offset between the control winding supply and the power winding supply [ROB-02]. The control has a direct effect on the synchronous load angle of the BDFM. This angle determines the torque of the machine, so the control of the machine can be fulfilled according to Fig 1.10.

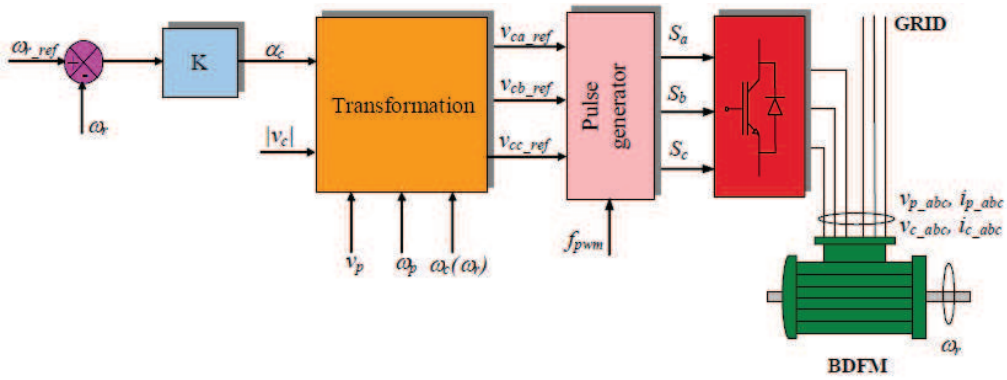

Fig I.10 Block diagram of the control winding phase angle control [ROB-02]

- *Speed and power factor control:*

The research has demonstrated that the power factor of the machine can be controlled by the amplitude of the voltage or by the control winding current, [SHO-02]. The speed of the machine is controlled by the control winding frequency.

In [ZHA-01], the control strategy of power factor of BDFM is studied and an important conclusion has been made, that changes the amplitude value of voltage or current of control winding which control the power factor of BDFM. Based on this theory, the control system is implemented by the conventional PI controller. However, that control strategy suffers from some shortcomings as follows:

- The control implementation depends on the mathematical model, so badly that the precision of control is decided by a veracity of model. Unfortunately, it is impossible to get quite precise mathematical model.

- Owing to the control system based on the mathematical model with rotor dq reference frame, some parameters change at a larger scale during motor operation, but the control system does nothing with it.

The control strategy has been improved in [SHO-02] that a fuzzy PID controller, instead of a conventional PID controller, is utilized to adjust the system's power factor and the rotor speed as shown in FigI.11.

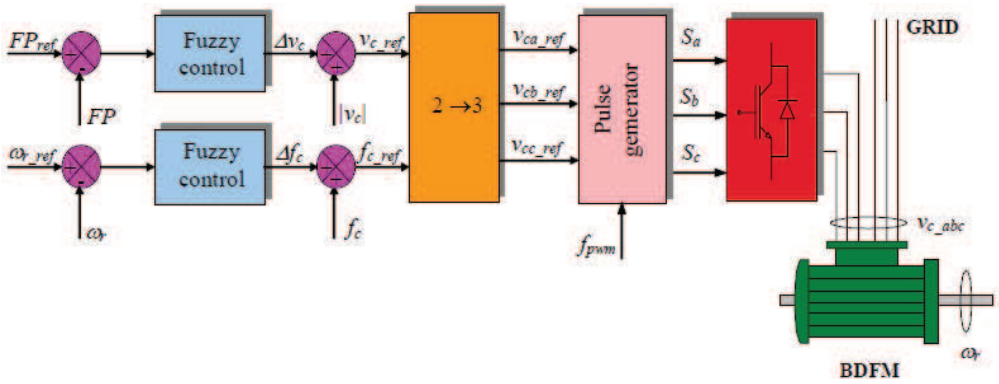

Fig I.11 Speed and power factor control, [SHO-02]

Simulation shows that the power factor and the speed of BDFM can be controlled efficiently by adjusting voltage or current amplitude of control winding through the fuzzy controller.

One advantage of this strategy is the robustness of the controller against the variations of the system parameters and the external disturbances.

- *Vector control:*

The vector control is based on the dynamic *dq* model, an exact model being necessary to obtain good results. Different dynamic models techniques exist and these are based on two vector controls strategies [BOG-95, ZHO-94, POZ-03]:

- The model referred to the rotor of the machine where a vector control with the rotor flux orientation is developed, [ZHO-94, BOG-95, SPE-96, ZHO-97].
- The unified *dq* reference frame model referred to the power winding where a vector control with the power winding flux orientation is developed [POZ-06, SHI-08].

Rotor flux orientation vector control:

In [ZHO-97] two synchronous reference frames are used; each one is synchronized with its own source of excitation. The rotor oriented control algorithm is designed and uses a power subsystem prediction or electrical torque estimator. The controller requires the measurement of the power winding variables and the angle of the rotor.

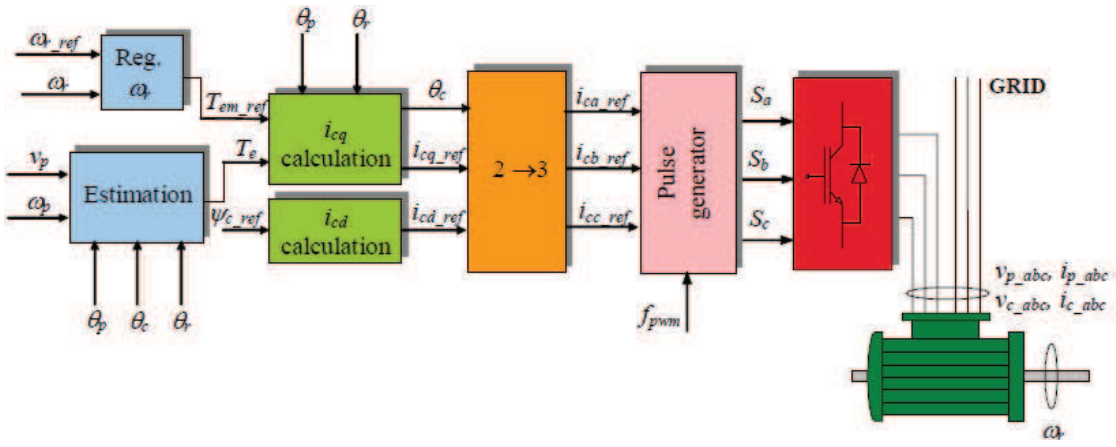

Fig I.12 Block diagram of the rotor flux orientation control [ZHO-97]

The angle between these two frames is defined as the BDFM synchronous angle. Varying this angle the electromagnetic torque of the machine can be modified. In order to calculate the synchronous angle, a non-linear function requiring the real time evaluation of the arcsine and the arctangent is used. This control method leads to good results, but it is quite complicated to be implemented it experimentally.

Power winding flux oriented control:

Javier Poza and *Daniel Roye* presented a new vector control algorithm for the BDFM [POZ-02]. The purpose of the proposed method depending on the two main currents control of the machine are the first one is to generate the torque and the second one is to provide the flux. This scheme control is similar to the one that has been used with very good results for the induction machine control during several years. For doing so, all variables of the machine are related to the PW synchronous reference frame.

The principle regulation in cascade is used as illustrated in *FigI.13*. The control algorithm is as follows:

- Control of the power winding reactive power:

$$Q_{p\_ref} \rightarrow i_{pd\_ref} \rightarrow i_{cd\_ref} \rightarrow v_{cd\_ref}$$

- Control of the speed or power winding active power:

$$\omega_{r_{ref}} \rightarrow T_{em_{ref}} \rightarrow i_{pq_{ref}} \rightarrow i_{cq_{ref}} \rightarrow v_{cq_{ref}}$$

$$P_{p\_ref} \rightarrow i_{pq\_ref} \rightarrow i_{cq\_ref} \rightarrow v_{cq\_ref}$$

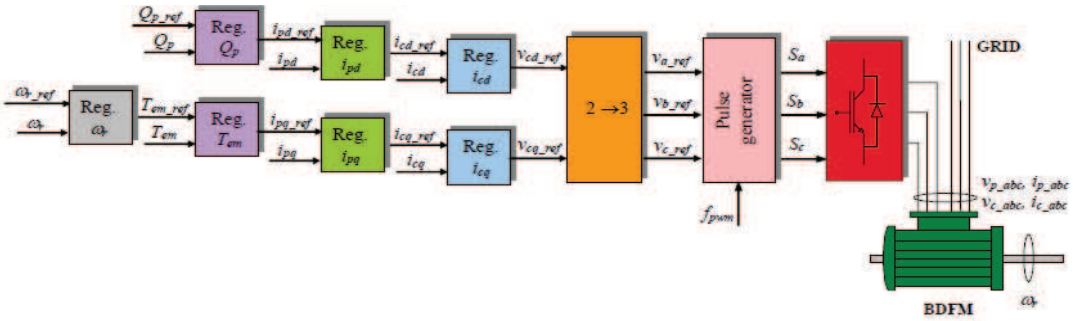

Fig I.13 Block diagram of the vector control with PW flux orientation [POZ-09]

To implement this control strategy, flux and torque estimations are necessary.

- *Direct torque control:*

In [BRA-96], a predictive direct torque control is used for the BDFM. In similar manner of that of the doubly fed machine.

The predictive calculations use measured terminal quantities, rotor speed, position and machine parameters. Space vector pulse width modulation (PWM) is used to determine the inverter switching function, resulting in a constant switching frequency.

This direct torque control does not act directly on the inverter commutations, and requires a PWM modulator as shown in Fig I.14.

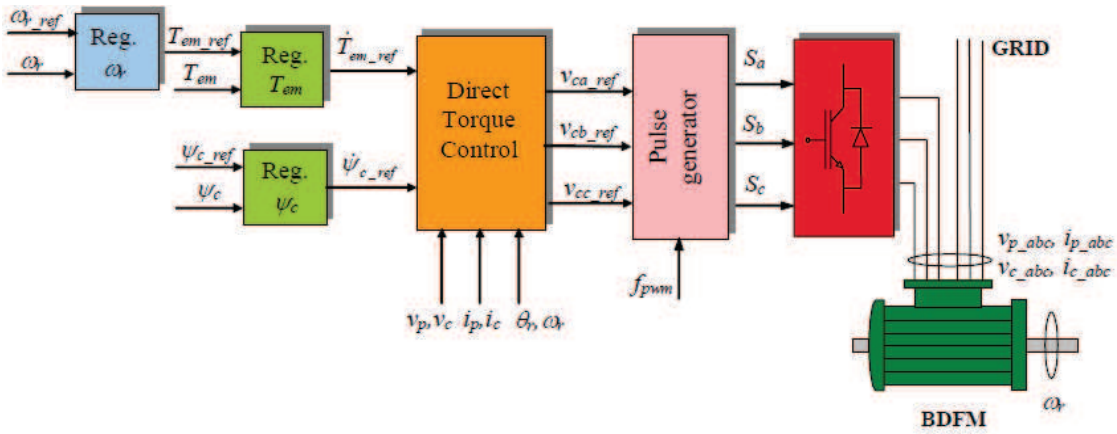

Fig I.14 Direct torque control, [BRA-96]

This technique giving good performances in simulation, however, an efficient implementation of this control method is difficult to achieve [POZ-02].

I.4.5 Main applications of the BDFM:

The BDFM then has some very attractive features: it is brushless in operation, offers high power factor operation when operating as variable speed drive, and can achieve variable speed operation with a fractionally rated inverter. The fractional rating of the inverter will lead to significant economic benefits, as typically the cost of a variable speed drive is dominated by the cost of the inverter [ROB-05].

The most promising applications therefore are applications requiring variable speed generation preferably over a limited speed range and in hostile environments where high power factor and lack of brushes are highly required.

There is, however, a cost penalty for using a BDFM as compared to a conventional induction machine based drive. The rotor is to be more complex, hence manufacturing cost will be slightly higher. However the benefits will certainly outweigh the costs in an appropriate number of application areas.

Chapter Two:

OPERATION PRINCIPLE AND DYNAMIC MODELE ANALYSIS OF THE BDFM

This chapter presents firstly the principle operation of the BDFM. It will show the topology of this machine and the different operation modes describing the magnetic couplings effects.

Next, it will treat the mathematical model for the BDFM based on coupled magnetic circuit theory formulated in complex space vector notation. Then they obtained dynamic model of the machine will be *finally tested in simulation workbench using MATLAB/SIMULINK in order to verify the proposed model.*

II.I CONSTITUTION AND OPERATION OF THE BDFM

II.1.1 Topology of the Machine

The BDFM system consists of an induction-based machine and a bidirectional converter as shown in Fig II.1. The machine is built with two three phase stator winding systems with different pole-pair numbers: the Power Winding (PW) having p_p.pole-pairs and Control Winding (CW) having p_c, pole-pairs.

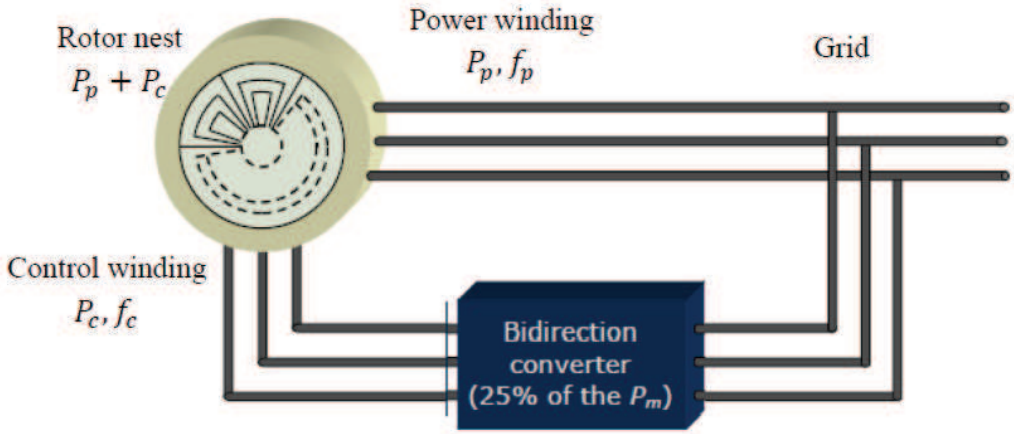

Fig II.1: BDFM system.

The rotor is constructed by a modified cage form which has the potential to be compacted, similar to the conventional squirrel cage rotors of the induction machines. The number of the rotor nests is equal to the sum of the stator windings pair-poles [WIL-97]. Each nest number has one or more copper loops as clearly seen in appendices D. Fig II.2 shows the nested loop rotor. This machine has 4 and 8 pole stator windings (2 and 4 pair-poles) which are used as control and as power windings, respectively. Hence, the number of rotor nests is 6. There are 3 loops in each nest: inner, middle, and outer loops. All the loops are short-circuited through a common end ring at one end of the rotor (*FigII-2*).

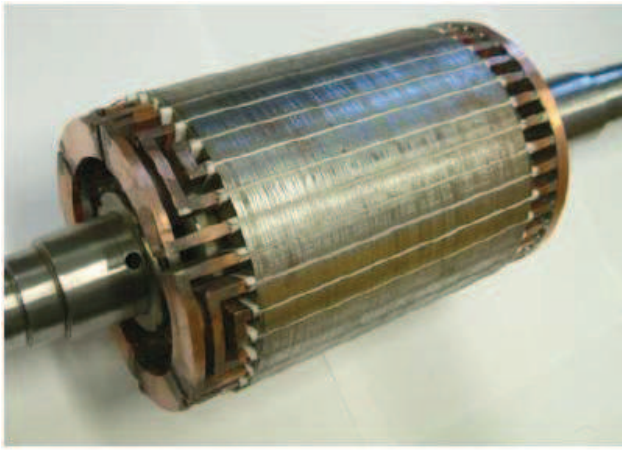

Fig.II.2: Nested loop rotor cage of Cambridge prototype [FAR-08]

For the BDFM the major interest is the operation in synchronous mode, the essential feature of synchronous operation is the electromagnetic coupling of one stator winding system with the other, exclusively through the rotor. Since the stator windings which can be assumed to be sinusoidally distributed for different pole-pair numbers, there is (intentionally) no direct coupling between both stator windings. However, each stator winding can be coupled directly with the rotor. The induced rotor currents from both stator windings should be have an appropriate sequence and frequency. It results that the rotor current creates the appropriate fields which can induce voltages in the power windings (stator) initially due to control windings currents, and vice versa. This indirect induction mechanism is referred to as ***cross coupling*** which is illustrated in Fig II.3.

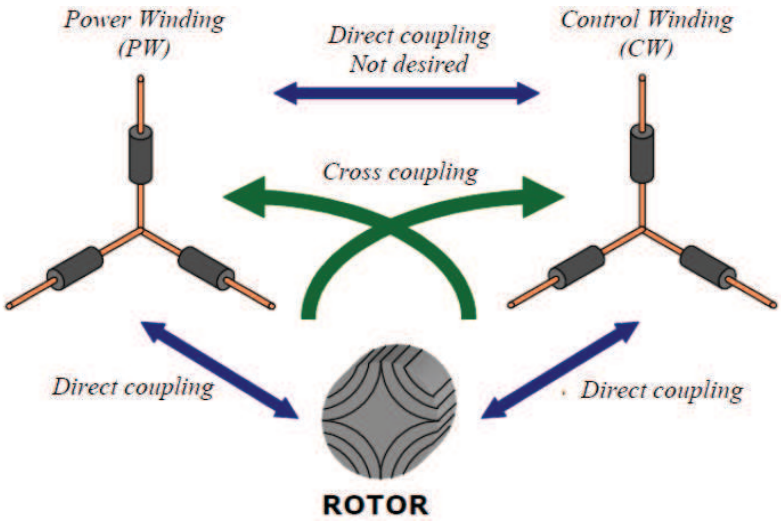

Fig II.3 BDFM coupling mechanism schematic

II.I.2 Operation modes of the BDFM

It can be shown that the BDFM exhibits two modes of operation: the induction mode (IM) and the synchronous mode (SM). The synchronous mode is the most interesting applications for variable speed generations. Table II-1 summarizes the different operation modes for an experimental BDFM [RUQ-91].

Operation mode	Power Winding	Control Winding
1) **Induction mode**	Grid frequency	Open circuit
2) **Induction mode**	Grid frequency	Short circuit
3) **Induction mode**	Grid frequency	Variable frequency
4) **Synchronous mode**	Grid frequency	Variable frequency

Table II.1: Different operation modes of the BDFM in steady state conditions

a) Induction mode:

The shaft speed in this mode of operation is depending on the load.

✓ *First case (CW open circuit):* the power winding creates a rotating field at the angular velocity $\boldsymbol{\omega_p = 2\pi f_p/p_p}$. The speed of the machine is approached to this angular velocity (synchronous speed). The induced current by the PW in the rotor will create a voltage in the CW. However, the CW is an open circuit and no current is circulating in this winding, the machine operate as an asynchronous (induction) motor with a single supplying voltage. It should be noted, however, that the equivalent asynchronous machine has a high relative rotor leakage impedance (rotor_ CW mutual inductance wich acts as a leakage inductance).

✓ *Second case (CW short circuit)*: CW short circuit current is induced by the PW-CW cross-coupling and its frequency is given by $\boldsymbol{\omega_c = -[\,\omega_p - (p_p + p_c)\Omega]}$. Therefore, the induced rotor current from the CW may be synchronized. The operation was equivalent to an asynchronous machine with $\boldsymbol{(p_p + p_c)}$ pair-poles.

✓ *Third case (doubly-fed mode):* two power and control windings create two separate fields that rotate at the speeds $\boldsymbol{\omega_p = 2\pi f_p/p_p}$and $\boldsymbol{\omega_c = 2\pi f_c/p_c}$, respectively. Each of these fields induce respectively in the rotor an electromotive forces system at the frequencies $\boldsymbol{f_{rp}}$ and $\boldsymbol{f_{rc}}$ and so they circulate simultaneously inside the rotor through an current with two system frequencies $\boldsymbol{f_{rp}}$ and $\boldsymbol{f_{rc}}$. This combined current may induce two electromotive voltages at different frequencies into the primary supplies (PW & CW). This mode of operation is inappropriate study, and will only be admitted during the transient synchronization.

All the previous cases are induction operation modes where the shaft speed is related to the machine load. However, in doubly-fed mode, the BDFM has another particular synchronous mode operation which is desired one, and for which the machine design to be optimized.

b) **Synchronous mode:**

Synchronous operation mode is established when the frequencies of the rotor currents induced by both rotating stator fields become identical [IZA-08]. In this mode, both stator windings are fed from isolated sources with different frequencies where the machine operation relies on ***cross coupling*** between stators winding and rotor winding [WIL-97].

By design, this cross coupling does not occur directly between PW and CW because they are chosen to be no coupled. Ended, this choice is guaranty with the pole number of each different field of stators [ROB-05].

II.I.3 Magnetic Couplings:

Two magnetic fields are generated in the BDFM when the power and control windings are supplied with three-phase balanced voltages. The magnetic flux density distribution established in the air gap by both windings can be expressed as follows [WIE-95] (ignoring any fixed angular offsets):

$$b_p(\theta,t) = B_p \cos\left(\omega_p t - p_p\theta\right) \quad \textbf{[Eq2\_1]}$$

$$b_c(\theta,t) = B_c \cos\left(\omega_c t - p_c\theta\right) \quad \textbf{[Eq2\_2]}$$

Where $\mathbf{B_p}, \mathbf{B_c}$ are the peak magnetic flux densities and $\boldsymbol{\theta}$ is the airgap angular position.
If the rotor is rotating at an angular velocity $\boldsymbol{\Omega}$, then the fundamental flux density equations may be written in the rotor reference frame as $\boldsymbol{\theta = \Omega t + \grave{\theta}}$:

$$b_p(\theta,t) = B_p \cos[\left(\omega_p - p_p\Omega\right)t - p_p\grave{\theta}] \quad \textbf{[Eq2\_3]}$$

$$b_c(\theta,t) = B_c \cos[\left(\omega_c - p_c\Omega\right)t - p_c\grave{\theta}] \quad \textbf{[Eq2\_4]}$$

The essential requirement for BDFM action is that the ***frequency*** and ***distribution*** of the currents induced in the rotor by the first airgap field matches that induced by the second one [WIL-97]. Both stator windings will then be coupled via the rotor.

The condition that the two rotor current distributions have the same frequency may be determined directly by equalize the frequency terms of the two previous equations.

$$\omega_p - p_p\Omega = \omega_c - p_c\Omega \quad \textbf{[Eq2\_5]}$$

This leads to:

$$\Omega = \frac{\omega_p - \omega_c}{p_p - p_c} \quad \textbf{[Eq2\_6]}$$

To assure the same distribution for the two rotors currents a physical structure of the rotor should satisfy the following equation:

$$\frac{2\pi}{N_r}p_p = \frac{2\pi}{N_r}p_c + 2\pi q \quad , \quad q = 0, \pm1, \pm2 \ldots\ldots\ldots \quad \textbf{[Eq2\_7]}$$

Where **Nr** is the number of the rotor nests. $\mathbf{N_r}$ is then expressed by:

$$N_r = \frac{P_p - P_c}{q} \quad \textbf{[Eq2\_8]}$$

For practical values of $\boldsymbol{P_p}$ and $\boldsymbol{P_c}$, the values of $\boldsymbol{q}$ other than unity will produce an unfeasibly small numbers of rotor nests, so:

$$N_r = p_p - p_c \qquad \textbf{[Eq2\_9]}$$

[Eq2_8] gives the number of the rotor nest that produce ***cross coupling,*** hence **[Eq2_6]** shows the rotor speed at which produces synchronous operation. But since the equation **[Eq2_4]** is fulfilled that $\boldsymbol{cos(A) = cos(-A)}$ there exists another alternative to ensure this form of the synchronous and cross coupling phenomena, that we can write:

$$b_c(\theta, t) = B_c \cos[-(\omega_c - p_c\Omega)t + p_c\grave{\theta}] \qquad \textbf{[Eq2\_10]}$$

Calculating these combinations in the same way as in the previous case, we obtain:

$$\Omega = \frac{\omega_p + \omega_c}{p_p + p_c} \qquad \textbf{[Eq2\_11]}$$

Where,

$$N_r = p_p + p_c \qquad \textbf{[Eq2\_12]}$$

So there are two possible solutions that may be illustrated in the following table:

Solution 1	Solution 2
$\boldsymbol{\Omega = \frac{\omega_p - \omega_c}{p_p - p_c}}$	$\boxed{\Omega = \frac{\omega_p + \omega_c}{p_p + p_c}}$
$\boldsymbol{N_r = p_p - p_c}$	$\boxed{N_r = p_p + p_c}$

Table II.2: Magnetic coupling conditions

It is more convenient to choose ***Nr*** in accordance with the second solution because it results in a greater number of rotor nests. Therefore, the rotor speed can be expressed as follows:

$$\Omega = \frac{\omega_p + \omega_c}{p_p + p_c} \qquad \textbf{[Eq2\_13]}$$

When$\boldsymbol{f_c} > 0$, the control winding current has the same sequence as the power winding one and when, if $\boldsymbol{f_c} < 0$, the sequences are different.

So there are two operation cases: the subsynchronous case where ω_c takes negative values; and the supersynchronous case, where $\boldsymbol{\omega_c}$ takes positive values [POZ-06].

The BDFM is characterized by the so-called natural speed when the control winding is supplied by DC voltage ($\boldsymbol{f_c = 0}$):

$$\Omega_{\mathrm{n}} = \frac{\omega_p}{p_p + p_c} \qquad [\mathbf{Eq2\_14}]$$

From [**Eq2_13**], we can conclude an important feature for the BDFM control which represents in a direct relationship between the rotor speed of the machine and the control winding frequency. So, we can get a regular speed of the machine by controlling the control winding frequency.

II.2 DYNAMIC MODEL OF THE BDFM:

The good dynamic model of the machine is very important to analyze its operation mode and to implement the different control strategies. BDFM is composed of two three-phase windings in the stator and a special rotor winding. Thanks to a specific design of the BDFM, the control winding can act on the rotor current which is being induced by the power winding as we have seen previously. This is achieved by an electromagnetic ***cross coupling*** effect between the two stator windings through the rotor. The existence of multiple reference frames related to the stator windings and the rotor makes it too difficult to exploit the well known standard induction-machine control strategies.

Li, Wallace and Spee was developed the dynamic vector model of the BDFM referred to the rotor shaft position [LI-91]. later than, the same group has generalized their work to any number of pair-poles [BOG-95].

Next, a BDFM model was derived assuming that the machine was composed of two superposed subsystems [ZHO-97, ZHO-94]. Each subsystem contains the dynamic of one of the two stator windings (PW or CW) and the corresponding rotor dynamics. PW or CW subsystem equations were written in two different synchronous reference frames related to each pole-pair distribution.

Later, Munoz and Lipo have proposed dynamic complex vector models for both machines: cage induction machine [MUN-99] and dual-stator-winding induction machine [MUN-00]. These models are based on complex space vector notation.

After that, based on this theory, ***J. Poza*** developed a unified $\boldsymbol{dq}$ reference frame model for BDFM.

Afterward, ***P. C. Roberts*** proposed a generalized 'synchronous reference frame' model which has been derived in a different way [ROB-05], but this purpose becomes identical to the unified reference frame model obtained by ***J. Poza***.

The objective of this section is to develop the unified $\boldsymbol{dq}$ reference frame model of the BDFM based on the space vector notation.

II.2.1 General electrical machine coupled-circuit model

It is assumed that the stator has two sinusoidally distributed windings with different number of poles ($\boldsymbol{p_p \neq p_c}$). The rotor of the BDFM is configured with $\boldsymbol{n}$ symmetrical nests as shown in Fig II.4. In such a way, that the second solution [**Eq2_13**] is fulfilled where each nest can be built of several isolated loops, one unique loop per nest will be initially considered.

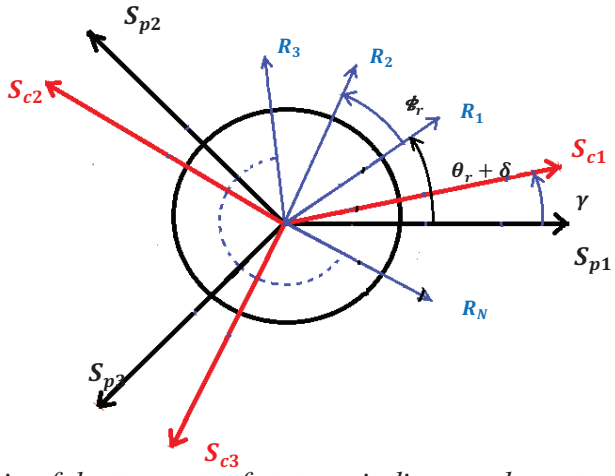

Fig II.4 Schematic of the two sets of stator windings and n rotor nests of the BDFM

Based on the magnetic circuit theory, a full model of the induction machine can be developed. The general coupled circuit model can be expressed as:

$$V = Ri + \frac{d\varphi}{dt} \qquad \textbf{[Eq2_15]}$$

Where: $\boldsymbol{V}$, $\boldsymbol{i}$ and $\boldsymbol{\varphi}$ are the terminal voltage, current and flux linkage in each circuit; and $\boldsymbol{R}$ is the resistances matrix. Applying this general equation to the BDFM leads to its full model.

II.2.1.1 Stator voltage equation

A) Power winding equation:

Stator voltage equation of power winding is expressed as:

$$v_{Sp} = R_{Sp} i_{Sp} + \frac{d\varphi_{Sp}}{dt} \qquad \textbf{[Eq2_16]}$$

Where, $\boldsymbol{R_{Sp} = R_{Sp123}}$ is a diagonal 3×3 matrix, in which the diagonal value depends on the resistances per phase of the power winding equation set, and also:

$$v_{Sp} = \begin{pmatrix} v_{Sp1} \\ v_{Sp2} \\ v_{Sp3} \end{pmatrix};\ i_{Sp} = \begin{pmatrix} i_{Sp1} \\ i_{Sp2} \\ i_{Sp3} \end{pmatrix};\ \varphi_{Sp} = \begin{pmatrix} \varphi_{Sp1} \\ \varphi_{Sp2} \\ \varphi_{Sp3} \end{pmatrix}.$$

The flux linkage can be written as the contribution of three components as:

$$\varphi_{Sp} = \varphi_{Sp}^{Sp} + \varphi_{Sc}^{Sp} + \varphi_{R}^{Sp} \qquad \textbf{[Eq2\_17]}$$

The first term in the previous equation represents the stator power winding flux linkage due to the power winding stator currents, the second term is the flux linkage due to the stator control winding currents and the last term is the contribution of the rotor current.

More detailed explanations of each term will be developed separately in the following sub-sections.

a) Stator flux linkage in the power winding due to power winding currents:

Stator flux linkage of the power winding due to the power winding currents can be expressed as:

$$\varphi_{Sp}^{Sp} = \begin{pmatrix} \varphi_{Sp1}^{Sp} \\ \varphi_{Sp2}^{Sp} \\ \varphi_{Sp3}^{Sp} \end{pmatrix} = \begin{pmatrix} l_{lp} + L_{p1p1} & m_{p1p2} & m_{p1p3} \\ m_{p2p1} & l_{lp} + L_{p2p2} & m_{p2p3} \\ m_{p3p1} & m_{p3p2} & l_{lp} + L_{p3p3} \end{pmatrix} \begin{pmatrix} i_{Sp1} \\ i_{Sp2} \\ i_{Sp3} \end{pmatrix} \qquad \textbf{[Eq2\_18]}$$

Where:

$l_{lp}\ and\ L_{pipi}$ are the Leakage and self inductances of power windings, respectively $l_p = l_{lp} + L_{pipi}$

$m_{p1p2} = m_{p1p3} = m_{p2p1} = m_{p2p3} = m_{p3p1} = m_{p3p2} = m_p$**:** Mutual inductances of the power windings. Therefore we can write:

$$\varphi_{Sp}^{Sp} = \begin{pmatrix} \varphi_{Sp1}^{Sp} \\ \varphi_{Sp2}^{Sp} \\ \varphi_{Sp3}^{Sp} \end{pmatrix} = \begin{pmatrix} l_p & m_p & m_p \\ m_p & l_p & m_p \\ m_p & m_p & l_p \end{pmatrix} \begin{pmatrix} i_{Sp1} \\ i_{Sp2} \\ i_{Sp3} \end{pmatrix} \qquad \textbf{[Eq2\_19]}$$

Since:

$$i_{Sp1} + i_{Sp2} + i_{Sp3} = 0 \qquad \textbf{[Eq2\_20]}$$

Therefore the equation [**Eq2_19**] becomes

$$\varphi_{Sp}^{Sp} = \begin{pmatrix} L_p & 0 & 0 \\ 0 & L_p & 0 \\ 0 & 0 & L_p \end{pmatrix} \begin{pmatrix} i_{Sp1} \\ i_{Sp2} \\ i_{Sp3} \end{pmatrix} = L_p \begin{pmatrix} i_{Sp1} \\ i_{Sp2} \\ i_{Sp3} \end{pmatrix} \qquad \textbf{[Eq2\_21]}$$

Where, $L_p = l_p - m_p$ is the cyclic self inductance of the power windings.

b) Stator flux linkage in the power windings due to control winding currents:

Two stator winding sets have different numbers of poles. Hence the mutual inductances between the stator winding sets are zero [POZ-03], which means that these two stator winding

sets are naturally decoupled. The stator flux linkage in the power winding set due to the control winding currents is always zero.

$$\varphi_{Sc}^{Sp} = 0 \qquad \textbf{[Eq2\_22]}$$

c) Stator flux linkage in power winding set due to the rotor currents.

The cage rotor having $\boldsymbol{n}$ rotor nest can be assumed as a system of $\boldsymbol{n}$ phases [MUN-99]. The total stator flux linkage due to the rotor currents can be derived as:

$$\varphi_R^{Sp} = \begin{pmatrix} \varphi_R^{S_{p1}} \\ \varphi_R^{S_{p2}} \\ \varphi_R^{S_{p3}} \end{pmatrix} = M_{0p} \begin{pmatrix} \cos p_p(\theta_r+\delta) & \cos p_p[(\theta_r+\delta)+\alpha_r] & \dots\dots & \cos p_p[(\theta_r+\delta)+(n-1)\alpha_r] \\ \cos[\frac{2\pi}{3}-p_p(\theta_r+\delta)] & \cos[\frac{2\pi}{3}-p_p[(\theta_r+\delta)+\alpha_r]] & \dots\dots & \cos[\frac{2\pi}{3}-p_p[(\theta_r+\delta)+(n-1)\alpha_r]] \\ \cos[\frac{4\pi}{3}-p_p(\theta_r+\delta)] & \cos[\frac{2\pi}{3}-p_p[(\theta_r+\delta)+\alpha_r]] & \dots\dots & \cos[\frac{4\pi}{3}-p_p[(\theta_r+\delta)+(n-1)\alpha_r]] \end{pmatrix} \begin{pmatrix} i_{r1} \\ i_{r2} \\ \vdots \\ \vdots \\ i_{rn} \end{pmatrix} \qquad \textbf{[Eq2\_23]}$$

So we can write, for example, for the first component of last flux vector:

$$\varphi_R^{Sp1} = \frac{M_{0p}}{2}\left\{ e^{jp_p(\theta_r+\delta)}\left[1\ b^{P_p}\ b^{2P_p}\ \dots\dots b^{(n-1)P_p}\right] + e^{-jp_p(\theta_r+\delta)}\left[1\ b^{-P_p}\ b^{-2P_p}\ \dots\dots b^{-(n-1)P_p}\right]\right\} \begin{pmatrix} i_{r1} \\ i_{r2} \\ \vdots \\ \vdots \\ i_{rn} \end{pmatrix} \qquad \textbf{[Eq2\_24]}$$

In the same way for $\boldsymbol{\varphi_R^{Sp2}, \varphi_R^{Sp3}}$, we can also obtain:

$$\varphi_R^{Sp} = \frac{M_{0p}}{2}\left\{ e^{jp_p(\theta_r+\delta)} \begin{pmatrix} 1 & b^{P_p} \dots\dots & b^{(n-1)P_p} \\ a^2(1 & b^{P_p} \dots\dots & b^{(n-1)P_p}) \\ a(1 & b^{P_p} \dots\dots & b^{(n-1)P_p}) \end{pmatrix} + e^{-jp_p(\theta_r+\delta)} \begin{pmatrix} 1 & b^{-P_p} \dots\dots & b^{-(n-1)P_p} \\ a(1 & b^{-P_p} \dots\dots & b^{-(n-1)P_p}) \\ a^2(1 & b^{-P_p} \dots\dots & b^{-(n-1)P_p}) \end{pmatrix} \right\} \begin{pmatrix} i_{r1} \\ i_{r2} \\ \vdots \\ \vdots \\ i_{rn} \end{pmatrix} \qquad \textbf{[Eq2\_25]}$$

Where: $\boldsymbol{b = e^{j\alpha_r}}$; $\boldsymbol{\alpha_r = \frac{2\pi}{n}}$; $\boldsymbol{a = e^{j\frac{2\pi}{3}}}$

So, [**Eq2_17**] becomes:

$$\varphi_{Sp} = L_p \begin{pmatrix} i_{Sp1} \\ i_{Sp2} \\ i_{Sp3} \end{pmatrix} + \frac{M_{0p}}{2}\left\{ e^{jp_p(\theta_r+\delta)} \begin{pmatrix} 1 & b^{P_p} \dots\dots & b^{(n-1)P_p} \\ a^2(1 & b^{P_p} \dots\dots & b^{(n-1)P_p}) \\ a(1 & b^{P_p} \dots\dots & b^{(n-1)P_p}) \end{pmatrix} + e^{-jp_p(\theta_r+\delta)} \begin{pmatrix} 1 & b^{-P_p} \dots\dots & b^{-(n-1)P_p} \\ a(1 & b^{-P_p} \dots\dots & b^{-(n-1)P_p}) \\ a^2(1 & b^{-P_p} \dots\dots & b^{-(n-1)P_p}) \end{pmatrix} \right\} \begin{pmatrix} i_{r1} \\ i_{r2} \\ \vdots \\ \vdots \\ i_{rn} \end{pmatrix} \textbf{[Eq2\_26]}$$

B) Control winding equation:

For the control winding set, the stator voltage equation is expressed as:

$$v_{Sc} = R_{Sc} i_{Sc} + \frac{d\varphi_{Sc}}{dt} \qquad \textbf{[Eq2\_27]}$$

Where, $\boldsymbol{R_{sc} = [R_{sc123}]}$ is a diagonal 3× 3 matrix, in which the diagonal values depend on the resistances per phase of the control winding set, and also:

$$v_{Sc} = \begin{pmatrix} v_{Sc1} \\ v_{Sc2} \\ v_{Sc3} \end{pmatrix};\ i_{Sc} = \begin{pmatrix} i_{Sc1} \\ i_{Sc2} \\ i_{Sc3} \end{pmatrix};\ \varphi_{Sc} = \begin{pmatrix} \varphi_{Sc1} \\ \varphi_{Sc2} \\ \varphi_{Sc3} \end{pmatrix}.$$

The flux linkage can be written as the contribution of three components as:

$$\varphi_{Sc} = \varphi_{Sc}^{Sc} + \varphi_{Sp}^{Sc} + \varphi_{R}^{Sc} \qquad \textbf{[Eq2\_28]}$$

Similar to the PW analysis we that can procede for CW analysis as follows:

a) *Stator flux linkage in the control winding set due to control winding currents is:*

$$\varphi_{Sc}^{Sc} = \begin{pmatrix} L_c & 0 & 0 \\ 0 & L_c & 0 \\ 0 & 0 & L_c \end{pmatrix} \begin{pmatrix} i_{Sc1} \\ i_{Sc2} \\ i_{Sc3} \end{pmatrix} = L_c \begin{pmatrix} i_{Sc1} \\ i_{Sc2} \\ i_{Sc3} \end{pmatrix} \qquad \textbf{[Eq2\_29]}$$

Where**:** $\boldsymbol{L_c}$ is the cyclic inductance of the control winding.

b) *Stator flux linkage in the control winding set due to the power winding currents is:*

$$\varphi_{Sp}^{Sc} = 0 \qquad \textbf{[Eq2\_30]}$$

c) *Stator flux linkage in the control winding set due to the rotor currents is:*

$$\varphi_{R}^{Sc} = \frac{M_{0c}}{2}\left\{ e^{jp_c[(\theta_r+\delta)-\gamma]} \begin{pmatrix} 1 & b^{P_c} \dots\dots & b^{(n-1)P_c} \\ a^2(1 & b^{P_c} \dots\dots & b^{(n-1)P_c}) \\ a(1 & b^{P_c} \dots\dots & b^{(n-1)P_c}) \end{pmatrix} + e^{-jp_c[(\theta_r+\delta)-\gamma]} \begin{pmatrix} 1 & b^{-P_c} \dots\dots & b^{-(n-1)P_c} \\ a(1 & b^{-P_c} \dots\dots & b^{-(n-1)P_c}) \\ a^2(1 & b^{-P_c} \dots\dots & b^{-(n-1)P_c}) \end{pmatrix} \right\} \begin{pmatrix} i_{r1} \\ i_{r2} \\ \vdots \\ \vdots \\ i_{rn} \end{pmatrix} \qquad \textbf{[Eq2\_31]}$$

Where: γ mechanical angular displacement of stator control winding.

So [**Eq2_28**] becomes:

$$\varphi_{Sc} = L_c \begin{pmatrix} i_{Sc1} \\ i_{Sc2} \\ i_{Sc3} \end{pmatrix} + \frac{M_{0c}}{2}\left\{ e^{jp_c[(\theta_r+\delta)-\gamma]} \begin{pmatrix} 1 & b^{P_c} \dots\dots & b^{(n-1)P_c} \\ a^2(1 & b^{P_c} \dots\dots & b^{(n-1)P_c}) \\ a(1 & b^{P_c} \dots\dots & b^{(n-1)P_c}) \end{pmatrix} + e^{-jp_c[(\theta_r+\delta)-\gamma]} \begin{pmatrix} 1 & b^{-P_c} \dots\dots & b^{-(n-1)P_c} \\ a(1 & b^{-P_c} \dots\dots & b^{-(n-1)P_c}) \\ a^2(1 & b^{-P_c} \dots\dots & b^{-(n-1)P_c}) \end{pmatrix} \right\} \begin{pmatrix} i_{r1} \\ i_{r2} \\ \vdots \\ \vdots \\ i_{rn} \end{pmatrix} \qquad \textbf{[Eq2\_32]}$$

II.2.1.2 Rotor voltage equation:

For the power winding set, the stator voltage equation is formulated as:

$$v_R = R_R i_R + \frac{d\varphi_R}{dt} \qquad \textbf{[Eq2\_33]}$$

Where, $R_R = [R_{R1\dots n}]$ is a $\boldsymbol{n} * \boldsymbol{n}$ matrix, in which each resistance value depends on the rotor nest, and also for n-dimension rotor vector can be written as follows:

$$v_R = \begin{pmatrix} v_{R1} \\ v_{R2} \\ \vdots \\ \vdots \\ v_{Rn} \end{pmatrix};\ i_R = \begin{pmatrix} i_{r1} \\ i_{r2} \\ \vdots \\ i_{rn} \end{pmatrix};\ \varphi_R = \begin{pmatrix} \varphi_{R1} \\ \varphi_{R2} \\ \vdots \\ \varphi_{Rn} \end{pmatrix}.$$

The rotor flux can be divided into three components, one due to the rotor currents and two due to the power winding and control winding currents.

$$\varphi_R = \varphi_R^R + \varphi_{Sp}^R + \varphi_{Sc}^R \qquad \textbf{[Eq2\_34]}$$

More detailed explanations of each term will be developed separately in the following subsections.

a) flux linkage in the rotor nest due to power winding currents:

$$\varphi_{Sp}^R = \begin{pmatrix} \varphi_{Sp}^{R1} \\ \varphi_{Sp}^{R2} \\ \vdots \\ \vdots \\ \varphi_{Sp}^{Rn} \end{pmatrix} = \frac{M_{0p}}{2}\left\{ e^{jp_p(\theta_r+\delta)} \begin{pmatrix} 1 & 1 & 1 \\ b^{P_p} & b^{P_p} & b^{P_p} \\ \vdots & \vdots & \vdots \\ b^{(n-1)P_p} & b^{(n-1)P_p} & b^{(n-1)P_p} \end{pmatrix} \begin{pmatrix} i_{Sp1} \\ a^2 i_{Sp2} \\ a i_{Sp3} \end{pmatrix} + e^{-jp_p(\theta_r+\delta)} \begin{pmatrix} 1 & 1 & 1 \\ b^{-P_p} & b^{-P_p} & b^{-P_p} \\ \vdots & \vdots & \vdots \\ b^{-(n-1)P_p} & b^{-(n-1)P_p} & b^{-(n-1)P_p} \end{pmatrix} \begin{pmatrix} i_{Sp1} \\ a i_{Sp2} \\ a^2 i_{Sp3} \end{pmatrix} \right\} \qquad \textbf{[Eq2\_35]}$$

b) flux linkage in the rotor nest due to control winding currents:

$$\varphi_{Sc}^R = \begin{pmatrix} \varphi_{Sc}^{R1} \\ \varphi_{Sc}^{R2} \\ \vdots \\ \vdots \\ \varphi_{Sc}^{Rn} \end{pmatrix} = \frac{M_{0c}}{2}\left\{ e^{jp_c[(\theta_r+\delta)-\gamma]} \begin{pmatrix} 1 & 1 & 1 \\ b^{P_c} & b^{P_c} & b^{P_c} \\ \vdots & \vdots & \vdots \\ b^{(n-1)P_c} & b^{(n-1)P_c} & b^{(n-1)P_c} \end{pmatrix} \begin{pmatrix} i_{Sc1} \\ a^2 i_{Sc2} \\ a i_{Sc3} \end{pmatrix} + e^{-jp_c[(\theta_r+\delta)-\gamma]} \begin{pmatrix} 1 & 1 & 1 \\ b^{-P_c} & b^{-P_c} & b^{-P_c} \\ \vdots & \vdots & \vdots \\ b^{-(n-1)P_c} & b^{-(n-1)P_c} & b^{-(n-1)P_c} \end{pmatrix} \begin{pmatrix} i_{Sc1} \\ a i_{Sc2} \\ a^2 i_{Sc3} \end{pmatrix} \right\}$$

[Eq2_36]

c) Rotor flux linkage in the rotor nest due to rotor nest currents:

The total flux linked by the $\boldsymbol{K_{th}}$ rotor nests and due only to the rotor currents is given by

$$\varphi_{Rk}^R = M_{k1} i_{r1} + M_{k2} i_{r2} + \ \ldots\ldots\ldots + M_{kk} i_{rk} + \ \ldots\ldots\ldots\ldots + M_{kn} i_{rn} \qquad \textbf{[Eq2\_37]}$$

Where$\boldsymbol{M_{ki}}$; represents the mutual magnetic coupling between rotor nests $\boldsymbol{k}$ and $\boldsymbol{i}$, and $\boldsymbol{M_{kk}}$ is the self inductance of the $\boldsymbol{K_{th}}$ nest.

Because of the structural symmetry of the rotor, [**Eq2_37**] is valid for every nest. Hence, $\boldsymbol{\varphi_R^R}$ can be rewritten in matrix form as:

$$\varphi_{\mathrm{R}}^{\mathrm{R}} = \begin{pmatrix} \varphi_{R1}^R \\ \varphi_{R2}^R \\ \vdots \\ \cdots \\ \varphi_{Rn}^R \end{pmatrix} = \begin{pmatrix} M_{11} & M_{12} \ldots\ldots & M_{1n} \\ M_{21} & M_{22} \ldots\ldots & M_{2n} \\ \vdots & \cdots \ \ldots\ldots\ldots & \vdots \\ M_{n1} & \cdots \ \ \ldots \ \ \ldots & M_{nn} \end{pmatrix} \begin{pmatrix} i_{r1} \\ i_{r2} \\ \vdots \\ i_{rn} \end{pmatrix} \qquad \textbf{[Eq2\_38]}$$

Therefore, [**Eq2_34**] becomes:

$$\varphi_R = \frac{M_{0p}}{2}\left\{ e^{jp_p(\theta_r+\delta)}\begin{pmatrix} 1 & 1 & 1 \\ b^{P_p} & b^{P_p} & b^{P_p} \\ \vdots & \vdots & \vdots \\ b^{(n-1)P_p} & b^{(n-1)P_p} & b^{(n-1)P_p} \end{pmatrix}\begin{pmatrix} i_{Sp1} \\ a^2 i_{Sp2} \\ a i_{Sp3} \end{pmatrix} + e^{-jp_p(\theta_r+\delta)}\begin{pmatrix} 1 & 1 & 1 \\ b^{-P_p} & b^{-P_p} & b^{-P_p} \\ \vdots & \vdots & \vdots \\ b^{-(n-1)P_p} & b^{-(n-1)P_p} & b^{-(n-1)p_p} \end{pmatrix}\begin{pmatrix} i_{Sp1} \\ a i_{Sp2} \\ a^2 i_{Sp3} \end{pmatrix}\right\} +$$

$$+\frac{M_{0c}}{2}\left\{ e^{jp_c[(\theta_r+\delta)-\gamma]}\begin{pmatrix} 1 & 1 & 1 \\ b^{P_c} & b^{P_c} & b^{P_c} \\ \vdots & \vdots & \vdots \\ b^{(n-1)P_c} & b^{(n-1)P_c} & b^{(n-1)P_c} \end{pmatrix}\begin{pmatrix} i_{Sc1} \\ a^2 i_{Sc2} \\ a i_{Sc3} \end{pmatrix} + e^{-jp_c[(\theta_r+\delta)-\gamma]}\begin{pmatrix} 1 & 1 & 1 \\ b^{-P_c} & b^{-P_c} & b^{-P_c} \\ \vdots & \vdots & \vdots \\ b^{-(n-1)P_c} & b^{-(n-1)P_c} & b^{-(n-1)P_c} \end{pmatrix}\begin{pmatrix} i_{Sc1} \\ a i_{Sc2} \\ a^2 i_{Sc3} \end{pmatrix}\right\} +$$

$$\begin{pmatrix} M_{11} & M_{12} \dots\dots & M_{1n} \\ M_{21} & M_{22} \dots\dots & M_{2n} \\ \vdots & \cdots \quad \dots\dots & \vdots \\ M_{n1} & \cdots \quad \dots \quad \dots & M_{nn} \end{pmatrix}\begin{pmatrix} i_{r1} \\ i_{r2} \\ \vdots \\ i_{rn} \end{pmatrix} \qquad \textbf{[Eq2\_39]}$$

II.2.2 Variables expressed in space vector:

The previous system equations [**Eq2_26**], [**Eq2_32**] and [**Eq2_39**]are formed by $\boldsymbol{n+6}$ equations and $\boldsymbol{n+6}$ unknown variables.

Now we will try to simplify this complex system by representing the variables of stator and rotor by vectorial form, so called space vector modeling inspired by professor Lipo. This method was used by A.R. Munoz and T.A. Lipo in [MUÑ-99] for dynamic modeling of induction machines without cage equivalent circuit for the rotor and taking into account the exact form of the rotor cage, and considering the physical positions of the coils. We can get the resulting space vector by expressing the temporal components of each phase as follows,

$$\vec{x} = \frac{2}{Kn}\left[x_1 + x_2\, e^{jP_i\alpha_2} + x_3\, e^{jP_i\alpha_3} \ \dots\dots + x_n\, e^{jP_i\alpha_n}\right] \qquad \textbf{[Eq2\_40]}$$

Where:

$\frac{\boldsymbol{2}}{\boldsymbol{n}}$: **A**mplitude conservation factor

p_i: Number of the space harmonic

α_i : Mechanical angle between coil $\boldsymbol{i}$ and coil 1

K: Arbitrary transformation ratio that modifies the amplitude of the vectors or normalizing gain. Note that $K = 1$ represents the similar assertion in Clarke three phases conform transformation. In similar case, the three phase's space vector (n=3) can be expressed as:

$$\vec{x} = \frac{2}{3}\left[x_1 + a x_2 + a^2 x_3\right] \qquad \textbf{[Eq2\_41]}$$

Where: $\boldsymbol{a = e^{j\frac{2\pi}{3}}}$

II.2.2.1 Voltage equations for the BDFM expressed in space vectors:

A) Stator voltage equation expressed in space vector

a) *Resistive voltage drops:*

In matrix form, the copper voltage drop successively of power (index, *sp*) and control (index, *sc*) windings may be done as followed (multiplying the second and third lines by $\boldsymbol{a}$ and $\boldsymbol{a^2}$, respectively):

$$\vec{V}_{R(sp,sc)} = \begin{pmatrix} v_{R(sp,sc)1} \\ av_{R(sp,sc)2} \\ a^2 v_{R(\,p,sc)3} \end{pmatrix} = \begin{pmatrix} R_{sp,sc} & 0 & 0 \\ 0 & R_{sp,sc} & 0 \\ 0 & 0 & R_{sp,sc} \end{pmatrix} \begin{pmatrix} i_{(sp,sc)1} \\ ai_{(sp,sc)2} \\ a^2 i_{(sp,sc)3} \end{pmatrix} = R_{sp,sc} \begin{pmatrix} i_{(sp,sc)1} \\ ai_{(sp,sc)2} \\ a^2 i_{(sp,sc)3} \end{pmatrix} \quad \textbf{[Eq2\_42]}$$

So,

$$\vec{V}_{R(sp,sc)} = R_{sp,sc}\vec{i}_{sp,sc} \quad \textbf{[Eq2\_43]}$$

[**Eq2_42**], performed as the equivalent resistance for the stator windings equal to the single resistance phase. This result may be generalized in such a way that the equivalent resistance of the rotor matches to the single equivalent value resistance nest [POZ-03].

b) <u>Flux linkage in power winding set :</u>

From [**Eq2_26**], after multiplying each component of PW stator flux successively by $(1, a, a^2)$, we can get:

$$\begin{pmatrix} \varphi_{Sp1} \\ a\varphi_{Sp2} \\ a^2\varphi_{Sp3} \end{pmatrix} = L_p \begin{pmatrix} i_{Sp1} \\ ai_{Sp2} \\ a^2 i_{Sp3} \end{pmatrix} + \frac{M_{0p}}{2} \left\{ e^{jp_p(\theta_r+\delta)} \begin{pmatrix} 1 & b^{P_p} \dots\dots & b^{(n-1)P_p} \\ 1 & b^{P_p} \dots\dots & b^{(n-1)P_p} \\ 1 & b^{P_p} \dots\dots & b^{(n-1)P_p} \end{pmatrix} + e^{-jp_p(\theta_r+\delta)} \begin{pmatrix} 1 & b^{-P_p} \dots\dots & b^{-(n-1)P_p} \\ a^2(1 & b^{-P_p} \dots\dots & b^{-(n-1)P_p}) \\ a(1 & b^{-P_p} \dots\dots & b^{-(n-1)P_p}) \end{pmatrix} \right\} \begin{pmatrix} i_{\_1} \\ i_{r2} \\ \vdots \\ \vdots \\ i_{rn} \end{pmatrix} \quad \textbf{[Eq2\_44]}$$

Therefore, that is leads to

$$\frac{3}{2}\overrightarrow{\varphi_{Sp}} = L_p\left(i_{Sp1} + ai_{Sp2} + a^2 i_{Sp3}\right) + \frac{M_{0p}}{2}\left\{ e^{jp_p(\theta_r+\delta)} 3(1, b^{P_p}, \dots, b^{(n-1)P_p}) + e^{-jp_p(\theta_r+\delta)}(1 + a^2 + a)(1, b^{-P_p}, \dots, b^{-(n-1)P_p}) \right\} \begin{pmatrix} i_{r1} \\ i_{r2} \\ \vdots \\ \vdots \\ i_{rn} \end{pmatrix}$$

[Eq2_45]

Since $(1 + a + a^2 = 0)$, **[Eq2_46]**

then [**Eq2_45**] is rewritten as

$$\frac{3}{2}\vec{\varphi}_{sp} = \frac{3}{2}L_p\vec{i}_{sp} + \frac{3}{2}\,M_{0p}\left\{ e^{jp_p(\theta_r+\delta)}(i_{r1} + i_{r2}b^{P_p} + \cdots + i_{rn}b^{(n-1)P_p}) \right\} \quad \textbf{[Eq2\_47]}$$

So, [**Eq2_47**] becomes

$$\vec{\varphi}_{sp} = L_p\vec{i}_{sp} + K\frac{n}{2}\,M_{0p}\,e^{jp_p(\theta_r+\delta)}\,\vec{i}_R^{\,xyp} \quad \textbf{[Eq2\_48]}$$

Where,

$$\vec{i}_R^{\,xyp} = \frac{2}{Kn}(i_{r1} + i_{r2}b^{P_p} + \cdots + i_{rn}\,b^{(n-1)P_p}) \quad \textbf{[Eq2\_49]}$$

As a result, the power winding voltage equation may be done as

$$\begin{cases}\vec{V}_{sp} = R_{sp}\vec{i}_{sp} + \dfrac{d\vec{\varphi}_{sp}}{dt} \\ \vec{\varphi}_{sp} = L_p\vec{i}_{sp} + K\dfrac{n}{2}\,M_{0p}\,e^{jp_p(\theta_r+\delta)}\,\vec{i}_R^{\,xyp}\end{cases} \qquad \textbf{[Eq2\_50]}$$

c) Flux linkage in control winding set :

As in the case of the stator PW we can also obtain the same formulation for **[Eq2_32]**, as followed

$$\begin{pmatrix}\varphi_{Sc1}\\ a\varphi_{Sc2}\\ a^2\varphi_{Sc3}\end{pmatrix} = L_c\begin{pmatrix}i_{Sc1}\\ ai_{Sc2}\\ a^2i_{Sc3}\end{pmatrix} + \frac{M_{0c}}{2}\left\{ e^{jp_c[(\theta_r+\delta)-\gamma]}\begin{pmatrix}1 & b^{P_c} \dots\dots & b^{(n-1)P_c}\\ 1 & b^{P_c} \dots\dots & b^{(n-1)P_c}\\ 1 & b^{P_c} \dots\dots & b^{(n-1)P_c}\end{pmatrix} + e^{-jp_c[(\theta_r+\delta)-\gamma]}\begin{pmatrix}1 & b^{-P_c} \dots\dots & b^{-(n-1)P_c}\\ a^2(1 & b^{-P_c} \dots\dots & b^{-(n-1)P_c})\\ a(1 & b^{-P_c} \dots\dots & b^{-(n-1)P_c})\end{pmatrix}\right\}\begin{pmatrix}i_{r1}\\ i_{r2}\\ \vdots\\ \vdots\\ i_{rn}\end{pmatrix}$$

[Eq2_51]

And therefore,

$$\vec{\varphi}_{sc} = L_c\vec{i}_{sc} + K\frac{n}{2}M_{0c}\,e^{jp_c[(\theta_r+\delta)-\gamma]}\vec{i}_R^{\,xyc} \qquad \textbf{[Eq2\_52]}$$

Where, $\vec{i}_R^{\,xyc} = \dfrac{2}{kn}\,(i_{r1} + i_{r2}b^{P_c} + \cdots + i_{rn}b^{(n-1)P_c})$ **[Eq2_53]**

So, the control winding stator voltage equation becomes

$$\begin{cases}\vec{V}_{sc} = R_{sc}\vec{i}_{sc} + \dfrac{d\vec{\varphi}_{sc}}{dt} \\ \vec{\varphi}_{sc} = L_c\vec{i}_{sc} + K\dfrac{n}{2}M_{0c}\,e^{jp_c[(\theta_r+\delta)-\gamma]}\vec{i}_R^{\,xyc}\end{cases} \qquad \textbf{[Eq2\_54]}$$

B) Rotor voltage equation expressed in space vector

a) Flux linkage in rotor nests due to the rotor nests current :

Multiplying **[Eq2_38]** by $(\mathbf{1}, \boldsymbol{b^{P_p}}, \dots, \boldsymbol{b^{(n-1)P_p}})$ yields to the following serial equations

$$\left(1, b^{P_p}, b^{2P_p}, \dots, b^{(n-1)P_p}\right)\begin{pmatrix}\varphi_{R1}^R\\ \varphi_{R2}^R\\ \varphi_{R3}^R\\ \vdots\\ \vdots\\ \vdots\\ \varphi_{Rn}^R\end{pmatrix} = \left(1, b^{P_p}, b^{2P_p}, \dots, b^{(n-1)P_p}\right)\begin{pmatrix}M_{11} & M_{12} & M_{13} & \vdots & \vdots & \vdots & M_{1n}\\ M_{21} & M_{22} & M_{23} & \vdots & \vdots & \vdots & M_{2n}\\ M_{31} & M_{32} & M_{33} & \vdots & \vdots & \vdots & M_{3n}\\ \vdots & \vdots & \vdots & \vdots & \vdots & \vdots & \vdots\\ \vdots & \vdots & \vdots & \vdots & \vdots & \vdots & \vdots\\ \vdots & \vdots & \vdots & \vdots & \vdots & \vdots & \vdots\\ M_{n1} & M_{n2} & M_{n3} & \vdots & \vdots & \vdots & M_{nn}\end{pmatrix}\begin{pmatrix}i_{r1}\\ i_{r2}\\ i_{r3}\\ \vdots\\ \vdots\\ \vdots\\ i_{rn}\end{pmatrix} \qquad \textbf{[Eq2\_55]}$$

$$\begin{pmatrix}\varphi_{R1}^R\\ b^{P_p}\varphi_{R2}^R\\ b^{2P_p}\varphi_{R3}^R\\ \vdots\\ \vdots\\ \vdots\\ b^{(n-1)P_p}\varphi_{Rn}^R\end{pmatrix} = \left\{\left(1, b^{P_p}, b^{2P_p}, \dots, b^{(n-1)P_p}\right)\begin{pmatrix}M_{11}\\ M_{21}\\ M_{31}\\ \vdots\\ \vdots\\ \vdots\\ M_{n1}\end{pmatrix}; \left(1, b^{P_p}, b^{2P_p}, \dots, b^{(n-1)P_p}\right)\begin{pmatrix}M_{12}\\ M_{22}\\ M_{32}\\ \vdots\\ \vdots\\ \vdots\\ M_{n2}\end{pmatrix}; \dots\dots\dots; \left(1, b^{P_p}, \text{?}^{2P_p}, \dots, b^{(n-1)P_p}\right)\begin{pmatrix}M_{1n}\\ M_{2n}\\ M_{3n}\\ \vdots\\ \vdots\\ \vdots\\ M_{nn}\end{pmatrix}\right\}\begin{pmatrix}i_{r1}\\ i_{r2}\\ i_{r3}\\ \vdots\\ \vdots\\ \vdots\\ i_{rn}\end{pmatrix} =$$

$$\left\{\left(1, b^{P_p}, b^{2P_p}, \dots, b^{(n-1)P_p}\right)\begin{pmatrix}M_{11}\\ M_{21}\\ M_{31}\\ \vdots\\ \vdots\\ \vdots\\ M_{\text{?}1}\end{pmatrix}; b^{P_p}\left(\text{?}^{-P_p}, 1, b^{P_p}, \dots, b^{(n-2)P_p}\right)\begin{pmatrix}M_{12}\\ M_{22}\\ M_{32}\\ \vdots\\ \vdots\\ \vdots\\ M_{n2}\end{pmatrix}; \dots\dots\dots; b^{(n-1)P_p}\left(b^{-(n-1)P_p}, b^{-(n-2)P_p}, b^{-(n-3)P_p}, \dots, b^{-P_p}, 1\right)\begin{pmatrix}M_{1n}\\ M_{2n}\\ M_{3n}\\ \vdots\\ \vdots\\ \vdots\\ M_{nn}\end{pmatrix}\right\}\begin{pmatrix}i_{r1}\\ i_{r2}\\ i_{r3}\\ \vdots\\ \vdots\\ \vdots\\ i_{rn}\end{pmatrix}$$

Using the identity formulation $\boxed{\boldsymbol{b^{(n+m)P_p} = b^{mP_p}}}$, we can get

$$\left(1, b^{P_p}, b^{2P_p}, \dots, b^{(n-1)P_p}\right)\begin{pmatrix} M_{11} \\ M_{21} \\ M_{31} \\ \vdots \\ \vdots \\ \vdots \\ M_{n1} \end{pmatrix} = \left(b^{-P_p}, 1, b^{P_p}, \dots, b^{(n-2)P_p}\right)\begin{pmatrix} M_{12} \\ M_{22} \\ M_{32} \\ \vdots \\ \vdots \\ \vdots \\ M_{n2} \end{pmatrix} = \cdots \dots \dots \dots . = \left(b^{-(n-1)P_p}, b^{-(n-2)P_p}, b^{-(n-3)P_p}, \dots, b^{-P_p}, 1\right)\begin{pmatrix} M_{1n} \\ M_{2n} \\ M_{3n} \\ \vdots \\ \vdots \\ \vdots \\ M_{nn} \end{pmatrix}$$

So,

$$\begin{pmatrix} \varphi_{R1}^{R} \\ b^{P_p}\varphi_{R2}^{R} \\ b^{2P_p}\varphi_{R3}^{R} \\ \vdots \\ \vdots \\ \vdots \\ b^{(n-1)P_p}\varphi_{Rn}^{R} \end{pmatrix} = \left(1, b^{P_p}, b^{2P_p}, \dots, b^{(n-1)P_p}\right)\begin{pmatrix} M_{11} \\ M_{21} \\ M_{31} \\ \vdots \\ \vdots \\ \vdots \\ M_{n1} \end{pmatrix}\left\{\left(1, b^{P_p}, b^{2P_p}, \dots, b^{(n-1)P_p}\right)\begin{pmatrix} i_{r1} \\ i_{r2} \\ i_{r3} \\ \vdots \\ \vdots \\ \vdots \\ i_{r\,nr} \end{pmatrix}\right\} \qquad \textbf{[Eq2\_56]}$$

And therefore,

$$\Rightarrow \vec{\varphi}_R^R = L_r \vec{i}_R^{\,xy_p} \qquad \textbf{[Eq2\_5〈]}$$

With, $L_r = \left(1, b^{P_p}, b^{2P_p}, \dots, b^{(n-1)P_p}\right)\begin{pmatrix} M_{11} \\ M_{21} \\ M_{31} \\ \vdots \\ \vdots \\ \vdots \\ M_{n1} \end{pmatrix} = M_{11} + b^{P_p}M_{12} + b^{2P_p}M_{13} + \cdots + b^{(n-1)P_p}M_{1n}$

The proportionality constant L_r corresponds on the equivalent rotor self inductance. Note that its value is expressed only in terms of rotor nest's dimension.

b) <u>flux linkage in rotor nests due to the power winding current:</u>

From **[Eq2_35],** after multiplying each component of rotor flux successively by $\left(1, b^{P_p}, b^{2P_p}, \dots, b^{(n-1)P_p}\right)$, we can get:

$$\begin{pmatrix} \varphi_{Sp}^{R1} \\ b^{P_p}\varphi_{Sp}^{R2} \\ \vdots \\ \vdots \\ b^{(n-1)P_p}\varphi_{Sp}^{Rn} \end{pmatrix} = \frac{M_{0p}}{2}\left\{ e^{jp_p(\theta_r+\delta)}\begin{pmatrix} 1 & 1 & 1 \\ b^{2P_p} & b^{2P_p} & b^{2P_p} \\ \vdots & \vdots & \vdots \\ b^{2(n-1)P_p} & b^{2(n-1)P_p} & b^{2(n-1)P_p} \end{pmatrix}\begin{pmatrix} i_{Sp1} \\ a^2 i_{Sp2} \\ a i_{Sp3} \end{pmatrix} + e^{-jp_p(\theta_r+\delta)}\begin{pmatrix} 1 & 1 & 1 \\ 1 & 1 & 1 \\ \vdots & \vdots & \vdots \\ 1 & 1 & 1 \end{pmatrix}\begin{pmatrix} i_{Sp1} \\ a i_{Sp2} \\ a^2 i_{Sp3} \end{pmatrix}\right\} \textbf{[Eq2\_58]}$$

With $\boldsymbol{\left(1 + b^{2P_p} + \cdots + b^{2(n-1)P_p} = 0\right)}$**, t**he rotor nests flux linkage due to the power winding current becoms:

$$\vec{\varphi}_{Sp}^{R} = \frac{3}{2}\frac{M_{0p}}{K}e^{-jp_p(\theta_r+\delta)}\,\vec{i}_{sp}^{\,\alpha\beta p} \qquad \textbf{[Eq2\_59]}$$

c) Flux linkage in rotor nests due to control winding current:

This term represents the rotor nest's flux vector of $p_p$pole-pairs distribution produced by the control winding current of p_c pole-pairs distribution. The calculation of this magnetic coupling effect is vital to determine the machine operation, since its existence produces a ***cross coupling*** being well indicated by *Fig II.3***,** between both stator windings through the rotor. Once the ***cross coupling*** is produced, the current of each stator winding will not solely depend on its own supply voltage, but it will also vary according to the voltage of the other stator winding. On the other hand, if the ***cross coupling*** does not produce, the electrical machine would operate like two independent asynchronous machines with the same axis.

From [**Eq2_36**]**,** after multiplying each component of rotor flux successively by $\left(1, b^{P_p}, b^{2P_p}, \dots, b^{(n-1)P_p}\right)$, which defines the ***cross coupling,*** we can obtain

$$\begin{pmatrix} \varphi_{Sc}^{R1} \\ b^{P_p}\varphi_{Sc}^{R2} \\ \vdots \\ \vdots \\ b^{(n-1)P_p}\varphi_{Sc}^{Rn} \end{pmatrix} = \frac{M_{0c}}{2}\left\{ e^{jp_c[(\theta_r+\delta)-\gamma]} \begin{pmatrix} 1 & 1 & 1 \\ b^{P_p+P_c} & \vdots & \vdots \\ \vdots & b^{(n-1)(P_p+P_c)} & b^{(n-1)(P_p+P_c)} \\ b^{(n-1)(P_p+P_c)} & & \end{pmatrix} \begin{pmatrix} i_{Sc1} \\ a^2 i_{Sc2} \\ a i_{Sc3} \end{pmatrix} + e^{-jp_c[(\theta_r+\delta)-\gamma]} \begin{pmatrix} 1 & 1 & 1 \\ b^{P_p-P_c} & \vdots & \vdots \\ \vdots & b^{(n-1)(P_p-P_c)} & b^{(n-1)(P_p-P_c)} \\ b^{(n-1)(P_p-P_c)} & & \end{pmatrix} \begin{pmatrix} i_{Sc1} \\ a i_{Sc2} \\ a^2 i_{Sc3} \end{pmatrix} \right\}$$

[**Eq2_60**]

As shown in [**Eq2_60**], the rotor flux vector due to CW currents depends on the selected values of $\boldsymbol{p_p}$ and $\boldsymbol{p_c}$pole-pairs. By analyzing different combinations, there are two possible cases:

Possibility 1:

$\vec{\boldsymbol{\varphi}}_{\boldsymbol{Sc}}^{\boldsymbol{R}} = \boldsymbol{0} \Longrightarrow \boldsymbol{b}^{(\boldsymbol{P_p}+\boldsymbol{P_c})}$ & $\boldsymbol{b}^{(\boldsymbol{P_p}-\boldsymbol{P_c})} \neq \boldsymbol{1} \Longrightarrow$ Inexistence of a ***cross coupling*** between the both stator windings through the rotor current.

Possibility 2:

$\vec{\boldsymbol{\varphi}}_{\boldsymbol{Sc}}^{\boldsymbol{R}} \neq \boldsymbol{0} \Longrightarrow \boldsymbol{b}^{(\boldsymbol{P_p}+\boldsymbol{P_c})}$ *or* $\boldsymbol{b}^{(\boldsymbol{P_p}-\boldsymbol{P_c})} = \boldsymbol{1} \Longrightarrow$ The existence of a ***cross coupling*** between the two stator windings through the rotor current. There are two possible configurations:

- ✓ *configuration* 1: $\boldsymbol{b}^{(\boldsymbol{P_p}-\boldsymbol{P_c})} = \boldsymbol{e}^{\boldsymbol{j}\frac{\boldsymbol{2\pi}}{\boldsymbol{n}}(\boldsymbol{P_p}-\boldsymbol{P_c})} = \boldsymbol{1} \Longrightarrow \boxed{\boldsymbol{n} = \frac{(\boldsymbol{P_p}-\boldsymbol{P_c})}{\boldsymbol{q}}}$ [**Eq2_61**]
- ✓ *configuration* 2: $\boldsymbol{b}^{(\boldsymbol{P_p}+\boldsymbol{P_c})} = \boldsymbol{e}^{\boldsymbol{j}\frac{\boldsymbol{2\pi}}{\boldsymbol{n}}(\boldsymbol{P_p}+\boldsymbol{P_c})} = \boldsymbol{1} \Longrightarrow \boxed{\boldsymbol{n} = \frac{(\boldsymbol{P_p}+\boldsymbol{P_c})}{\boldsymbol{q}}}$ [**Eq2_62**]

Where, $\boldsymbol{q} = \boldsymbol{0}, \pm\boldsymbol{1}, \pm\boldsymbol{2} \dots\dots\dots\dots\dots$

In this way, we have the same ***cross coupling*** conditions which were obtained in equations[**Eq2_9**] and [**Eq2_12**]**.** So, to ensure this ***cross coupling*** effect, we should chose the second configuration [**Eq2_62**] which maximizes the number of rotor nest's i.e $(\boldsymbol{q} = \boldsymbol{1})$**.** So, $\boldsymbol{n} = \boldsymbol{p_p} + \boldsymbol{p_c}$ impling that

$$\vec{i}_R^{\,xyp} = \frac{2}{kn}(i_{r1} + i_{r2}b^{P_p} + \cdots + i_{rn}b^{(n-1)P_p}) \quad \textbf{[Eq2\_63]}$$

$$\boldsymbol{p_p = n - p_c} \Longrightarrow$$

$$\begin{aligned}\vec{i}_R^{\,xy_P} &= \frac{2}{kn}\left(i_{r1} + i_{r2}b^{n-P_c} + \cdots + i_{rn}b^{(n-1)(n-P_c)}\right)\\ &= \frac{2}{kn}\left(i_{r1} + i_{r2}b^{-P_c} + \cdots + i_{rn}b^{(n-1)(-P_c)}\right)\\ &= \vec{i}_R^{\,*xy_c}\end{aligned}$$

So,

$$\boxed{\vec{i}_R^{\,xy_P} = \vec{i}_R^{\,*xy_c}} \quad \textbf{[Eq2\_64]}$$

So we conclude that, in last configuration, one of the current vectors behaves as the conjugate of the other. According to this relation, it becomes straightforward to change from a $p_p - type$ reference frame to a $p_c - type$ one or vice versa. This one constitutes the key step for the derivation of the unified $\boldsymbol{dq}$ reference frame model.

Replacing with $\boldsymbol{n = p_p + p_c}$ in [**Eq2_60**], yields to

$$\begin{pmatrix} \varphi_{Sc}^{R1} \\ b^{P_p}\,\mathcal{LL}_{Sc}^{R2} \\ \vdots \\ \vdots \\ b^{(n-1)P_p}\varphi_{Sc}^{Rn} \end{pmatrix} = \frac{M_{0c}}{2}\left\{ e^{jp_c[(\theta_r+\delta)-\gamma]} \begin{pmatrix} 1 & 1 & 1 \\ 1 & 1 & 1 \\ \vdots & \vdots & \vdots \\ 1 & 1 & 1 \end{pmatrix} \begin{pmatrix} i_{Sc1} \\ a^2 i_{Sc2} \\ a i_{Sc3} \end{pmatrix} \right\} \quad \textbf{[Eq2\_65]}$$

And so, $\vec{\varphi}_{Sc}^{R} = \frac{\mathbf{3}}{\mathbf{2}}\frac{M_{0c}}{\boldsymbol{K}}\, e^{jp_c[(\theta_r+\delta)-\gamma]}\, \vec{i}_{sc}^{\,*\alpha\beta c}$ **[Eq2_66]**

With, $\vec{i}_{sc}^{\,*\alpha\beta c} = (i_{Sc1} + a^2 i_{Sc2} + a i_{Sc3}) = (i_{Sc1} + a^{-1} i_{Sc2} + a^{-2}\,\mathcal{L}_{Sc3})$

So the rotor nest's voltage equation is given by

$$\boxed{\begin{cases} \vec{V}_R = R_r\vec{i}_R + \frac{d\vec{\varphi}_R}{dt} \\ \vec{\varphi}_R = L_r\vec{i}_R + \frac{3}{2}\frac{M_{0p}}{K}e^{-jp_p(\theta_r+\delta)}\,\vec{i}_{sp}^{\,\alpha\beta p} + \frac{3}{2}\frac{M_{0c}}{K}\, e^{jp_c[(\theta_r+\delta)-\gamma]}\,\vec{i}_{sc}^{\,*\alpha\beta c} \end{cases}} \quad \textbf{[Eq2\_67]}$$

In [**Eq2_50**], [**Eq2_54**] and [**Eq2_67**], in order to obtain the same equivalent mutual inductance from rotor to stator as from stator to rotor, the following constraint must be fulfilled:

$$K\frac{n}{2}M_{0(p,c)} = \frac{3}{2}\frac{M_{0(p,c)}}{K} \quad \textbf{[Eq2\_68]}$$

The normalizing gain is identified as

$$\boldsymbol{K = \sqrt{\frac{3}{n}}} \quad \textbf{[Eq2\_69]}$$

Taking into account the obtained value from [**Eq2_69**], we can write the equations system from [**Eq2_50**], [**Eq2_54**] and [**Eq2_67**] as follows:

$$\begin{cases} \vec{V}_{sp} = R_{sp}\vec{\imath}_{sp} + \frac{d\vec{\varphi}_{sp}}{dt} \\ \vec{\varphi}_{sp} = L_p\vec{\imath}_{sp} + M_p\, e^{jp_p(\theta_r+\delta)}\vec{\imath}_R \\ \vec{V}_{sc} = R_{sc}\vec{\imath}_{sc} + \frac{d\vec{\varphi}_{sc}}{dt} \\ \vec{\varphi}_{sc} = L_c\vec{\imath}_{sc} + M_c\, e^{jp_c[(\theta_r+\delta)-\gamma]}\ \vec{\imath}^{\,*}_R \\ \vec{V}_r = R_r\vec{\imath}_R + \frac{d\vec{\varphi}_r}{dt} \\ \vec{\varphi}_r = L_r\vec{\imath}_R + M_p e^{-jp_p(\theta_r+\delta)}\,\vec{\imath}_{sp} + M_c\, e^{jp_c[(\theta_r+\delta)-\gamma]}\,\vec{\imath}^{\,*}_{sc} \end{cases} \quad \textbf{[Eq2\_70]}$$

The system defined by [**Eq2_70**] is given in assuming that the following lightening nomenclature:

$\vec{\imath}_{sp} \equiv \vec{\imath}_{sp}^{\alpha\beta p}$: Power winding reference frame in a $\boldsymbol{p_p}$ pole-pairs distribution

$\vec{\imath}_{sc} \equiv \vec{\imath}_{sc}^{\alpha\beta c}$: Control winding reference frame in a $\boldsymbol{p_c}$ pole-pairs distribution.

$\vec{\imath}_R \equiv \vec{\imath}_R^{\,xy_p}$: Rotor references related to $\boldsymbol{p_p}, \boldsymbol{p_c}$ pole-pairs distribution.

With, $M_{p,c} = \frac{\sqrt{3n}}{2} M_{0(p,c)}$ **[Eq2_71]**

II.2.3 Unified reference frame model of the BDFM:

As it can be observed the initial set of [**Eq2_70**] is referred to three different frames and tow possible pole-pairs distributions may be considered. The goal is to get a set of equations with a unified reference frame with a given pole-pairs distribution (e.g. $\boldsymbol{p_p}$) located at an arbitrary mechanical position $\left(\frac{\boldsymbol{\theta_{obsp}}}{\boldsymbol{p_p}}\right)$ in $\boldsymbol{\alpha\beta_p}$ reference frame. This is easily achieved if we followed the steps given in appendix B. First, the transformation relationship between $\boldsymbol{\alpha\beta_p}$ and $\boldsymbol{\alpha\beta_c}$ systems is developed. Next, we can define a generic dq reference frame with a $\boldsymbol{p_p}$ pole-pair distribution and located at any mechanical position $\left(\frac{\boldsymbol{\theta_{obsp}}}{\boldsymbol{P_p}}\right)$ in $\boldsymbol{\alpha\beta_p}$.

Vector transformations from original reference frames to generic $\boldsymbol{dq_p}$ reference frame are obtained. Finally by means of these vector transformations the machine model [**Eq2_70**] is expressed in a common ***dq***-generic reference frame where ***dq*** symbol indices have been removed to simplify resulting expressions which are given as follows

$$\vec{V}_p = R_p\,\vec{\imath}_p + \frac{d\,\vec{\varphi}_p}{dt} + j\omega_{obsp}\vec{\varphi}_p \quad \textbf{[Eq2\_72]}$$

$$\vec{\varphi}_p = L_p\vec{\imath}_p + M_p\,\vec{\imath}_r \quad \textbf{[Eq2\_73]}$$

$$\vec{V}_c = R_c\vec{i}_c + \frac{d\vec{\varphi}_c}{dt} + j[\omega_{obsp} - (p_p + p_c)\Omega]\vec{\varphi}_c \quad \textbf{[Eq2\_74]}$$

$$\vec{\varphi}_c = L_c\vec{i}_c + M_c\vec{i}_r \quad \textbf{[Eq2\_75]}$$

$$\vec{V}_r = R_r\vec{i}_r + \frac{d\vec{\varphi}_r}{dt} + j[\omega_{obsp} - p_p\Omega]\vec{\varphi}_r \quad \textbf{[Eq2\_76]}$$

$$\vec{\varphi}_r = L_r\vec{i}_r + M_p\vec{i}_p + M_c\vec{i}_c \quad \textbf{[Eq2\_77]}$$

This model is similar to the vector model of the induction machine in presence of two stator winding. The expressions related to stator power winding are the same as that of the induction machine. In rotor flux equation, the influence of the two stator currents is well represented. In stator control winding, the factor $[\boldsymbol{\omega_{obs_p}} - (\boldsymbol{p_p} + \boldsymbol{p_c})\boldsymbol{\Omega}]$ characterizes the relative angular velocity between the reference frames $\boldsymbol{dq}$ and $\boldsymbol{\alpha\beta_p}$ [POZ-06].

The vector transformation from generic $\boldsymbol{dq_p}$ reference frame rotating at the speed of $\boldsymbol{\omega_{obs_p}}$ to the $\boldsymbol{dq_c}$ reference frame rotating at the speed of $\boldsymbol{\omega_{obs_c}}$ as follows (see Appendix B):

$$\vec{x}^{dq_p} = \vec{x}^{dq_p}{}^{*}_{.}\, e^{-j(\theta_{xp} + \theta_{xc})} \quad \textbf{[Eq2\_78]}$$

While,

$$\theta_{xp} = \theta_{obs_p} - P_p(\theta_r + \delta) \quad \textbf{[Eq2\_79]}$$

$$\theta_{xc} = \theta_{obs_c} - P_c(\theta_r + \delta - \gamma) \quad \textbf{[Eq2\_80]}$$

Applying the transformation [**Eq2_78**] on the generic $\boldsymbol{dq_p}$ reference frame model, we can obtain a $\boldsymbol{dq_c}$ reference frame model formulated as

$$\vec{V}_p = R_p\,\vec{i}_p + \frac{d\,\vec{\varphi}_p}{dt} + j[\omega_{obs_c} - (p_p + p_c)\Omega]\vec{\varphi}_p \quad \textbf{[Eq2\_81]}$$

$$\vec{\varphi}_p = L_p\vec{i}_p + M_p\,\vec{i}_r \quad \textbf{[Eq2\_82]}$$

$$\vec{V}_c = R_c\vec{i}_c + \frac{d\vec{\varphi}_c}{dt} + j\omega_{obs_c}\vec{\varphi}_c \quad \textbf{[Eq2\_83]}$$

$$\vec{\varphi}_c = L_c\vec{i}_c + M_c\vec{i}_r \quad \textbf{[Eq2\_84]}$$

$$\vec{V}_r = R_r\vec{i}_r + \frac{d\vec{\varphi}_r}{dt} + j[\omega_{obs_c} - p_c\Omega]\vec{\varphi}_r \quad \textbf{[Eq2\_85]}$$

$$\vec{\varphi}_r = L_r\vec{i}_r + M_p\vec{i}_p + M_c\vec{i}_c \quad \textbf{[Eq2\_86]}$$

II.2.4 Torque calculation:

The power absorbed by the machine caused by three excitations PW, CW and rotor is given by:

$$P_{abs} = \mathcal{R}_e\left\{\vec{V}_p.\vec{i}_p^{*}\right\} + \mathcal{R}_e\left\{\vec{V}_c.\vec{i}_c^{*}\right\} + \mathcal{R}_e\left\{\vec{V}_r.\vec{i}_r^{*}\right\} \quad \textbf{[Eq2\_87]}$$

Multiplying the equations [**Eq2_72**], [**Eq2_74**] , [**Eq2_76**] by $\vec{i}_p^*, \vec{i}_c^*, \vec{i}_r^*$ respectively and taking the real part we can write:

$$\mathcal{R}_e\left\{\vec{V}_p.\vec{i}_p^*\right\} = R_p i_p^2 + \mathcal{R}_e\left\{\frac{d\vec{\varphi}_p}{dt}.\vec{i}_p^*\right\} + \mathcal{R}_e\left\{j\omega_{obsp}\vec{\varphi}_p.\vec{i}_p^*\right\} \quad [\mathbf{Eq2\_88}]$$

$$\mathcal{R}_e\left\{\vec{V}_c.\vec{i}_c^*\right\} = R_c i_c^2 + \mathcal{R}_e\left\{\frac{d\vec{\varphi}_c}{dt}.\vec{i}_c^*\right\} + \mathcal{R}_e\left\{j[\omega_{obsp} - (p_p + p_c)\Omega]\vec{\varphi}_c.\vec{i}_c^*\right\} \quad [\mathbf{Eq2\_89}]$$

$$\mathcal{R}_e\left\{\vec{V}_r.\vec{i}_r^*\right\} = \underbrace{R_r i_r^2}_{P_{J_{pcr}}} + \underbrace{\mathcal{R}_e\left\{\frac{d\vec{\varphi}_r}{dt}.\vec{i}_r^*\right\}}_{P_{a_{pcr}}} + \underbrace{\mathcal{R}_e\left\{j[\omega_{obsp} - p_p\Omega]\vec{\varphi}_r.\vec{i}_r^*\right\}}_{P_{em_{pcr}}} \quad [\mathbf{Eq2\_90}]$$

Three terms appear in each active power expression, whereas

$P_{J_{pcr}}$: Power dissipated as Joule losses in PW, CW and Rotor

$P_{a_{pcr}}$: Transient active power instantaneously stored in PW, CW and Rotor

$P_{em_{pcr}}$: Power linked to the rotating field (electromagnetic power)

By definition, the torque may be obtained from the relationship of the total electromagnetic power at the rotor shaft speed Ω

$$T_{em} = \frac{P_{em_{pcr}}}{\Omega} \quad [\mathbf{Eq2\_91}]$$

$$P_{em_{pcr}} = \omega_{obsp}\mathcal{R}_e\left\{j\vec{\varphi}_p.\vec{i}_p^*\right\} + [\omega_{obsp} - (p_p + p_c)\Omega]\mathcal{R}_e\left\{j\vec{\varphi}_c.\vec{i}_c^*\right\} + [\omega_{obsp} - p_p\Omega]\mathcal{R}_e\left\{j\vec{\varphi}_r.\vec{i}_r^*\right\} \quad [\mathbf{Eq2\_92}]$$

A simple identity shows that:

$$\mathcal{R}_e\left\{j\vec{X}_A.\vec{X}_B^*\right\} = \Im_m\left\{\vec{X}_B.\vec{X}_A^*\right\} = -\Im_m\left\{\vec{X}_A.\vec{X}_B^*\right\} \quad [\mathbf{Eq2\_93}]$$

So, [**Eq2_92**] becomes:

$$P_{em_{pcr}} = \omega_{obsp}\Im_m\left\{\vec{i}_p.\vec{\varphi}_p^*\right\} + [\omega_{obsp} - (p_p + p_c)\Omega]\Im_m\left\{\vec{i}_c.\vec{\varphi}_c^*\right\} + P_{em_r} \quad [\mathbf{Eq2\_94}]$$

Where,

$$P_{em_r} = [\omega_{obsp} - p_p\Omega]\Im_m\left\{\vec{i}_r.\vec{\varphi}_r^*\right\} \quad [\mathbf{Eq2\_95}]$$

Conjugate of [**Eq2_77**] is

$$\vec{\varphi}_r^* = L_r\vec{i}_r^* + M_p\vec{i}_p^* + M_c\vec{i}_c^* \quad [\mathbf{Eq2\_96}]$$

Replacing [**Eq2_96**] in [**Eq2_95**] yields

$$P_{em_r} = [\omega_{obsp} - p_p\Omega]\Im_m\left\{M_p\vec{i}_r.\vec{i}_p^* + M_c\vec{i}_r.\vec{i}_c^*\right\} \quad [\mathbf{Eq2\_97}]$$

From [**Eq2_73**], [**Eq2_75**] we get also

$$\vec{i}_r = \frac{\vec{\varphi}_p}{M_p} - \frac{L_p}{M_p}\vec{i}_p \quad \textbf{[Eq2\_98]}$$

$$\vec{i}_r = \frac{\vec{\varphi}_c}{M_c} - \frac{L_c}{M_c}\vec{i}_c \quad \textbf{[Eq2\_99]}$$

[**Eq2_98**], [**Eq2_99**] in[**Eq2_97**] conduct to

$$P_{em_r} = [\omega_{obsp} - p_p\Omega]\Im_m\left\{\vec{\varphi}_p.\vec{i}_p^* + \vec{\varphi}_c.\vec{i}_c^*\right\} \quad \textbf{[Eq2\_100]}$$

Replacing [**Eq2_100**] in [**Eq2_92**] and after arrangement we get

$$P_{em_{pcr}} = p_p\Omega\Im_m\left\{\vec{\varphi}_p^*.\vec{i}_p\right\} + p_c\Omega\Im_m\left\{\vec{\varphi}_c.\vec{i}_c^*\right\} \quad \textbf{[Eq2\_101]}$$

From [**Eq2_91**] of the electromagnetic torque, which is given by the contribution of PW and CW, can be expressed as:

$$T_{em} = T_{em\_p} + T_{em\_c} \quad \textbf{[Eq2\_102]}$$

Whereas,

$$T_{em_p} = p_p\Im_m\left\{\vec{\varphi}_p^*.\vec{i}_p\right\} \quad \textbf{[Eq2\_103]}$$

$$T_{em\_c} = p_c\Im_m\left\{\vec{\varphi}_c.\vec{i}_c^*\right\} \quad \textbf{[Eq2\_104]}$$

In addition, we can express the electromagnetic torque by the PW, CW and rotor currents as follows

$$T_{em_p} = p_p M_p\Im_m\left\{\vec{i}_p.\vec{i}_r^*\right\} \quad \textbf{[Eq2\_105]}$$

$$T_{em\_c} = p_c M_c\Im_m\left\{\vec{i}_r.\vec{i}_c^*\right\} \quad \textbf{[Eq2\_106]}$$

II.3 DYNAMIC MODEL SIMULATIONS RESULTS:

To test the BDFM, the model has been implemented using MATLAB/SIMULINK package as shown, in Fig II.5 which presents open loop speed scalar control scheme from CW. Note that two cases will be considered: CW short circuited and CW fed controlled while PW is always grid supplied, relevant parameter employed for simulation tasks are collected in appendix C.

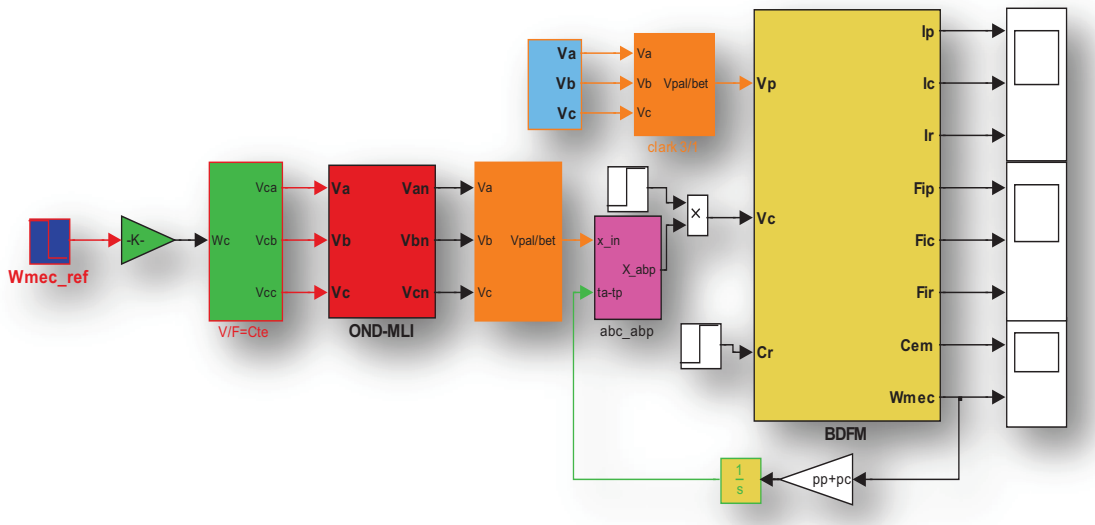

FigII.5: Open loop speed scalar control scheme.

II.3.1 Singly fed induction mode operation

In this mode the PW is connected to the grid and the CW is short-circuited. The existence of a single power supply in the machine facilitates enormously the synchronization of the both windings stator currents.

FigII.6.a shows the simulated BDFM start-up speed-time response under no-load condition, the obtained curve resembles very closely to that of an induction motor. It will be observed that once the synchronous speed is reached ($\Omega = 77.58\, rad/sec$), the frequency of CW is quite small near zero as shown in *Fig.II.6.b*

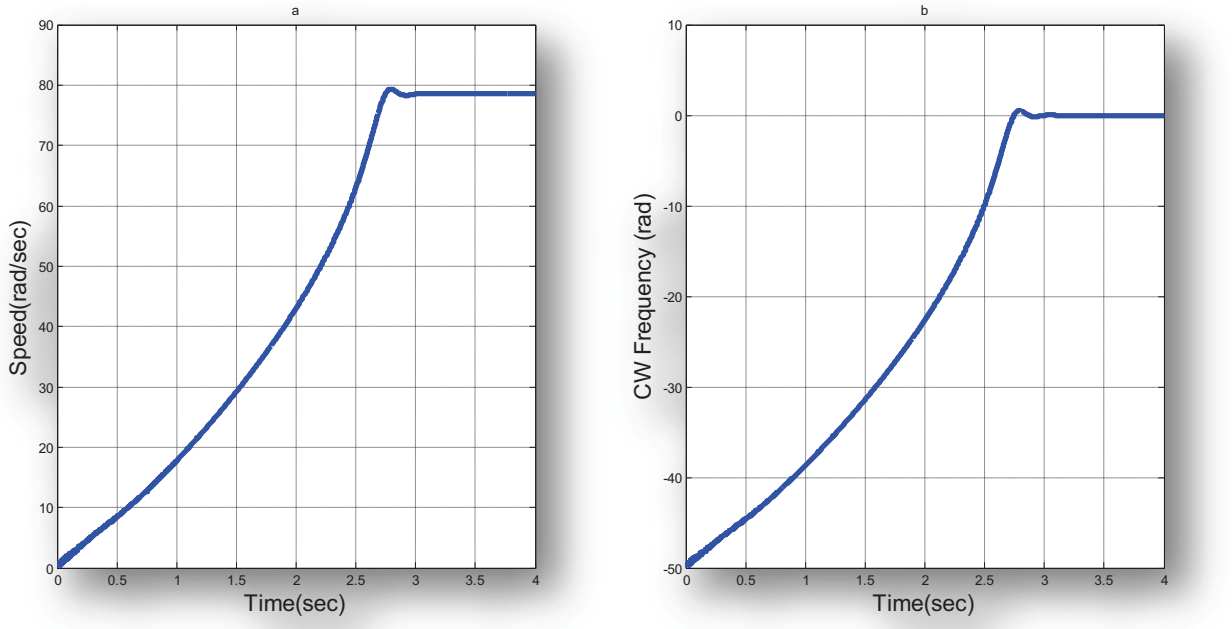

Fig II.6 Rotor speed and CW frequency responses in time

Fig II.7 shows the Temporal values of the phase currents for both stator windings.

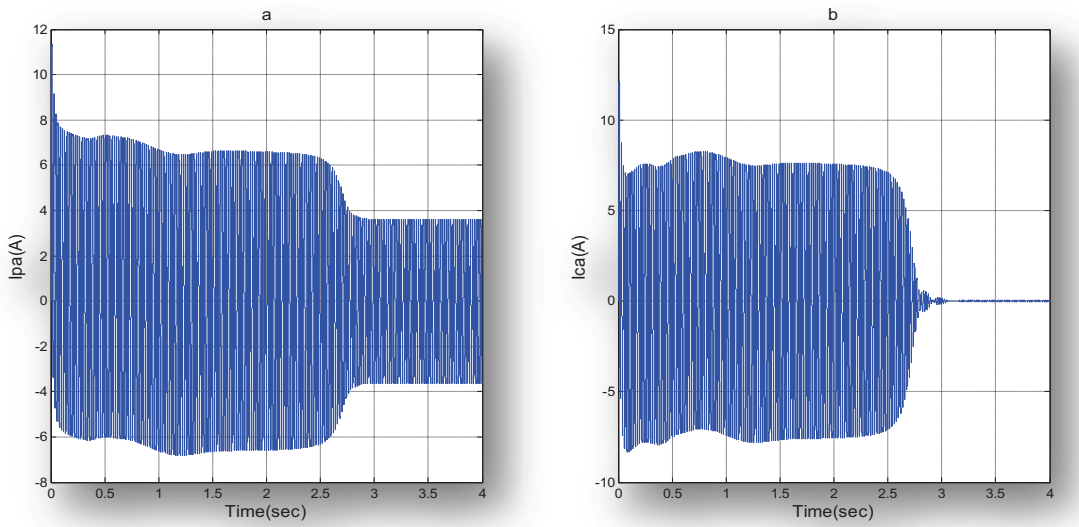

Fig II.7 PW and CW time response currents

The starting torque-speed characteristic is also of great interest. Simulation results are shown in *Figures II.8.* As would be expected, the BDFM follows the torque-speed characteristic of induction motor. Note that the total electromagnetic torque,$\boldsymbol{T_{em}}$ produced by the machine is composed of two components, $\boldsymbol{T_{emp}}$ and $\boldsymbol{T_{emc}}$. $\boldsymbol{T_{emp}}$, is produced by the PW pole-pairs system while$\boldsymbol{T_{emc}}$, is due to the CW pole-pairs system. Interaction between both torques can be clearly observed.

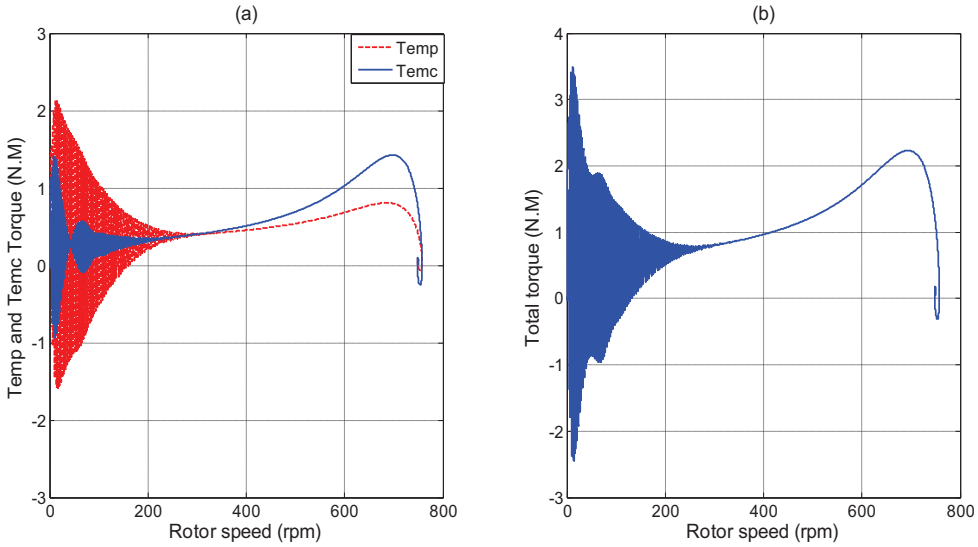

FigII.8: Electromagnetic torque-rotor speed characteristics

Free acceleration and steady state operation of the BDFM provides the same machine characteristics compared with an induction motor. In order to achieve the desired open loop speed control, doubly fed synchronous operation mode should be essential.

II.3.2 Doubly-fed synchronous operation mode:

In this case the controllability of the system is tested when an external voltage is applied on the CW side which follows a conventional Volt/Hertz law ($\boldsymbol{V_c/f_c}$ = constant).

Fig.II.9.b shows the variation of time speed response. Switching from the short-circuit case to the step of $\boldsymbol{f_c = -2Hz}$ at t=3.5s, and after it decreases once more until the step $\boldsymbol{f_c = -4Hz}$ at t = 6s.

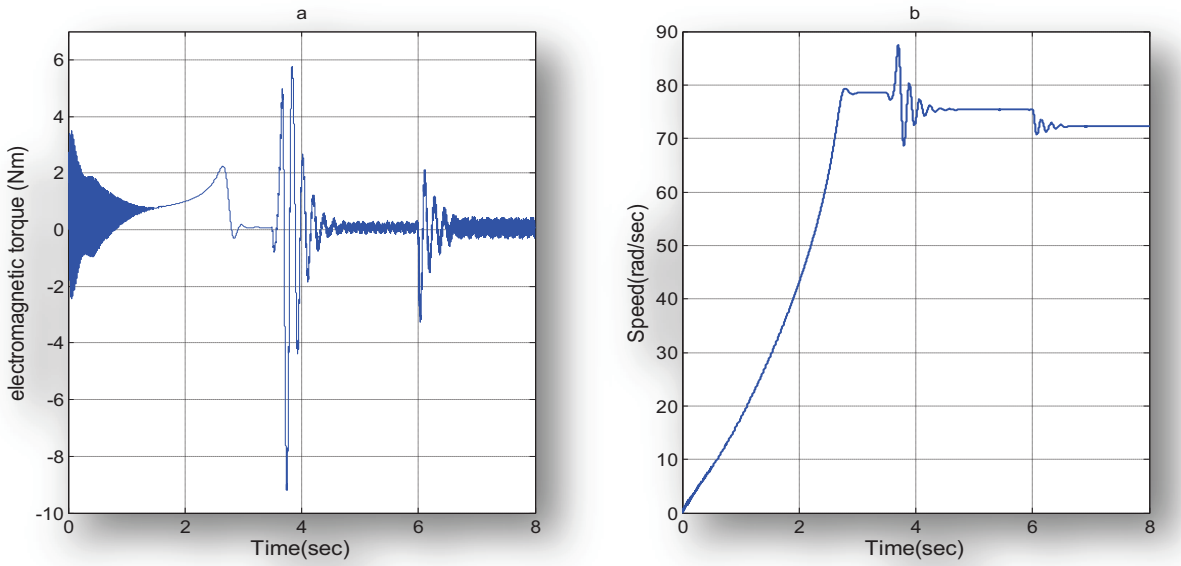

Fig. II.9 Rotor speed and electromagnetic torque

Oscillations of the first transition in *Fig.II.9-b at* t = 3.5s are very high relatively to the second one which occurs at t=6s. Step change for the first step explains the moment of CW connection after its short circuit regime.

Fig II.10 show time responses of speed and torque corresponding to the synchronous, the subsynchronous and the fault tolerant behavior of the BDFM system.

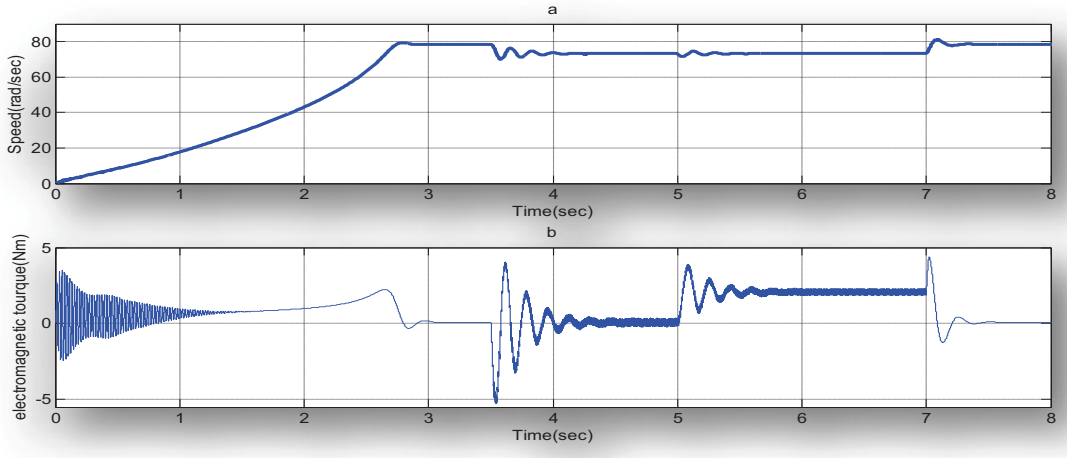

Fig. II.10: Speed and electromagnetic torque time response under load torque

Initially, the machine was running synchronously at 750 rpm (78.5rad/sec) with unload torque. At t=3.5 seconds, the CW excitation voltage is applied. The BDFM Speed decreases from synchronous to subsynchronous regimes and the electromagnetic torque is remained after the transient unchanged.

At t=5.0 seconds, load torque is applied up from zero to 2 Nm. Similar to conventional synchronous machines, in this case, the rotor speed remains after the transient to its initial value. Thus, the machine presents a synchronous operation at speed of 750 rpm (78.5rad/sec), in which the rotor speed depends only on the supply frequencies.

At t=7 seconds, we can see from *Fig II.10,* the dynamic responses for a sudden loss of the CW excitation when a short circuit is applied to the CW terminals accompagned with unload machine. An advantage of the BDFM drive system is that a loss of synchronism does not lead to a catastrophic situation and the machine can remain connected to the grid. As a result, the drive system still operates in the singly-fed induction mode and can be re-synchronized again.

II.4 CONCLUSION

This chapter has provided the detailed analysis of the BDFM principle operations, in which its dynamic model has been developed both in separate and in unified references frame. The second one has been based on the generic ***dq*** reference frame that will be used in vector control strategies. This model has been validated in MATLAB/SIMULINK packages where the BDFM has been controlled in open loop Volt/Hertz. The simulation results attest the BDFM literature assertion. As expected, the speed of BDFM can be controlled through adjusting the voltage applied to the CW. The model discussed above is an important part of this work, which offers the basis for the vector control strategy that will be discussed in the last chapter.

Chapter Three

STEADY STATE ANALYSIS OF THE BDFM

This chapter will present a steady-state model and performance study of the BDFM Initially, the steady state model of the machine will be developed.

Then, we will treat the mathematical relation between different electrical variables of the both stator windings at different rotor speeds.

After, the equivalent circuit for the BDFM will be determined its all parameters referred to the power winding.

Finally, from the steady state model, graphical simulation will be presented; they will illustrate the behavior of the machine for different rotor speeds.

The steady state study of the machine is needed to analyze its behavior in different operating conditions. This also allows the dimensioning and analyzing the system at different points of operation.

The reference [WIL-97a] presents a complete analysis of the BDFM steady state synchronous operation with developing a general harmonic analysis which obtains an accurate mathematical model. The model is validated experimentally in [WIL-97b], where iron losses and the effects of saturation are considered.

III.1 STEADY STATE MODEL OF THE MACHINE

In this section, we will present the BDFM operation analysis in steady state mode with its typical connection. We shall see that the electrical variables of the CW depend directly on the PW desired current [POZ-03]. The corresponding functions may be not linear caused by the rotor speed effect. Thanks to additional approximations, We shall assume a linear and stationary relation in the entire machine operating range.

III.1.1 Machine model according to PW variables

BDFM steady state analysis has been done from the previous developed dynamic model. The model is referred to PW, oriented with a generic $\boldsymbol{dq_p}$reference frame system. It is assumed that the machine is already in a synchronous operating mode. In this way, the desired rotor speed is defined by the CW frequency as

$$\Omega = \frac{\omega_p + \omega_c}{P_p + P_c} \quad \text{With } \omega_R = s_p \omega_p = -s_c \omega_c \qquad [\mathbf{Eq3\_1}]$$

Steady state analysis assumes the sinusoidal balanced excitations at both stators, then the corresponding equations may be written as follows

$$\vec{V_p} = R_p \vec{I_p} + j\omega_p L_p \vec{I_p} + j\omega_p M_p \vec{I_r} \qquad [\mathbf{Eq3\_2}]$$

$$\vec{V_c} = R_c \vec{I_c} - j\omega_c L_c \vec{I_c} - j\omega_c M_c \vec{I_r} \qquad [\mathbf{Eq3\_3}]$$

$$0 = R_r \vec{I_r} + js_p \omega_p L_r \vec{I_r} + js_p \omega_p M_p \vec{I_p} + js_p \omega_p M_c \vec{I_c} \qquad [\mathbf{Eq3\_4}]$$

$$T_{em} = \frac{3}{2} P_p M_p \Im_m\{\vec{I_p}.\vec{I_r^*}\} + \frac{3}{2} P_c M_c \Im_m\{\vec{I_r}.\vec{I_c^*}\} \qquad [\mathbf{Eq3\_5}]$$

In these equations, we can observe the two stator windings variables coupling through the rotor current. From[**Eq3_4**], we can deduce the rotor current as follows

$$\boxed{\vec{I_r} = -j \frac{s_p \omega_p}{R_r + j s_p \omega_p L_r} (M_p \vec{I_p} + M_c \vec{I_c})} \qquad [\mathbf{Eq3\_6}]$$

In equation[**Eq3_6**], if $s_p = 0$ ($\omega_p = P_p \Omega$) the rotor current is also equal to zero, and in this case, the ***cross-coupling*** could not be established.

Substituting [**Eq3_6**] in [**Eq3_2**], the voltage equations of both stator windings may be expressed as

$$\vec{V_p} = R_p \vec{I_p} + j\omega_p L_p \vec{I_p} + j\omega_p M_p \left[-j \frac{s_p \omega_p}{R_r + j s_p \omega_p L_r} (M_p \vec{I_p} + M_c \vec{I_c}) \right] \qquad [\mathbf{Eq3\_7}]$$

$$\vec{V_p} = \left[(R_p + j\omega_p L_p) + M_p \frac{M_p s_p {\omega_p}^2}{R_r + j s_p \omega_p L_r}\right]\vec{I_p} + M_c \frac{M_p s_p {\omega_p}^2}{R_r + j s_p \omega_p L_r}\vec{I_c} \quad \textbf{[Eq3\_8]}$$

And therefore, we can write the following relationship

$$\boxed{\vec{V_p} = \left[A_p + M_p G_p\right]\vec{I_p} + M_c G_p \vec{I_c}} \quad \textbf{[Eq3\_9]}$$

Where, $A_p = R_p + j\omega_p L_p, G_p = \frac{M_p s_p {\omega_p}^2}{R_r + j s_p \omega_p L_r}$ **[Eq3_10]**

In the same manner introducing **[Eq3_6]** in **[Eq3_3]**, the consecutive equations may be written as

$$\vec{V_c} = R_c\vec{I_c} - j\omega_c L_c\vec{I_c} - j\omega_c M_c\left[-j\frac{s_p\omega_p}{R_r + j s_p \omega_p L_r}(M_p\vec{I_p} + M_c\vec{I_c})\right] \quad \textbf{[Eq3\_11]}$$

$$\vec{V_c} = [R_c - j\omega_c L_c]\vec{I_c} - \frac{\omega_c M_c s_p \omega_p}{R_r + j s_p \omega_p L_r}(M_p\vec{I_p} + M_c\vec{I_c}) \quad \textbf{[Eq3\_12]}$$

$$\vec{V_c} = \left[(R_c - j\omega_c L_c) - M_c\frac{\omega_c M_c s_p \omega_p}{R_r + j s_p \omega_p L_r}\right]\vec{I_c} - M_p\frac{\omega_c M_c s_p \omega_p}{R_r + j s_p \omega_p L_r}\vec{I_p} \quad \textbf{[Eq3\_13]}$$

And therefore, we can write the following relationship

$$\boxed{\vec{V_c} = [A_c - M_c G_c]\vec{I_c} - M_p G_c \vec{I_p}} \quad \textbf{[Eq3\_14]}$$

Where, $A_c = R_c - j\omega_c L_c, G_c = \frac{\omega_c M_c s_p \omega_p}{R_r + j s_p \omega_p L_r}$ **[Eq3_15]**

Equations **[Eq3_9]** , **[Eq3_14]**, demonstrate that the voltage of each winding depends of two stator currents. Thus **[Eq3_9]** may be formulated as

$$\boxed{\vec{I_c} = \frac{1}{M_c G_p}\vec{V_p} - \frac{[A_p + M_p G_p]}{M_c G_p}\vec{I_p}} \quad \textbf{[Eq3\_16]}$$

The introduction of **[Eq3_16]** in **[Eq3_14]**, yields the following equation

$$\vec{V_c} = [A_c - M_c G_c]\left[\frac{1}{M_c G_p}\vec{V_p} - \frac{[A_p + M_p G_p]}{M_c G_p}\vec{I_p}\right] - M_p G_c \vec{I_p} \quad \textbf{[Eq3\_17]}$$

And finally, we obtain the following relationship

$$\boxed{\vec{V_c} = \frac{[A_c - M_c G_c]}{M_c G_p}\vec{V_p} - \left[\frac{[A_c - M_c G_c][A_p + M_p G_p]}{M_c G_p} + M_p G_c\right]\vec{I_p}} \quad \textbf{[Eq3\_18]}$$

We can note that CW voltage and current depend on their counterparts PW ones as expressed in **[Eq3_16]** , **[Eq3_18]**.

As the machine operates at a fixed terminal PW voltage, from [**Eq3_16**], a quasi direct relation between the two stator currents may be deduced as follows

$$\boxed{\vec{I}_p = \frac{1}{[A_p + M_p G_p]}\vec{V}_p - \frac{M_c G_p}{[A_p + M_p G_p]}\vec{I}_c} \quad [\mathbf{Eq3\_19}]$$

It should be observed that, as we have mentioned in the previous chapter, BDFM with the CW open circuited is equivalent to an induction machine of p_p pole-pairs "incorrectly calculated". This machine gives substantially a non-competitive in terms of torque and power factor interests.

Supposing that $\vec{\boldsymbol{I}}_{\boldsymbol{p}}$, of [**Eq3_19**], may be divided into two components: $\vec{\boldsymbol{I}}_{\boldsymbol{pi}}$, PW proper induction mode current and $\vec{\boldsymbol{I}}_{\boldsymbol{pc}}$, CW coupling current. This assertion leads to write the following expression

$$\vec{I}_p = \vec{I}_{pi} + \vec{I}_{pc} \quad [\mathbf{Eq3\_20}]$$

Where,

$$\vec{I}_{pi} = \frac{1}{[A_p + M_p G_p]}\vec{V}_p = \vec{K}_V \frac{\vec{V}_p}{\omega_p} \quad [\mathbf{Eq3\_21}]$$

$$\vec{I}_{pc} = -\frac{M_c G_p}{[A_p + M_p G_p]}\vec{I}_c = \vec{K}_i \vec{I}_c \quad [\mathbf{Eq3\_22}]$$

The gains $\boldsymbol{K_V}$ and $\boldsymbol{K_i}$ depend on $\boldsymbol{s_p}$and vary with the rotor speed. From [**Eq3_19**], we can write

$$\vec{I}_p = \vec{K}_V \frac{\vec{V}_p}{\omega_p} + \vec{K}_i \vec{I}_c \quad [\mathbf{Eq3\_23}]$$

Consequently, the CW current expression may be expressed as

$$\boxed{\vec{I}_c = \frac{1}{\vec{K}_i}\vec{I}_p - \frac{\vec{K}_V}{\vec{K}_i}\frac{\vec{V}_p}{\omega_p}} \quad [\mathbf{Eq3\_24}]$$

III.1.2 Simplified model:

In the preceding section, it has been noted that the machine model depends on the rotor speed. The first simplified approach might be done in assuming that

$$R_r \ll s_p \omega_p L_r \quad [\mathbf{Eq3\_25}]$$

This assumption, [**Eq3_25**], transforms [**Eq3_6**]to a stationary relationship in all operating range

$$\boxed{\vec{I}_r \approx -\frac{1}{L_r}(M_p \vec{I}_p + M_c \vec{I}_c)} \quad [\mathbf{Eq3\_27}]$$

Using [**Eq3_27**] and neglecting the resistive losses of the both stator windings, the previous gains factors might be transformed to simple constant parameters as follows

$$\vec{K}_i \approx K_i = \frac{M_p M_c}{\sigma_p L_p L_r} \quad [\mathbf{Eq3\_28}]$$

$$\vec{K}_V \approx jK_V, K_V = -\frac{1}{\sigma_p L_p} \quad [\mathbf{Eq3\_29}]$$

The alignement of the PW voltage on d-axis conducts to transform the [**Eq3_24**] as follows

$$\vec{I}_c = \frac{1}{K_i}\vec{I}_p - j\frac{K_V}{K_i}\frac{V_p}{\omega_p} \quad [\mathbf{Eq3\_30}]$$

After, *dq-**Park*** transformation, [**Eq3_30**] may becoms

$$\boxed{I_{dp} = K_i I_{dc}} \quad [\mathbf{Eq3\_31}]$$

$$I_{qc} = \frac{1}{K_i} I_{qp} - \frac{K_V}{K_i}\frac{V_p}{\omega_p} \Rightarrow \boxed{I_{qp} = K_i I_{qc} + K_V \frac{V_p}{\omega_p}} \quad [\mathbf{Eq3\_32}]$$

From [**Eq3_31**] and[**Eq3_32**], we can observe a linear amplification effect between both stator windings currents.

This result is very significant to understand the vector control algorithm that will be developed in the next chapter.

Taking into account the above approximation, equation [**Eq3_18**]becomes

$$\vec{V}_c = \frac{\omega_c}{\omega_p} L_{ec1} V_p - j\omega_c L_{ec2}\vec{I}_p \quad [\mathbf{Eq3\_33}]$$

Where

$$L_{ec1} = -\frac{L_c L_r \sigma_c}{M_c M_r} \quad [\mathbf{Eq3\_34}]$$

$$L_{ec2} = \left(\frac{L_c L_p}{M_c M_p}\frac{L_r^2 \sigma_p \sigma_c}{} + \frac{M_c M_p}{L_r}\right) \quad [\mathbf{Eq3\_35}]$$

With, $\sigma_c = 1 - \frac{M_c^2}{L_c L_r}$

Calculating $(\boldsymbol{dq})$Park components, we get the following relationships

$$\boxed{V_{dc} = \frac{L_{ec1} V_p}{\omega_p}\boldsymbol{\omega_c} + L_{ec2} I_{qp}\boldsymbol{\omega_c}} \quad [\mathbf{Eq3\_36}]$$

$$\boxed{V_{qc} = -L_{ec2} I_{dp}\boldsymbol{\omega_c}} \quad [\mathbf{Eq3\_37}]$$

Analysis of these expressions in assuming that the PW current as constant, shows that the CW voltage component increase linearly with CW frequency; in this way, the relationship $\frac{V_c}{f_c}$ may be kept constant.

III.1.3 Equivalent circuit model

It is well known that the electrical machinery equivalent circuit model represents a simpler method to study its steady-state performances, particularly BDFM type [ROB-05b]. Since the meaning of the model parameters has a comprehensible physical interpretation, the model can be very helpful to understand the design and optimization of the machine. The equivalent circuit model offers a straightforward way for practical calculation of efficiency, power factor and other steady-state variables.

From[**Eq3_2**] , [**Eq3_3**] and [**Eq3_4**], we can write

$$\vec{V_p} = R_p\,\vec{I_p} + j\omega_p L_p \vec{I_p} + j\omega_p M_p\,\vec{I_r} \qquad \textbf{[Eq3_38]}$$

$$\vec{V_c} = R_c\vec{I_c} + j\omega_p s_s L_c \vec{I_c} + j\omega_p s_s M_c \vec{I_r} \qquad \textbf{[Eq3_39]}$$

$$0 = R_r\vec{I_r} + js_p\omega_p L_r \vec{I_r} + js_p\omega_p M_p \vec{I_p} + js_p\omega_p M_c \vec{I_c} \qquad \textbf{[Eq3_40]}$$

Where, $s_s = \frac{\omega_p - (p_p + p_c)\Omega}{\omega_p}$ **[Eq3_41]**

Some mathematical arrangements of these last equations conduct successively to write

$$\vec{V_p} = R_p\,\vec{I_p} + j\omega_p(L_p - \boldsymbol{M_p})\vec{I_p} + j\omega_p M_p(\boldsymbol{\vec{I_p}} + \vec{I_r}) \qquad \textbf{[Eq3_42]}$$

$$\frac{\vec{V_c}}{s_s} = \frac{R_c}{s_s}\vec{I_c} + j\omega_p(L_c - \boldsymbol{M_c})\vec{I_c} + j\omega_p M_c(\boldsymbol{\vec{I_c}} + \vec{I_r}) \qquad \textbf{[Eq3_43]}$$

$$0 = \frac{R_r}{s_p}\vec{I_r} + j\omega_p(L_r - \boldsymbol{M_p} - \boldsymbol{M_c})\vec{I_r} + j\omega_p M_p(\boldsymbol{\vec{I_r}} + \vec{I_p}) + j\omega_p M_c(\boldsymbol{\vec{I_r}} + \vec{I_c}) \qquad \textbf{[Eq3_44]}$$

From the previous equations [**Eq3_42**], [**Eq3_43**] and [**Eq3_44**], fundamental equivalent circuit for the BDFM may be drawn as shown below in *Fig.III.1* where all the parameters, particularly leakage inductance and magnetizing inductances of PW and CW, are referred to PW side (iron losses are negligible).

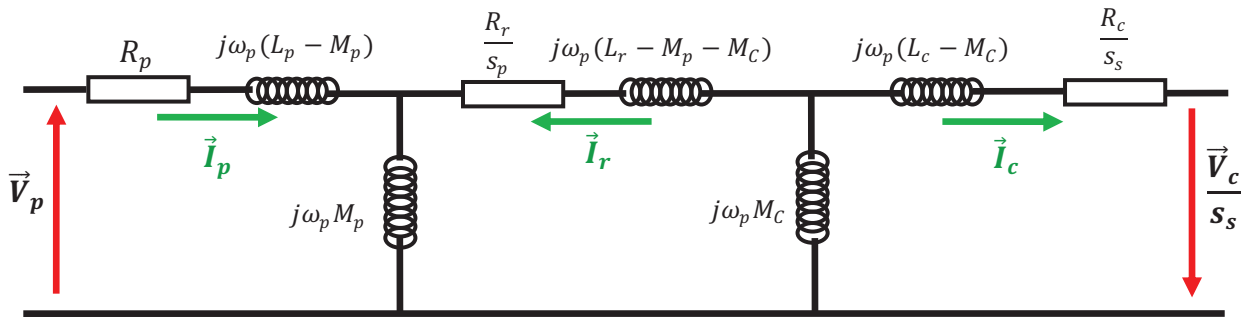

Fig.III.1: Referred per-phase equivalent circuit for the BDFM

From the above figure, we can deduce the equivalent circuit for the BDFM with only one supply, as shown in the *Fig.III.2,* this circuit resembles entirely to the conventional induction machine model.

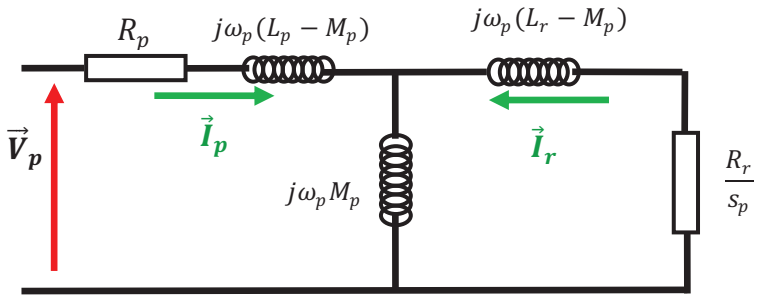

Fig.III.2: Referred per-phase equivalent circuit for the BDFM with only power supply.

The obtained equivalent circuit is very interesting to understand the operation mode of the BDFM. Although the BDFM model is more complicated, the operation mode may be considered as existing in DFIG, but in the BDFM case the second stator armature CW is only supplied the instead of the rotor windings of DFIG.

III.2 SIMULATION RESULTS

Normally we use the complete model to simulate the behavior of the machine; however the approximated relations presented in the previous section are very useful to simulate the machine operation and to establish the control principles and practical strategies to optimize the operation of the machine.

In this section, we will simulate the behavior of the machine at different rotor speeds by considering a constant value of the PW current. Consider a range of speeds which runs from up $\Omega = 300\,rpm$ to $\Omega = 1200rpm$ (natural synchronous speed $\Omega = 750\,rpm$). We have considered the PW variables (Vp and Ip) as inputs and calculate the electrical CW variables and the electromagnetic torque.

The considered values in this simulation are: $V_p = 243\,Vrms$ $I_p = 4.5\,Arms$, $P_p = 3208\,W$, $Q_p = 0VAR$.

The simulation results shown in the following figures depict how major quantities of the BDFM are varying with the rotor operational speed.

In the case of *Fig.III.3a*, the gain values are $K_v = -3.6660$ and $K_i = 0.4003$, and the CW current is greater than the PW current. The approximate form of the PW current, is expressed

numerically from [**Eq3_31**] and [**Eq3_32**] by calculating the PW current components (the values of voltage and current in RMS), so

$$\boxed{I_{dp} = 0.4003 I_{dc}} \qquad [\mathbf{Eq3\_45}]$$

$$I_{qp} = 0.4003 I_{qc} - 3.6660 \frac{V_p}{\omega_p} \Rightarrow \boxed{I_{qp} = 0.4003 I_{qc} - 2.5386} \qquad [\mathbf{Eq3\_46}]$$

Equation [**Eq3_45**] indicates that the I_{dc} controls the PW current component, which produces the reactive power in this winding

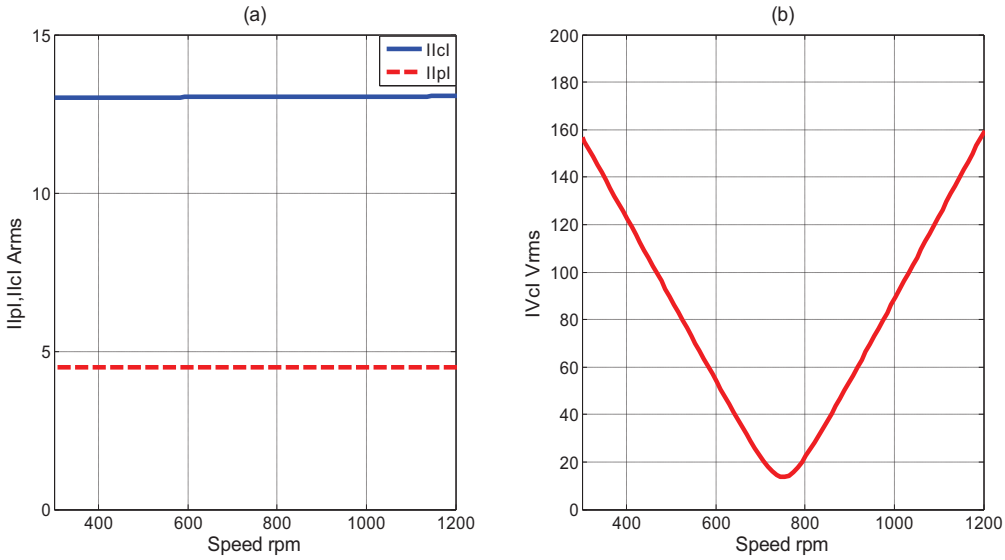

Fig.III.3: Electrical variables of the stator windings (RMS value).

The graph of *Fig.III.3b* shows the CW voltage module, if increases linearly when the rotor speed deviates from natural synchronous rotor speed Ω_n This linear increase is due to the ratio $\frac{V_c}{f_c}$ that remains constant as shown in [**Eq3_36**] and [**Eq3_37**].

From these results, it is possible to say that the required control voltage (*Fig.III.3b*) varies almost linearly with the rotor speed.

The graphs of Fig.III.4, show the CW active and reactive powers changing linearly with the rotor speed. So the total electrical power generated by the BDFM is linearly proportional to the rotor speed

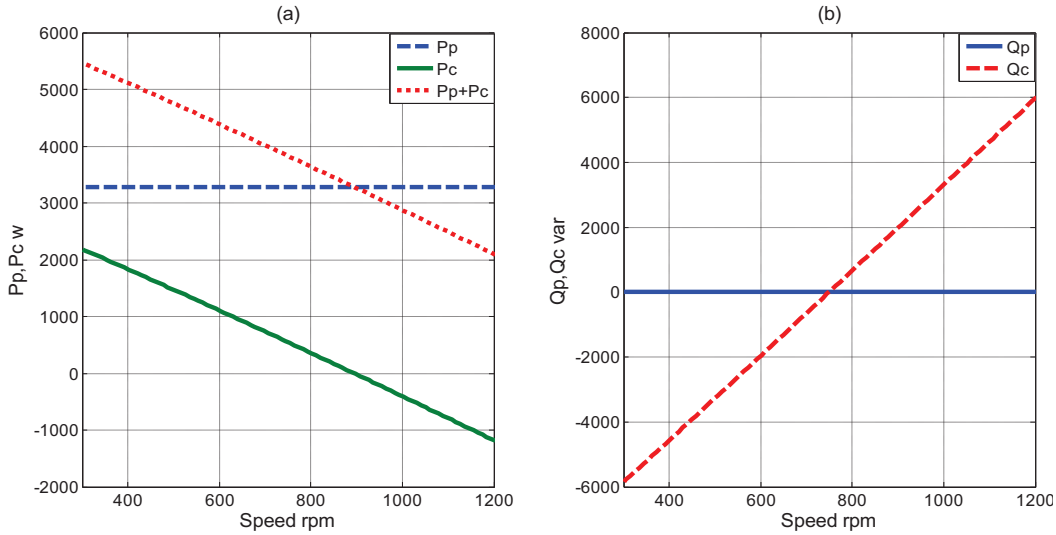

Fig.III.4: Evolution of the active and reactive powers of the stator windings with the rotor speed.

Now for the apparent power, the first graph of *Fig. III.5* shows the CW apparent power increases linearly when the rotor speed move away from its natural synchronous value. This feature is important, since limiting the range of rotor speed variation consequently limits the size of the frequency converter (an advantage of DFIG). For example, to limit VA rating of the power electronics converter to approx of $^{1}/_{3}$ of the PW rating (to approx. 1000VA) the generator speed range should be restricted to 690 rpm-820 rpm as shown in *FigIII.5.a*.

The torque in both stator windings is constant in the whole speed range as shown in *Fig.III.5.b* it can be noticed that the CW torque is higher than that of the PW.

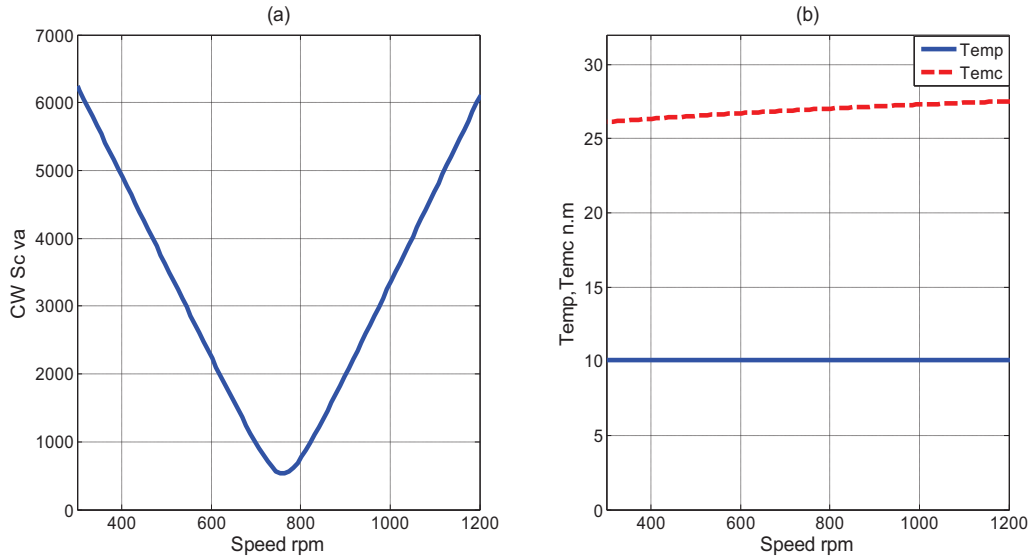

Fig.III.5: Evolution of the apparent power and electromagnetic torque with the rotor speed

III.3. CONCLUSION

In this chapter the steady state analysis has been carried out by referencing all machine to the same system of axis referred to the PW voltage

In summary, we can understand the operation of the machine using linear approximations which link the currents and voltages of the two stator windings.

With these relationships we can establish some basic principles of BDFM control, in this way; it was observed that by maintaining a Volt/Hertz law constant for the control winding, we have obtained a virtually constant electromagnetic torque.

The relations between currents can establish a principle of operation for a high performance vector control, in which we regulate the PW currents by varying the CW current, with the PW current components, that we can determine the operation mode of the machine, being the main objective of the next chapter.

Chapter Four

VECTOR CONTROL ALGORITHM FOR THE BDFM

The goal of the BDFM control is to achieve the same or higher dynamic performance as the wound rotor machine, exploiting the well known induction motor vector control philosophy. For this purpose a previous developed unified dq reference-frame model is preferred.

The purpose of the proposed method is the independent control of the two main currents of the machine: the one generating the torque and the other generating the flux. This scheme is similar to the one that has been used with very good results for the induction machine control during several years. For doing so, all variables of the machine are related to the PW synchronous reference frame.

VI.I: CONTROL STRATEGY

The objective of the vector control is to control the machine currents separately to control two different variables independently. The vector control is based on the dynamic ***dq*** model, an exact model being necessary to obtain the dynamic vector equations, then to design the most adequate control system.

IV.I.1: Control Principle:

In the previous chapter, a steady-state study of the BDFM in a synchronous operation mode has been presented giving some approximate expressions of the BDFM static operation. Taking the PW voltage as the reference phasor:

$$I_{dp} = K_i I_{dc} \qquad [\mathbf{Eq4.1}]$$

$$I_{qp} = K_v \frac{V_p}{w_p} - K_i I_{qc} \qquad [\mathbf{Eq4.2}]$$

Where K_i, and K_v, are constants depending on the electrical machine's parameters. In [POZ-03] the total electromagnetic torque is expressed as:

$$T_{em} \approx \frac{3}{2}\frac{P_p+P_c}{w_p} V_p I_{dp} - \frac{3}{2}\frac{P_p}{w_p} R_p \left|\vec{I}_p^2\right| \qquad [\mathbf{Eq4.3}]$$

From [**Eq4.1**] and [**Eq4.2**] we can conclude that the steady-state PW currents are linearly dependent of the steady-state CW currents (as demonstrated in the previous chapter). Similarly from [**Eq4.3**], the torque is mainly depending on the PW active current. Thus, the choice of the PW flux orientation as the reference frame seems to be the most adequate option.

When vector control is implemented in a ***dq*** PW flux orientation reference frame, the current I_p is related to the reactive power Q_p as follows,

$$Q_p = \frac{3}{2}\omega_p \varphi_p i_{dp} - \frac{d\varphi_p}{dt} i_{qp} \qquad [\mathbf{Eq4.4}]$$

Since the PW is connected to the 50 Hz grid constant voltage, so the PW flux is maintained almost constant $\frac{d\varphi_p}{dt} = 0$. In this way Q_p can be directly controlled by an adequate choice of i_{dp},.

The PW active power can be expressed as:

$$P_p = \frac{3}{2}\omega_p \varphi_p i_{qp} - \frac{d\varphi_p}{dt} i_{dp} + \frac{3}{2} R_p \left|\vec{i}_p\right|^2 \qquad [\mathbf{Eq4.5}]$$

In this case we also consider that i_{qp} is nearly proportional to the active power P_p.

The current i_{qp} can also be used to regulate the electromagnetic torque because:

$$T_{em} \approx \frac{3}{2}(p_p + p_c)\, \varphi_p i_{qp} \qquad [\mathbf{Eq4.6}]$$

Based on the above relations, we can establish the proposed control scheme as presented in the Fig.4.1. This scheme is based on the cascade regulation method. Two independent regulation paths are implemented:

- Reactive power control:

$$Q_{p\_ref} \Rightarrow I_{dc-ref} \Rightarrow V_{dc-ref}$$

- Active power , electromagnetic torque or speed Control:

$$P_{p\_ref} \Rightarrow I_{qc-ref} \Rightarrow V_{qc-ref}$$

Or

$$T_{em\_ref} \Rightarrow I_{qc-ref} \Rightarrow V_{qc-ref}$$

Or

$$\Omega_{ref} \Rightarrow I_{qc-ref} \Rightarrow V_{qc-ref}$$

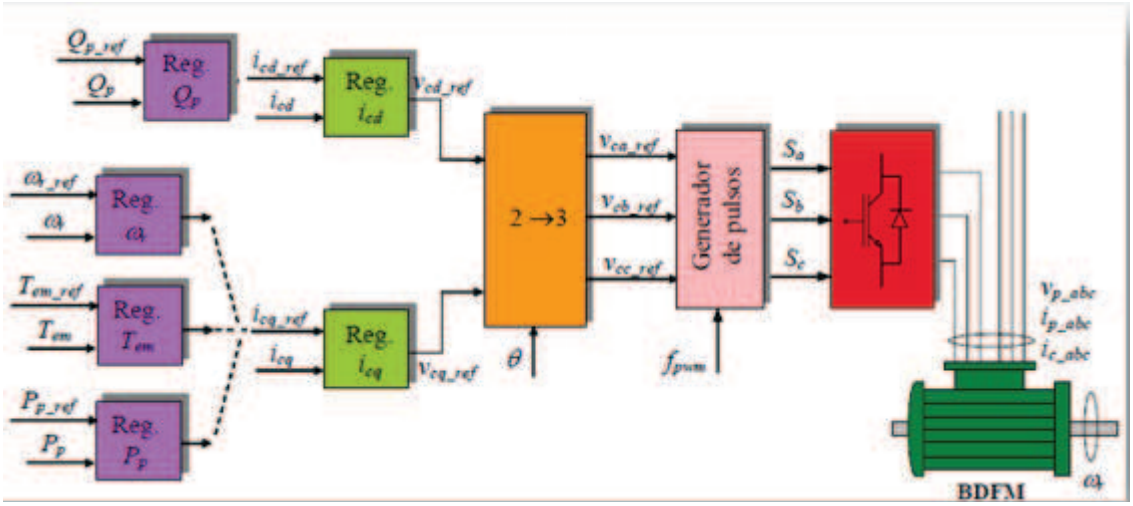

FigureIV.1: Vector control scheme of BDFM

IV.2: **PW FLUX REFERENCE FRAME MACHINE MODEL**

As we have said earlier, the best-suited reference frame for the proposed control principle is the PW flux orientation, so, $\varphi_{dp} = \left|\vec{\varphi}_p\right| = \varphi_p, \varphi_{qp} = 0$ are selected. The previous generic ***dq*** model of [**Eq2_72**] is expressed in this common reference frame can be expressed as follows

$$\vec{V}_p = R_p\,\vec{i}_p + \frac{d\,\varphi_p}{dt} + j\omega_p\,\varphi_p \qquad [\mathbf{Eq4.7}]$$

$$\varphi_p = L_p\vec{i}_p + M_p\,\vec{i}_r \qquad [\mathbf{Eq4.8}]$$

$$\vec{V}_c = R_c\vec{i}_c + \frac{d\vec{\varphi}_c}{dt} + j[\omega_p - (p_p + p_c)\Omega]\vec{\varphi}_c \qquad [\mathbf{Eq4.9}]$$

$$\vec{\varphi}_c = L_c\vec{i}_c + M_c\vec{i}_r \qquad [\mathbf{Eq4.10}]$$

$$0 = R_r\vec{i}_r + \frac{d\vec{\varphi}_r}{dt} + j[\omega_p - p_p\Omega]\vec{\varphi}_r \qquad [\mathbf{Eq4.11}]$$

$$\vec{\varphi}_r = L_r\vec{i}_r + M_p\vec{i}_p + M_c\vec{i}_c \qquad [\mathbf{Eq4.12}]$$

The electromagnetic torque can be expressed as:

$$T_{em} = \frac{3}{2} p_p Im\left[\varphi_p \vec{i}_p\right] + \frac{3}{2} p_c Im[\vec{\varphi}_c \vec{i}_c^*] \quad [\mathbf{Eq4.13}]$$

Suppose that the BDFM is running in steady state, and then the dynamic model can be transferred to the steady state model:

$$\vec{V}_p = R_p \vec{i}_p + j\omega_p L_p \vec{i}_p + j\omega_p M_p \vec{i}_r \quad [\mathbf{Eq4.14}]$$

$$\vec{V}_c = R_c \vec{i}_c + j[\omega_{rp} - p_c \Omega] L_c \vec{i}_c + j[\omega_{rp} - p_c \Omega] M_c \vec{i}_r \quad [\mathbf{Eq4.15}]$$

$$0 = R_r \vec{i}_r + j\omega_{rp} L_r \vec{i}_r + j\omega_{rp} M_p \vec{i}_p + j\omega_{rp} M_c \vec{i}_c \quad [\mathbf{Eq4.16}]$$

IV.3: DYNAMIC CONTROL FUNCTIONS:

IV.3.1: Control of power winding current:

From[**Eq4.16**]:

$$\vec{i}_r = -j \frac{\omega_{rp}}{R_r + j\omega_{rp} L_r} \left[M_p \vec{i}_p + M_c \vec{i}_c\right] \quad [\mathbf{Eq4.17}]$$

The introduction of [**Eq4.17**] in [**Eq4.14**] yields

$$\vec{V}_p = \left[R_p + j\omega_p L_p + \frac{\omega_p {M_p}^2 \omega_{rp}}{R_r + j\omega_{rp} L_r}\right] \vec{i}_p + \frac{\omega_p M_p \omega_{rp}}{R_r + j\omega_{rp} L_r} M_c \vec{i}_c \quad [\mathbf{Eq4.18}]$$

In order to introduce all the quantities in the reference frame. A common way is using equation [**Eq4.7**] and measuring the power winding voltage $\vec{V}_p$ while neglecting the power winding stator resistance R_p, [**Eq4.7**] becomes

$$\vec{V}_p = j\omega_p \varphi_p \quad [\mathbf{Eq4.19}]$$

Splitting equation [**Eq4.19**] into dq components yields,

$$V_{pd} = -\omega_p \varphi_{pq} = 0 \quad [\mathbf{Eq4.20}]$$

$$V_{pq} = \omega_p \varphi_{pd} \quad [\mathbf{Eq4.21}]$$

By considering the equations[**Eq4.18**], [**Eq4.20**] and [**Eq4.21**] and their arrangement, yields

$$\boldsymbol{i_{cd}} = \frac{L_p L_r \sigma_p}{M_p M_c} \boldsymbol{i_{pd}} - \frac{\varphi_p L_r}{M_p M_c} + \frac{L_p R_r}{\omega_{rp} M_p M_c} \boldsymbol{i_{pq}} \quad [\mathbf{Eq4.22}]$$

$$\boldsymbol{i_{cq}} = \frac{L_p L_r \sigma_p}{M_p M_c} \boldsymbol{i_{pq}} + \frac{\varphi_p R_r}{\omega_{rp} M_p M_c} - \frac{L_p R_r}{\omega_{rp} M_p M_c} \boldsymbol{i_{pd}} \quad [\mathbf{Eq4.23}]$$

The first term of equation[**Eq4.22**], $\frac{L_p L_r \sigma_p}{M_p M_c} \boldsymbol{i_{pd}}$

Defines the direct coupling between $\boldsymbol{i_{cd}}$ and$\boldsymbol{i_{pd}}$, and the coefficient is constant. The second term,

$-\frac{\varphi_p L_r}{M_p M_c}$ performs as a constant offset. Finally, the third term, $\frac{L_p R_r}{\omega_{rp} M_p M_c} \boldsymbol{i_{pq}}$

Reflects the cross coupling. Obviously, the only variable is $\boldsymbol{\omega_{rp}}$, and therefore this cross coupling term varies with the shaft speed. The coefficient of the cross coupling term can be neglected as compared to the direct coupling term [SHI-08].

As a conclusion, $\boldsymbol{i_{cd}}$ is linear with $\boldsymbol{i_{pd}}$ if the effect of the cross coupling term is neglected. Similar analysis applies to equation [**Eq4.23**], with a conclusion that $\boldsymbol{i_{cq}}$ is linear with $\boldsymbol{i_{pq}}$ *FigIV.2*, so [**Eq4.22**] and [**Eq4.23**] becomes,

$$\boldsymbol{i_{cd}} = \frac{L_p L_r \sigma_p}{M_p M_c} \boldsymbol{i_{pd}} - \frac{\varphi_p L_r}{M_p M_c} \qquad \textbf{[Eq4.24]}$$

$$\boldsymbol{i_{cq}} = \frac{L_p L_r \sigma_p}{M_p M_c} \boldsymbol{i_{pq}} + \frac{\varphi_p R_r}{\omega_{rp} M_p M_c} \qquad \textbf{[Eq4.25]}$$

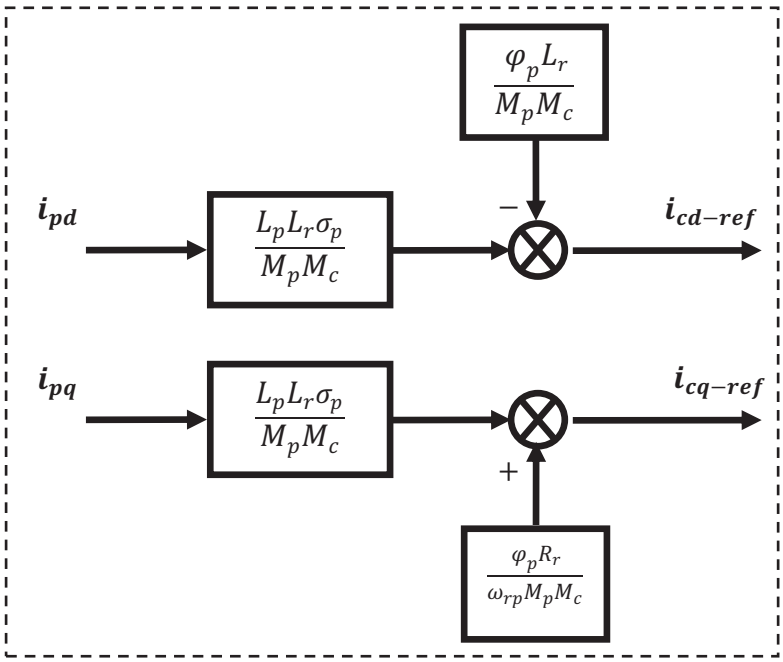

FigIV.2: Implemented PW current control

IV.3.2: Control of control winding current:

From [**Eq4.8**], we get,

$$\vec{i}_r = \frac{\varphi_p - L_p \vec{i}_p}{M_p} \qquad \textbf{[Eq4.26]}$$

Splitting [**Eq4.9**], [**Eq4.10**] and[**Eq4.26**], to become,

$$V_{cd} = R_c i_{cd} + \frac{d\varphi_{cd}}{dt} - [\omega_p - (p_p + p_c)\Omega]\varphi_{cq} \qquad \textbf{[Eq4.27]}$$

$$V_{cq} = R_c i_{cq} + \frac{d\varphi_{cq}}{dt} + [\omega_p - (p_p + p_c)\Omega]\varphi_{cd} \qquad \textbf{[Eq4.28]}$$

$$\varphi_{cd} = L_c i_{cd} + M_c i_{rd} \quad \textbf{[Eq4.29]}$$

$$\varphi_{cq} = L_c i_{cq} + M_c i_{rq} \quad \textbf{[Eq4.30]}$$

$$i_{rd} = \frac{\varphi_p - L_p i_{pd}}{M_p} \quad \textbf{[Eq4.31]}$$

$$i_{rq} = \frac{-L_p i_{pq}}{M_p} \quad \textbf{[Eq4.32]}$$

Subtitling [**Eq4.31**], [**Eq4.32**] in[**Eq4.29**], [**Eq4.30**] successively, the obtained result is replaced in [**Eq4.27**] and [**Eq4.28**], and after arrangement we get,

$$\boldsymbol{V_{cd}} = R_c \boldsymbol{i_{cd}} + L_c \frac{(\sigma_p + \sigma_c - 1)}{\sigma_p} \frac{d\boldsymbol{i_{cd}}}{dt} - [\omega_p - (p_p + p_c)\Omega] \left[L_c \boldsymbol{i_{cq}} - \frac{M_c L_p}{M_p} \boldsymbol{i_{pq}} \right] \quad \textbf{[Eq4.33]}$$

$$\boldsymbol{V_{cq}} = R_c \boldsymbol{i_{cq}} + L_c \frac{(\sigma_p + \sigma_c - 1)}{\sigma_p} \frac{d\boldsymbol{i_{cq}}}{dt} + [\omega_p - (p_p + p_c)\Omega] \left[L_c \boldsymbol{i_{cd}} + M_c \frac{\varphi_p - L_p \boldsymbol{i_{pd}}}{M_p} \right] \quad \textbf{[Eq4.34]}$$

Similar analysis as for the control of the power winding current can be applied to [**Eq4.33**], the first term, $\boldsymbol{R_c i_{cd}} + \boldsymbol{L_c} \frac{(\boldsymbol{\sigma_p + \sigma_c - 1})}{\boldsymbol{\sigma_p}} \frac{\boldsymbol{di_{cd}}}{\boldsymbol{dt}}$ shows direct relation between $\boldsymbol{V_{cd}}$ and $\boldsymbol{i_{cd}}$. The transfer function has first order, the second term, $-[\boldsymbol{\omega_p} - (\boldsymbol{p_p} + \boldsymbol{p_c})\boldsymbol{\Omega}] \left[\boldsymbol{L_c i_{cq}} - \frac{\boldsymbol{M_c L_p}}{\boldsymbol{M_p}} \boldsymbol{i_{pq}} \right]$ presents a cross coupling with lower order compared to the first terms, and therefore can be neglected [SHI-08].

Therefore, if cross coupling is neglected, $\boldsymbol{V_{cd}}$ and $\boldsymbol{i_{cd}}$ have a constant and a first order relation. A similar derivation can be applied to the analysis of [**Eq4.34**], concluding that the $\boldsymbol{V_{cq}}$ and $\boldsymbol{i_{cq}}$ also have a constant and a first order relation, as follows

$$\boldsymbol{V_{cd}} = R_c \boldsymbol{i_{cd}} + L_c \frac{(\sigma_p + \sigma_c - 1)}{\sigma_p} \frac{d\boldsymbol{i_{cd}}}{dt} \quad \textbf{[Eq4.35]}$$

$$\boldsymbol{V_{cq}} = R_c \boldsymbol{i_{cq}} + L_c \frac{(\sigma_p + \sigma_c - 1)}{\sigma_p} \frac{d\boldsymbol{i_{cq}}}{dt} \quad \textbf{[Eq4.36]}$$

In vector form,

$$\vec{\boldsymbol{V_c}} = R_c \vec{\boldsymbol{i_c}} + L_c \frac{(\sigma_p + \sigma_c - 1)}{\sigma_p} \frac{d\vec{\boldsymbol{i_c}}}{dt} \quad \textbf{[Eq4.37]}$$

FigIV.3 shows the proposed control scheme in order to obtain the CW reference values, obtaining the first-order transfer function between the CW current $\left(\vec{\boldsymbol{i_c}}\right)$ and the CW voltage $\left(\vec{\boldsymbol{V_c}}\right)$ terms, expressed as follows,

$$\frac{\vec{\boldsymbol{i_c}}}{\vec{\boldsymbol{V_c}}} = \frac{K_c}{1 + \tau_c s}, K_c = \frac{1}{R_c}, \tau_c = \frac{L_c}{R_c} \frac{(\sigma_p + \sigma_c - 1)}{\sigma_p} \quad \textbf{[Eq4.38]}$$

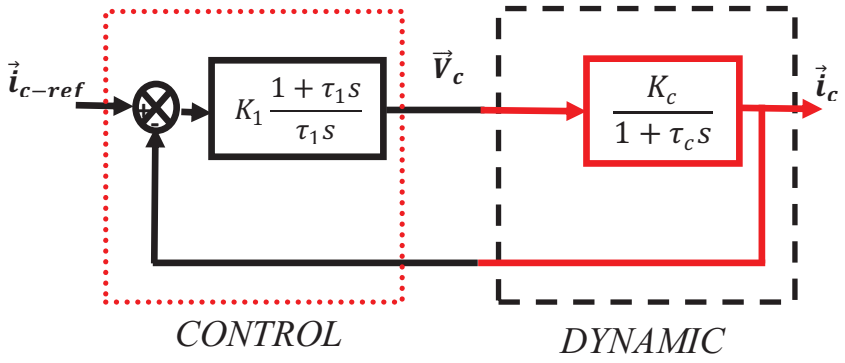

FigIV.3: CW current control loop

- *Regulator Calculation:*

Based on the conventional calculation of the first order transfer function we obtain:

$K_1 = \frac{n_c}{K_c}, n_c \geq 2 \;\; K_{i1} = \frac{n_c}{\tau_c K_c}$

IV.3.3: Control of torque:

From [**Eq4.13**]

$$T_{em} = \frac{3}{2} p_p \varphi_p i_{pq} + \frac{3}{2} p_c [i_{cd} \varphi_{cq} - i_{cq} \varphi_{cd}] \qquad [\mathbf{Eq4.39}]$$

By substuting [**Eq4.29**], [**Eq4.30**] in [**Eq4.39**] we get:

$$T_{em} = \frac{3}{2} p_p \varphi_p i_{pq} - \frac{3}{2} p_c \frac{M_c}{M_p} \varphi_p i_{cq} + \frac{3}{2} p_c \frac{M_c L_p}{M_p} [i_{pd} i_{cq} - i_{pq} i_{cd}] \qquad [\mathbf{Eq4.40}]$$

This equation is a function of $\vec{i}_p$ and $\vec{i}_c$ currents. In order to obtain a direct relation between T_{em} and $\vec{i}_p$, Substituting[**Eq4.22**] and [**Eq4.23**] expressions in [**Eq4.40**] an approximate torque equation may be obtained:

$$T_{em} \approx T_{em-d} + T_{em-c} \qquad [\mathbf{Eq4.41}]$$

Where:

$$T_{em-d} = \frac{3}{2} (p_p + p_c) \varphi_p i_{pq} \qquad [\mathbf{Eq4.42}]$$

$$T_{em-c} = \frac{3}{2} \frac{p_c R_r}{\omega_{rp} M_p^2} \left[2 L_p \varphi_p i_{pd} - \left(L_p^2 i_p^2 + \varphi_p^2 \right) \right] \qquad [\mathbf{Eq4.43}]$$

The first term, $\frac{3}{2}(p_p + p_c) \varphi_p i_{pq}$ Shows the fact that the torque of the BDFM is directly related to i_{qp}. The other term, $\frac{3}{2} \frac{p_c R_r}{\omega_{rp} M_p^2} \left[2 L_p \varphi_p i_{pd} - \left(L_p^2 i_p^2 + \varphi_p^2 \right) \right]$ shows time-varying relation and can be analyzed like the control of power winding and control winding current. Consequently, T_{em} is almost linear with i_{pq}.

IV.3.4: Speed control:

The mechanical equation of the machine is:

$$T_{em} - T_L = J\frac{d\Omega}{dt} + f\Omega \qquad \textbf{[Eq4.44]}$$

In the control scheme of Fig.4.1, the speed regulator gives directly the i_{qp} reference.

So by replacing [**Eq4.42**] in the mechanical equation of the machine we shall find:

$$\frac{3}{2}(p_p + p_c)\,\varphi_p\, i_{pq} = (Js + f)\Omega \Rightarrow$$

$$\Omega = \frac{K_\Omega}{1+\tau_\Omega s}\, i_{pq} \qquad \textbf{[Eq4.42]}$$

Where:

$$K_\Omega = \frac{3(p_p+p_c)\,\varphi_p}{2f}, \tau_\Omega = \frac{J}{f} \qquad \textbf{[Eq4.43]}$$

From [**Eq4.42**] we can obtain directly the $\boldsymbol{i_{qp}}$ reference from the speed regulator, for the calculation of the speed regulator parameters the CW current closed loop time response must be taken into account.

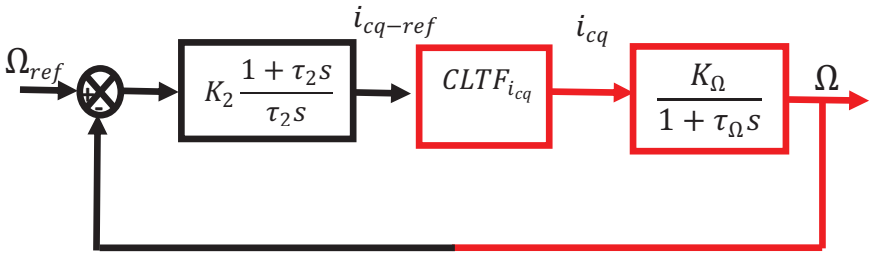

FigIV.4: Speed control loop

- *Regulator Calculation:*

OLTF:

$$T_\Omega = K_2\frac{1+\tau_2 s}{\tau_2 s}\,\frac{K_\Omega}{1+\tau_\Omega s} = \frac{K_2 K_\Omega}{\tau_2}\,\frac{1+\tau_2 s}{s}\,\frac{1}{1+\tau_\Omega s} \qquad \textbf{[Eq4.44]}$$

$$T_\Omega = K\frac{1+\tau_2 s}{s(1+\tau_\Omega s)}, K = \frac{K_2 K_\Omega}{\tau_\Omega} \qquad \textbf{[Eq4.45]}$$

CLTF:

$$F_\Omega = \frac{1+\tau_2 s}{\frac{\tau_\Omega}{K}S^2 + \frac{1+\tau_2 k}{K}S + 1} \equiv \frac{1+\tau_2 s}{\tau_n^2 S^2 + 2\xi\tau_n S + 1} \qquad \textbf{[Eq4.46]}$$

By identification,

$$\tau_n^2 = \frac{\tau_\Omega}{K}, 2\xi\tau_n = \frac{1+\tau_2 k}{K} \qquad \textbf{[Eq4.47]}$$

IV.3.5: PW power control:

The active and reactive powers of the PW exchanged with the machine depend only on the PW stator electric variable as follows:

$$Q_p = \Im_m\left\{\vec{V}_p.\vec{i}_p^*\right\} \quad \textbf{[Eq4.48]}$$

$$P_p = R_e\left\{\vec{V}_p.\vec{i}_p^*\right\} \quad \textbf{[Eq4.49]}$$

And also can be expressed as:

$$Q_p = \frac{3}{2}\omega_p\varphi_p i_{pd} - \frac{d\varphi_p}{dt} i_{pq} \quad \textbf{[Eq4.50]}$$

$$P_p = \frac{3}{2}\omega_p\varphi_p i_{pq} - \frac{d\varphi_p}{dt} i_{pd} + \frac{3}{2}R_p\left|\vec{i}_p\right|^2 \quad \textbf{[Eq4.51]}$$

The PW is connected to the 50 Hz grid constant voltage, so the PW flux is maintained almost constant $\boldsymbol{\frac{d\varphi_p}{dt} = 0}$. In this way $\boldsymbol{Q_p}$, can be directly controlled by an adequate choice of $\boldsymbol{i_{dp}}$.

Since the active power can be directly controlled using the $\boldsymbol{i_{pq}}$ reference value, the regulator will compensate the perturbation due to the joule losses. In order to get the regulator parameters, the PW current control time response must be taken into account.

- *Regulator Calculation:*

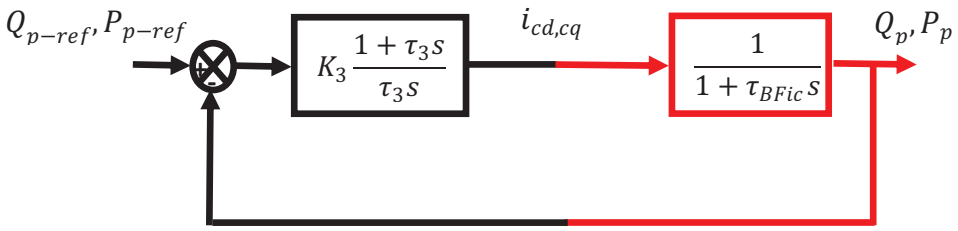

FigIV.5: Powers control loop

OLTF:

$$T_{Q_P} = K_3\frac{1+\tau_3 s}{\tau_3 s}\frac{1}{1+\tau_{BFicq}\,s}, \tau_3 = \tau_{BFic}, \tau_{BOQ_P} = \tau_{BFic} \Rightarrow \tau_{BOQ_P} = \tau_3 \quad \textbf{[Eq4.52]}$$

$$T_{Q_P} = \frac{K}{s}, K = \frac{K_3}{\tau_{BFic}} \quad \textbf{[Eq4.53]}$$

CLTF:

$$F_{Q_P} = \frac{1}{1+\tau_{BFQ_P}S}, \tau_{BFQ_P} = \frac{1}{K} \quad \textbf{[Eq4.54]}$$

$$\tau_{BFQ_p} = \frac{\tau_{BOQ_P}}{n_{Q_P}} \Rightarrow \frac{1}{K} = \frac{\tau_3}{n_{Q_P}} \Rightarrow K_3 = n_{Q_p}, K_{i3} = \frac{K_3}{\tau_3} \quad \textbf{[Eq4.55]}$$

In the previous section, the control scheme for the speed, active and reactive power control of the BDFM was developed, and the block diagrams for the controllers are established and carried out in Matlab/simulink. The results of this work are thoroughly explained in the next section.

IV.4: CONTROL SCHEME

Fig.IV.6 shows the proposed control scheme. This scheme is based on the cascade regulation method two independent regulation baths are implemented:

- Reactive power control:

$Q_{p\_ref} \Rightarrow I_{pd-ref} \Rightarrow I_{cd-ref} \Rightarrow V_{cd-ref}$

- Active power , electromagnetic torque or speed control:

$P_{p\_ref} \Rightarrow I_{pq-ret} \Rightarrow I_{cq-ref} \Rightarrow V_{cq-ref}$

Or

$T_{em\_ref} \Rightarrow I_{pq-ref} \Rightarrow I_{cq-ref} \Rightarrow V_{cq-ref}$

Or

$\Omega_{ref} \Rightarrow I_{pq-ref} \Rightarrow I_{cq-ref} \Rightarrow V_{cq-ref}$

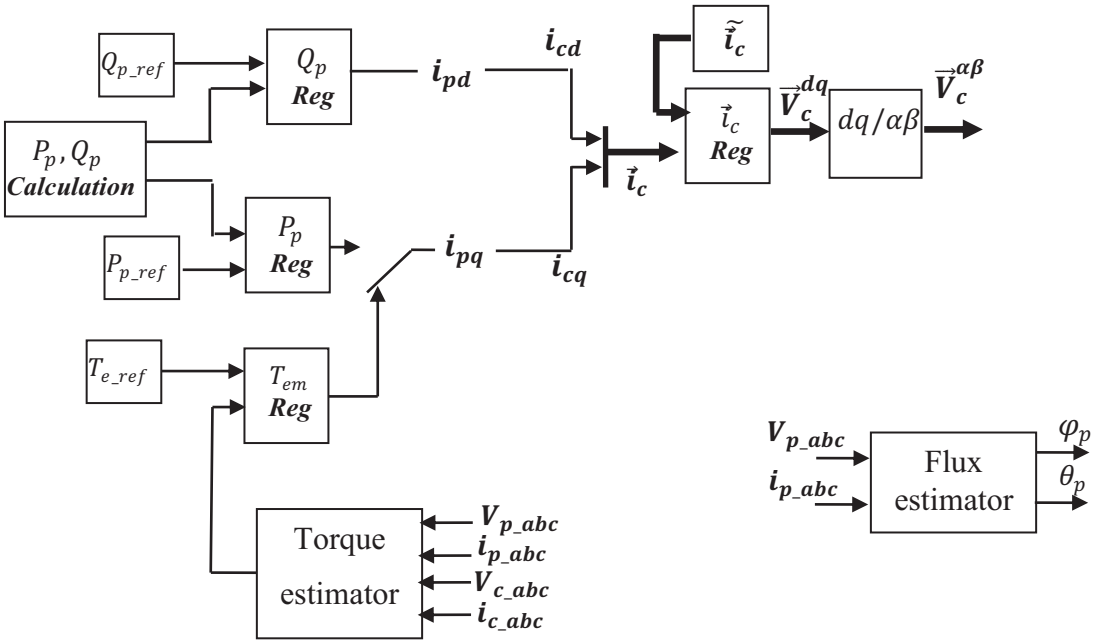

Fig.IV.6: General Vector Control bloc diagram

For the **dq** reference frame orientation it is necessary to know the PW flux position. So estimation is required. For doing so, a voltage model can be implemented, this method integrates directly the sinusoidal emf. Although this algorithm is simple, this flux estimator has been widely treated for the induction machine case.

The $\boldsymbol{T_{em}}$ estimation is needed for the torque, which is based on [**Eq2_103**]and [**Eq2_104**]expressed on the desired reference frame. In fact this CW flux estimation is required, this can be implemented via a current model or a voltage model.

The PW electric power is obtained through the measurements of the PW current and voltage values.

Finally, it should be noted that the rotor position is required for the transformations of the CW variables in the **dq** reference frame.

IV.4.1: PW flux estimator:

The PW flux position is obtained by means of a voltage-model-based estimator, which based on the voltage dynamic model of the machine.

The PW flux is obtained from the expression of [**Eq2_72**] that is referred to the generic $\boldsymbol{dq_p}$ reference frame. So if $\boldsymbol{dq_p}$ related to the PW reference ($\omega_{obsp} = 0$) its voltage becomes,

$$\vec{V}_p = R_p\,\vec{i}_p + \frac{d\,\vec{\varphi}_p}{dt} \qquad \textbf{[Eq4\_56]}$$

Therefore the PW $\boldsymbol{\alpha\beta_p}$ flux estimator becomes:

$$\widetilde{\vec{\varphi}_p} = \int \left(\vec{V}_p - R_p\,\vec{i}_p\right) dt \qquad \textbf{[Eq4\_57]}$$

In the same way, the CW flux is obtained from the expression of [**Eq2_83**]that is referred to the generic $\boldsymbol{dq_c}$ reference frame. So if $\boldsymbol{dq_c}$ related to the CW ($\omega_{obsc} = 0$) , its voltage becomes,

$$\vec{V}_c = R_c\,\vec{i}_c + \frac{d\,\vec{\varphi}_c}{dt} \qquad \textbf{[Eq4\_58]}$$

The CW $\boldsymbol{\alpha\beta_c}$ flux estimator becomes:

$$\widetilde{\vec{\varphi}_c} = \int \left(\vec{V}_c - R_c\,\vec{i}_c\right) dt \qquad \textbf{[Eq4\_59]}$$

IV.4.2: Torque Estimator:

The resulting flux estimations are used to obtain the torque estimation as follows:

From [**Eq2_103**] , we get

$$\widetilde{T}_{em_p} = \frac{3}{2} p_p \left\{\widetilde{\vec{\varphi}_p} \otimes \widehat{\vec{i}_p}\right\} \qquad \textbf{[Eq4\_60]}$$

[**Eq2_104**] yields

$$\widetilde{T}_{em_c} = \frac{3}{2} p_c \left\{\widehat{\vec{i}_c} \otimes \widetilde{\vec{\varphi}_c}\right\} \qquad \textbf{[Eq4\_61]}$$

The total torque estimation is:

$$\widetilde{T}_{em} = \widetilde{T}_{emp} + \widetilde{T}_{em_c} = \frac{3}{2} p_p \left\{\widetilde{\vec{\varphi}_p} \otimes \widehat{\vec{i}_p}\right\} + \frac{3}{2} p_c \left\{\widehat{\vec{i}_c} \otimes \widetilde{\vec{\varphi}_c}\right\} \qquad \textbf{[Eq4\_62]}$$

IV.5: SIMULATION RESULTS:

In the following, simulation results of vector control are presented, The PW is supplied with a constant voltage of 220 volts RMS per phase. All graphs below show the vector components using a park transformation (appendix A) which preserves its maximum values.

IV.5.1: CW current control results:

CW current loop, which is the inner control loop, is related to the PW reference frame.

In Fig. IV.7 the rotor speed is maintained constant (600 rpm) and the CW currents are regulated, under a step change of the $\boldsymbol{i_{cq}}$ reference. The control outputs are then transformed to obtain the sinusoidal **CW** voltages references (Fig. IV.7.d).

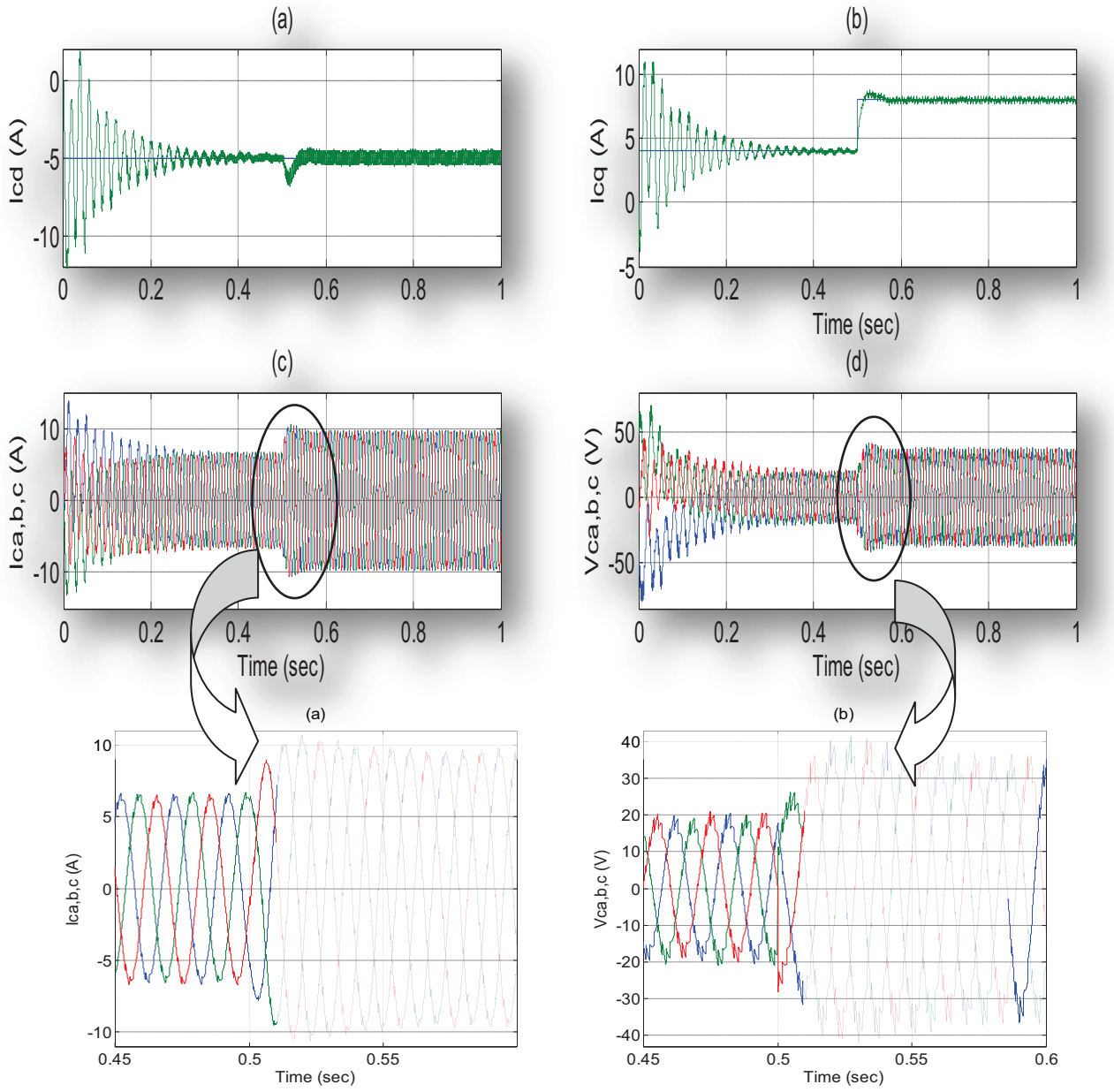

Fig IV.7: CW currents and voltage dynamic response

IV.5.2: Electromagnetic torque regulation results

Another operation mode is the torque control. In Fig IV.8 the rotor speed is fixed at 600 rpm while the PW reactive power is kept constant by the control. As it can be deduced from [**Eq4.42**] the torque is the result of the product $\boldsymbol{i_{pq}}$ and $\boldsymbol{\varphi_p}$, as the PW flux is constant, torque is linearly dependent of $\boldsymbol{i_{pq}}$ so $\boldsymbol{i_{pd}}$, is free to be used for any other purpose, as the control of the reactive power.

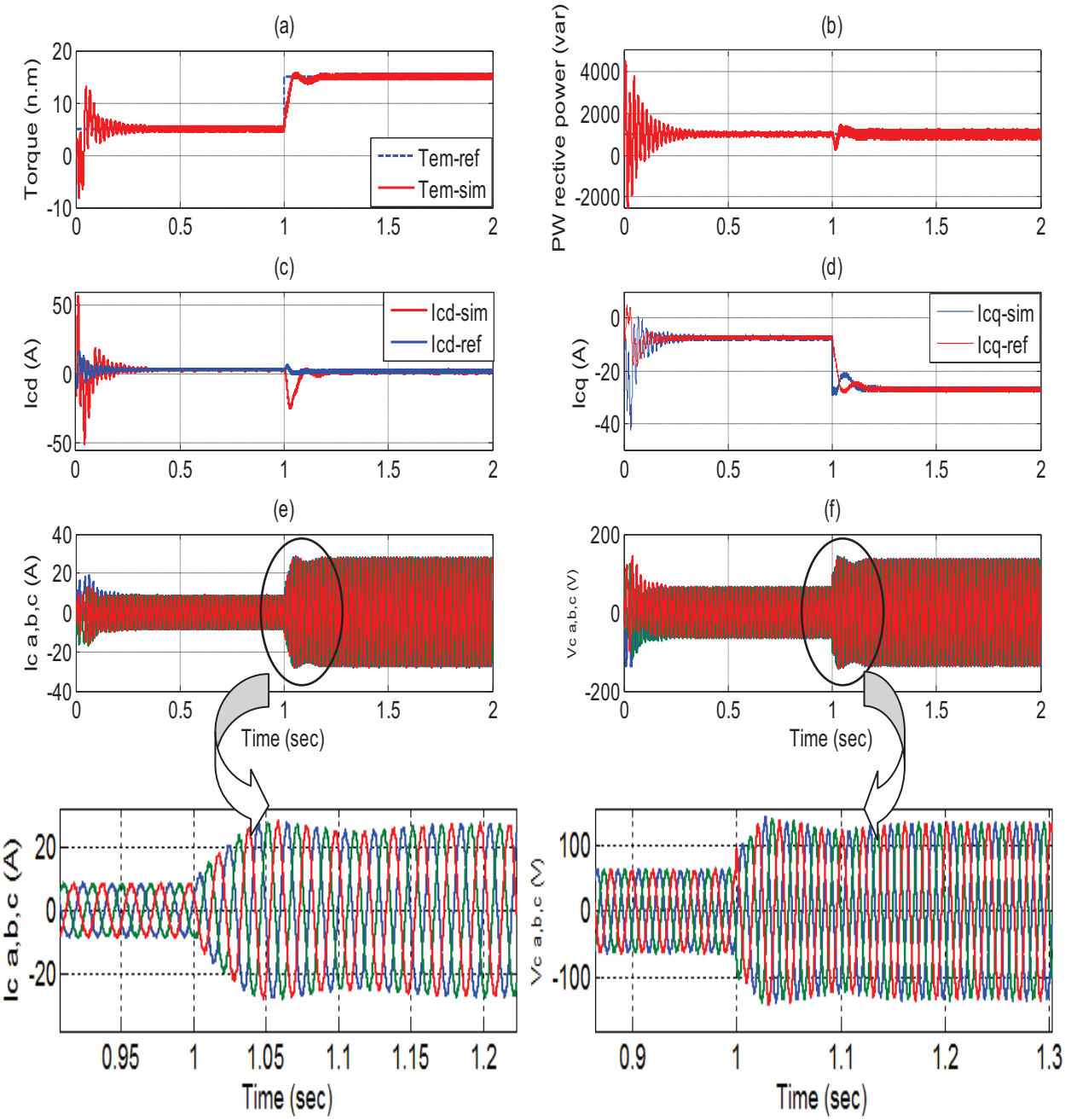

Fig IV.8 Torque control responses

IV.5.3 Dynamic of the speed control loop

Fig IV.9 shows control responses with speed reference steps (600 rpm to 680rpm). It can be remarked that speed response produces a dynamic impulse in the torque, maintaining its reactive power constant.

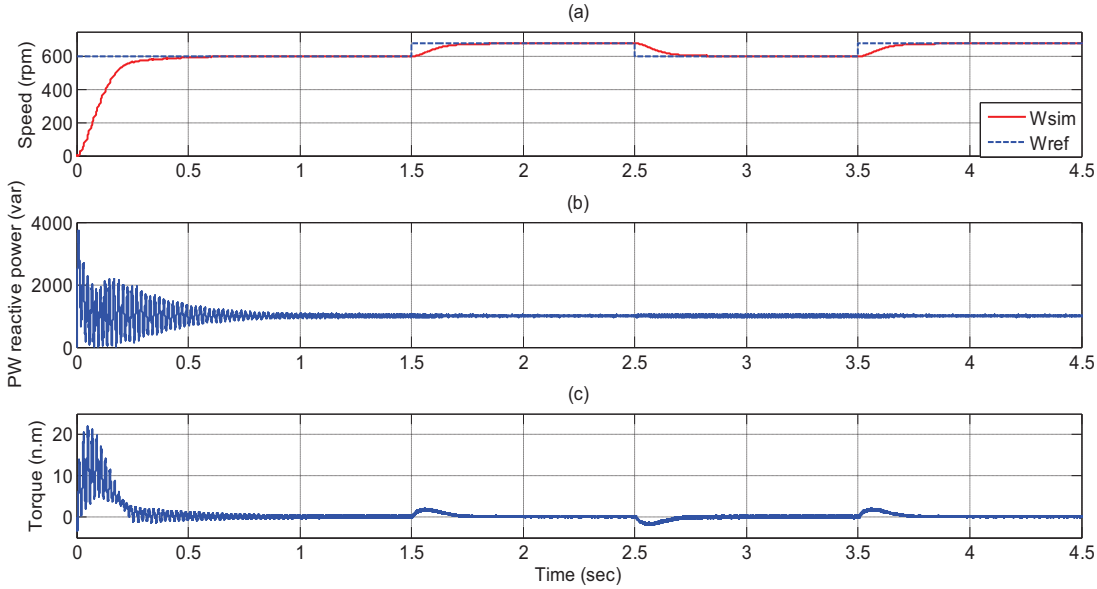

Fig IV.9 Control responses with steps of the rotor speed reference

IV.5.4 Load torque perturbation

The torque changes initially from 0 to 15 Nm to test the stability of the controller (Fig IV.10a). Both speed and reactive power come back to the reference values with an overshoot shown in Fig. IV.10 b, The speed regulator is able to compensate the load torque perturbation in a period of time close to 0.5 s, which displays the stability under the applied vector controller.

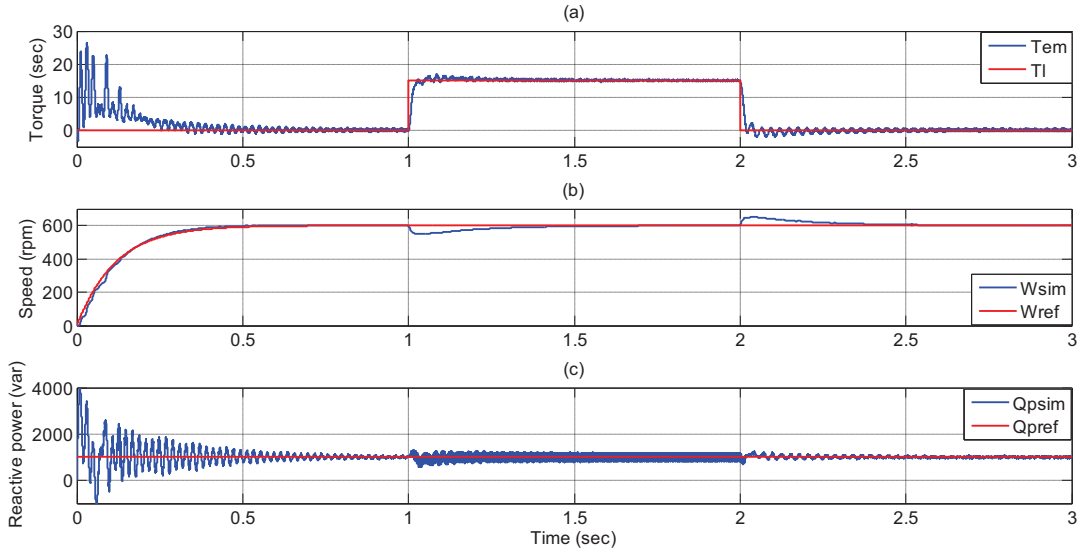

Fig IV.10 Control responses with a load perturbation

IV.5.6 Active and reactive power control

Among the important performances of the proposed scheme is the degree of the independence between the active and reactive power flows in the BDFIG.

Fig IV.11 shows the result of closed loop reactive power control dynamic response, the reactive power $Q_p$step while the active power is kept constant, the torque and i_{cd} current components are also kept constant.

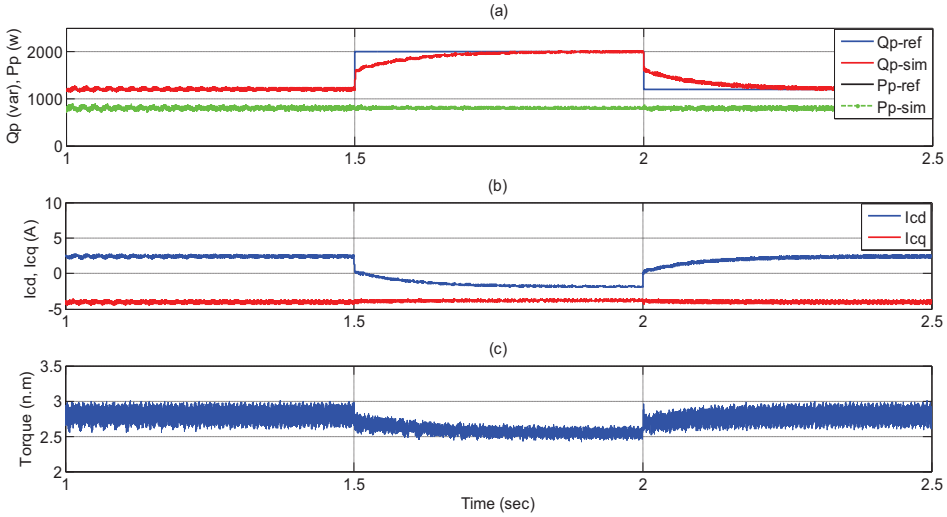

Fig IV.11 Reactive power control response

Fig IV.12 shows the result of closed loop active power control dynamic response while the reactive power imposed zero $\boldsymbol{Q_p = 0}$ that gives a unit power factor (only active power may be transferred, when the torque and the i_{cq} CW current components vary, the i_{cd} CW current components and reactive power are kept unchanged.

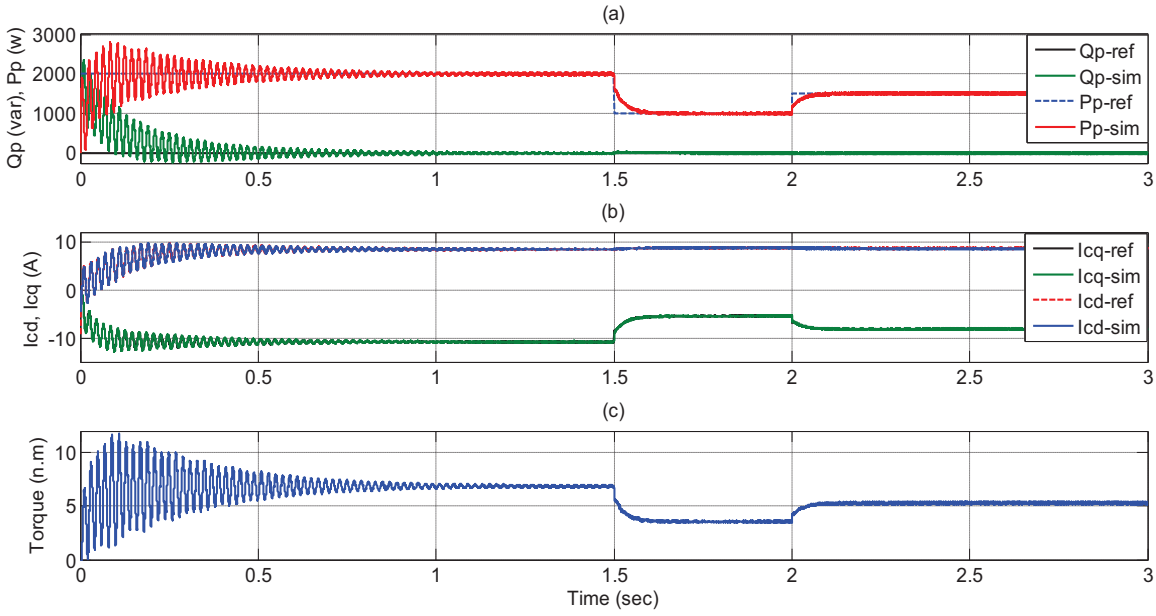

Fig IV.12 Active power control response

Fig IV.11 and Fig IV.12 indicate that this system can control the active and the reactive power independently and stably.

As discussed previously the rotor speed is directly proportional to the CW frequency, its absolute value increases when the rotor speed deviates from natural synchronous rotor speed Ω_n, as expressed by [**Eq2_13**].

In Fig IV.13 the machine starts at around 550 rpm and continues to operate as the speed picks up to 700 rpm then 750 rpm (natural synchronous rotor speed) and then increase up to 800 rpm and 1500 rpm in a 0.5-second interval.

Fig IV.13 (b) and (c) show the lowest current frequency corresponding to the nearly natural synchronous rotor speed and vice versa, according to [**Eq2_13**]. in order to accomplish the transition between the sub-synchronous and super-synchronous regions of operation, the CW current frequency would have to change its phase sequence as can be clearly seen from Fig IV.13 (d)

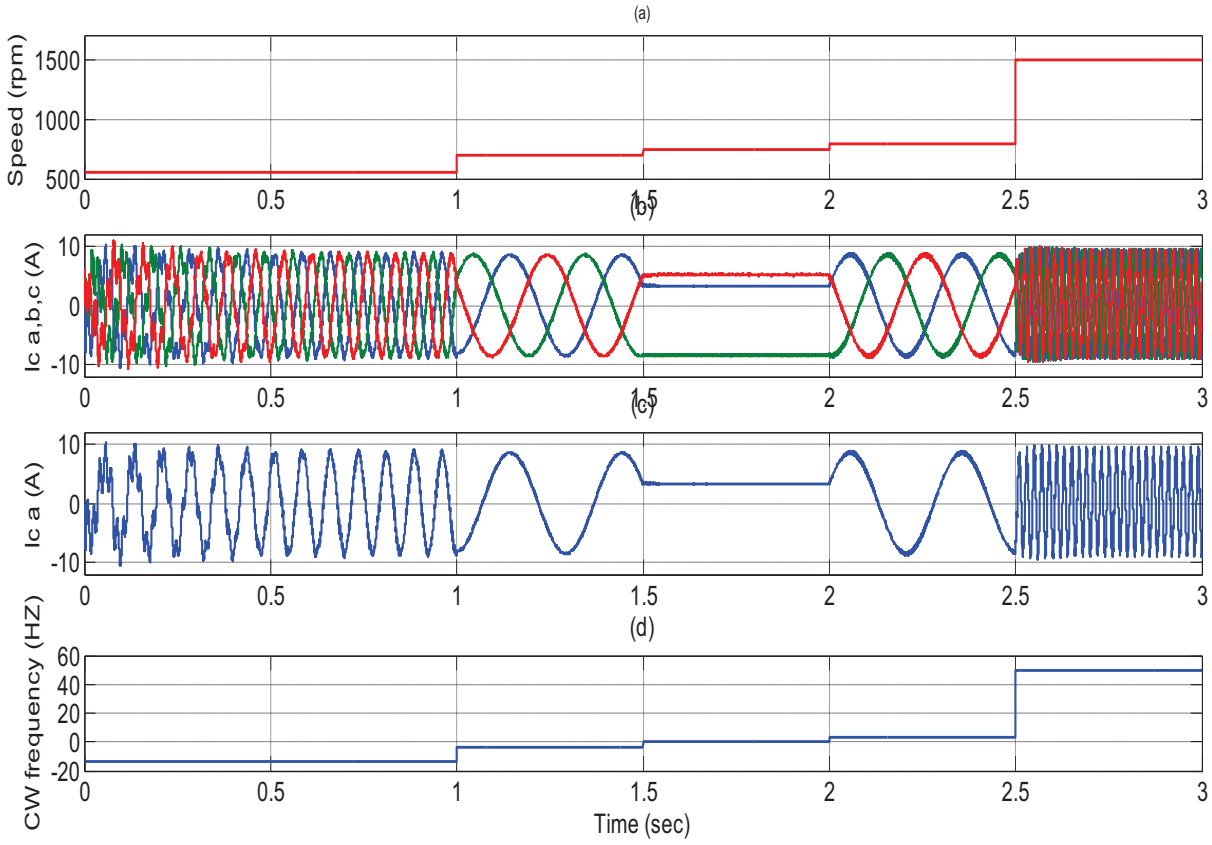

Fig IV.13 Speed, CW current and CW frequency time responces

Another test consists of applying a random wind turbine speed as shown in Fig IV.14 (a), the wind speed variations cause variations of the BDFM shaft speeds as shown in Fig IV.14 (b).

Fig IV.14 (c) shows the lowest current frequency corresponding to the nearly natural synchronous rotor speed (750 rpm) and vice versa, also as cited previously the transition between the sub-synchronous and super-synchronous regions of operation the CW current frequency would have to change its phase sequence as can be clearly seen from the Fig IV.14 (d).

Also, Fig IV.14 (e) and Fig IV.14 (f) performs the PW active and reactive powers are kept constant throughout the variation of the wind speed unless some disturbances can be shown in the PW active and reactive powers around its reference are clearly seen in the zooming Fig IV.14 (e) and Fig IV.14 (f).

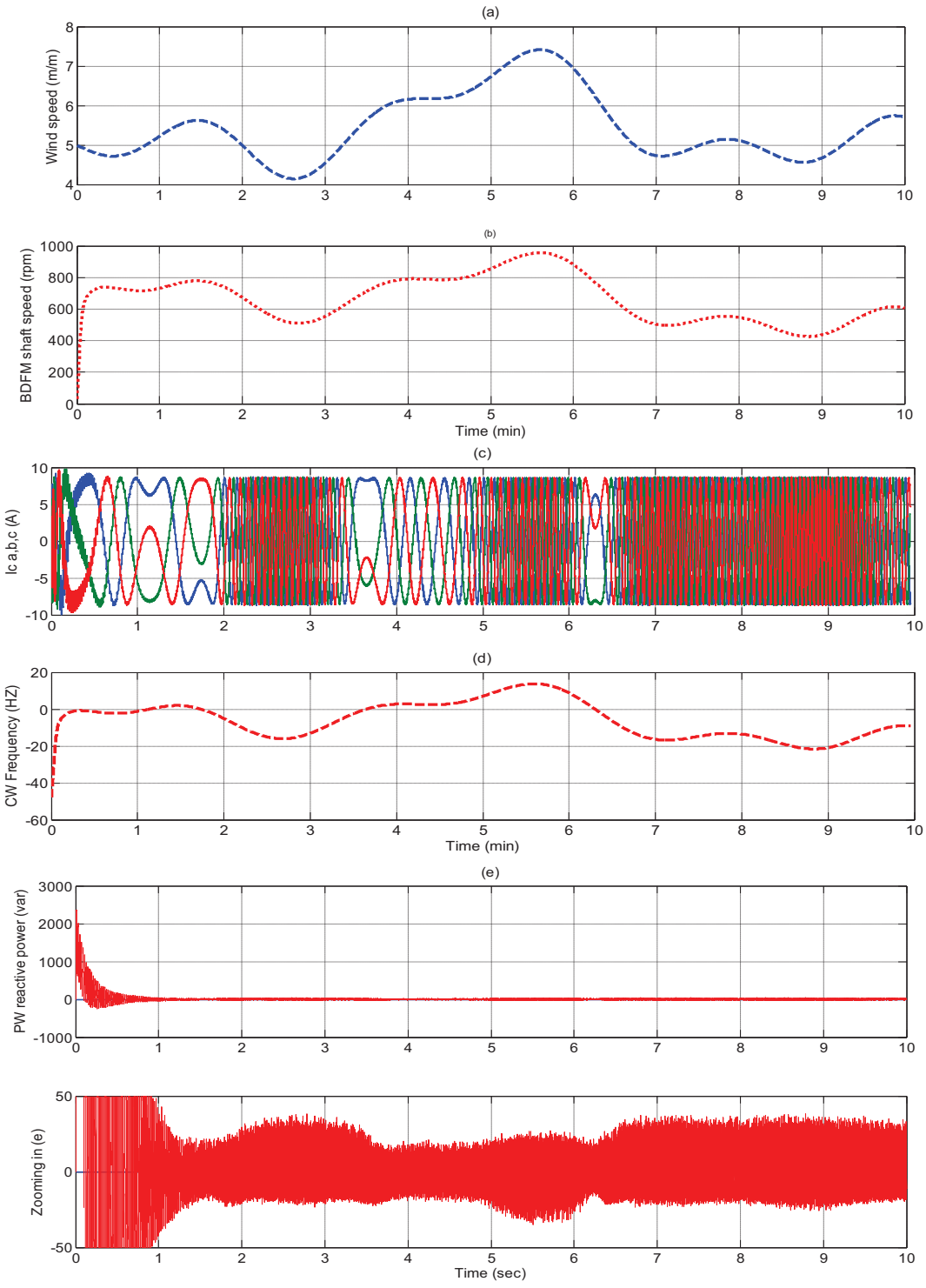

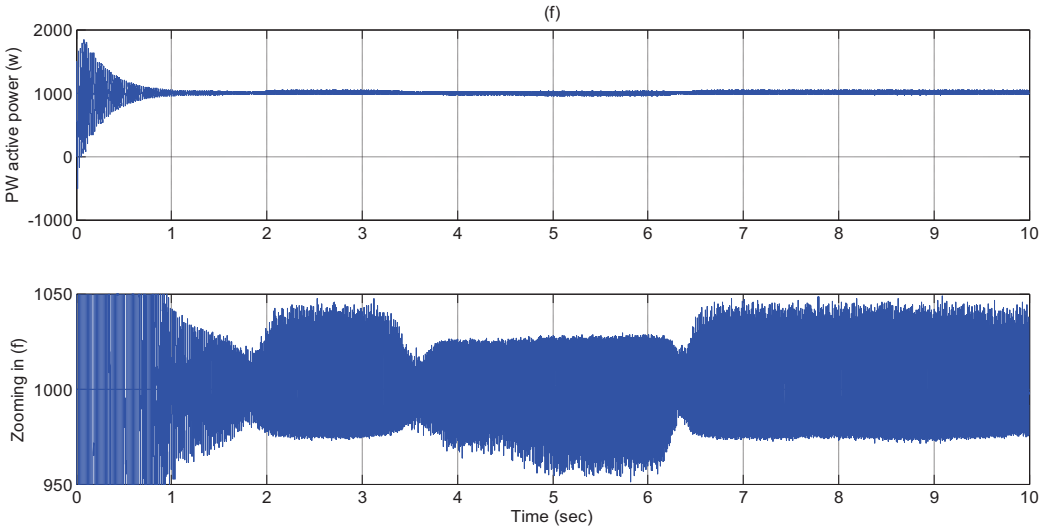

Fig IV.14 Speed, CW current, CW frequency PW active and reactive power time responces

IV.6) CONCLUSION:

This chapter proposes a simplified power winding flux oriented vector control scheme without the cross coupling compensator.

The PW stator flux orientation allows a very good non coupled response using at the same time simple linear regulators.

The vector control algorithm developed for the BDFM allows the regulation of the reactive power, the torque and the rotor speed with the same schema, detailed theoretical analysis is done to represent the decoupled control structure of the speed and reactive power control. The controller is able to regulate both the rotor speed and reactive power. The machine model and the controller have been implemented in MATLAB.

In summary, vector control has lead to a good dynamic performance and is stable throughout the operating range. Therefore, its potential application would be variable speed drives for high dynamic performance, as in the case of wind generation.

GENERAL CONCLUSION AND RECOMMANDATIONS

In this dissertation, a detailed mathematical derivation of the brushless doubly fed machine is has been developed.

This model is based on coupled magnetic circuit theory and complex space-vector notation. It is shown for the first time that, given the structural symmetry of the induction machine, the two stators and rotor circuits can be modeled by the simple set of only three vector coupled differential equations, More importantly, the number of equations does not depend on the number of rotor nests, the model derivation has lead to a simple derivation of unified dq reference frame model.

The unified dq reference frame model of the BDFM has the same structure as the well known vector models of standard induction machines. This is an important issue because it allows advantage to be taken of the set of control techniques and analysis tools that have previously been developed for other machines, especially for the cage induction machine and the wound rotor induction machine.

Based on dq reference frame model, this thesis applies PW flux oriented vector control technology to BDFM control, so the decoupling control of the active and reactive power of the generator is achieved.

With respect to the control algorithm proposed by [ZHO-97], The presented control scheme has the following advantages:

- ✓ The control system dynamic functions are simpler, so better dynamic responses could be obtained.
- ✓ The power winding current is regulated and a reactive power control is implemented.
- ✓ Non-linear functions are avoided (arcsine, arctangent).

Finally, vector control has yielded good dynamic performances and is stable throughout the operating range. Therefore, its potential application would be variable speed drives for high dynamic performance, as can be wind generation.

In this regard sums perspectives can be cited:

- ✓ Increase the robustness of the control face of load disturbances.
- ✓ Reduce the sensor requirements (the inclusion of a sensorless control strategy).
- ✓ Increase the insensitivity of the control against the uncertainty of the machine parameters.
- ✓ Study the direct torque control (DTC).
- ✓ Enhance the system robustness and simplify the control algorithm by applying the intelligent control approaches, such as fuzzy logic control.

APPENDICES

APPENDIX A

COORDINATE TRANSFORMATION

A.1) Clarke Transform:

A three-phase system can be represented in a two-phase system equivalent. Assuming that the axis of the three phase stationary system (a, b, c) and the (α, β)phase stationary system are in phase, the vector diagram would be:

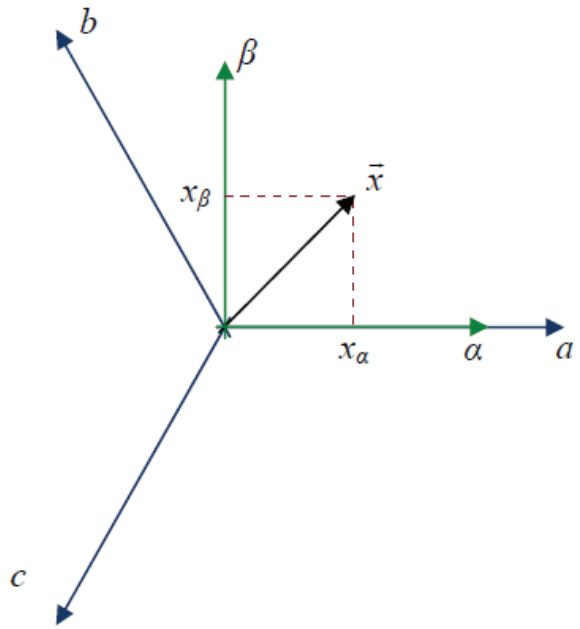

Figure A-1. Vector diagram of the Clarke transformation

The matrix form is:

$$\begin{bmatrix} x_\alpha \\ x_\beta \end{bmatrix} = \frac{2}{3}\begin{bmatrix} 1 & -\frac{1}{2} & -\frac{1}{2} \\ 0 & \frac{\sqrt{3}}{2} & -\frac{\sqrt{3}}{2} \end{bmatrix}\begin{bmatrix} x_a \\ x_b \\ x_c \end{bmatrix}$$

The inverse transformation is:

$$\begin{bmatrix} x_a \\ x_b \\ x_c \end{bmatrix} = \begin{bmatrix} 1 & 0 \\ -\frac{1}{2} & \frac{\sqrt{3}}{2} \\ -\frac{1}{2} & -\frac{\sqrt{3}}{2} \end{bmatrix} \begin{bmatrix} x_\alpha \\ x_\beta \end{bmatrix}$$

A.2) Park Transform:

The stationary two-phase system can be represented in a rotating two-phase system equivalent Figure A-2:

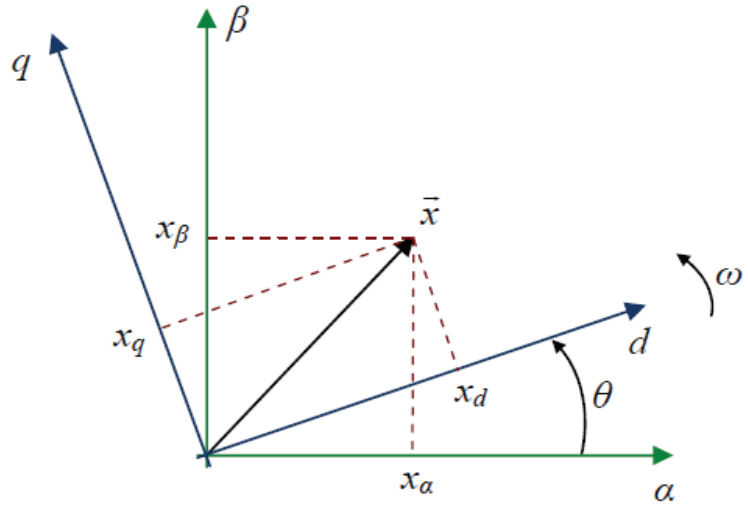

Figure A-2. Vector diagram of the Park transformation

The transformation in vector form is:

$$\vec{x}^{dq} = e^{-j\theta}\vec{x}^{\alpha\beta_p}$$

The inverse transformation is:

$$\vec{x}^{\alpha\beta_p} = e^{j\theta}\vec{x}^{dq}$$

APPENDIX B

TRANSFORMATION BETWEEN DIFFERENT REFERENCE FRAMES

The resulting model (***Eq2_70***) referred in three initial reference frames and two possible pole pair distribution (shown in Fig.b-1):

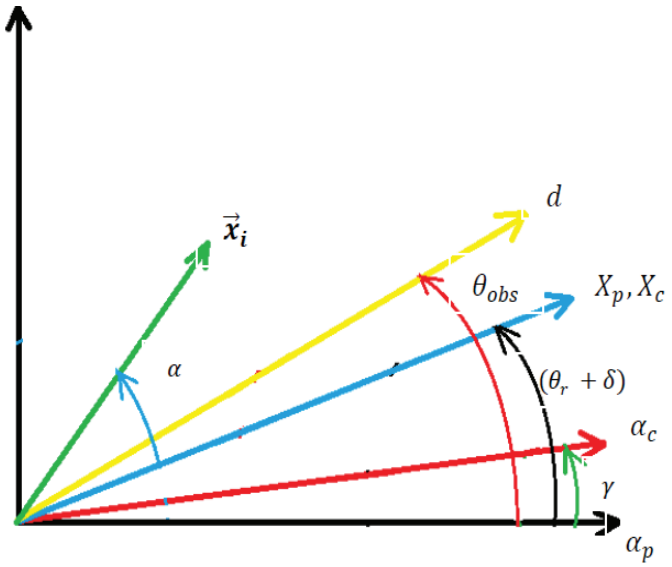

Fig.B-1: Unified reference frames (mechanical angle)

B.1) ***Coupling Relation*** $\vec{x}^{\alpha\beta_p} = \boldsymbol{f}\left(\vec{x}^{\alpha\beta_c}\right)$:

It is assumed that the rotor of the BDFM fulfils the second condition [$\boldsymbol{Eq2\_62}$]and maximizes the number of nests i.e. $\boldsymbol{p_p + p_c = n}$, which implies that:

$$\vec{x}^{xy_p} = \vec{x}^{xy_c{}^*} \quad (\mathbf{B\_1})$$

From (*Fig. B-1)* it can be deduced that:

$$\vec{x}^{\mathrm{xy}_p} = xe^{jP_p\alpha} \quad (\mathbf{B\_2})$$

$$\vec{x}^{\mathrm{xy}_c} = xe^{jP_c\alpha} \quad (\mathbf{B\_3})$$

$$\vec{x}^{\alpha\beta_p} = e^{jP_p(\theta_r+\delta)}\vec{x}^{\mathrm{xy}_p} \quad (\mathbf{B\_4})$$

$$\vec{x}^{\alpha\beta_c} = e^{jP_c(\theta_r+\delta-\gamma)}\vec{x}^{\mathrm{xy}_c} \quad (\mathbf{B\_5})$$

Combining(**B_1**),(**B_4**), (**B_5**) we get:

$$\vec{x}^{\alpha\beta_p} = \vec{x}^{\alpha\beta_c{}^*}e^{j\theta_a} \quad (\mathbf{B\_6})$$

With: $\theta_a = (p_p + p_c)(\theta_r + \delta) - p_c\gamma$ (**B_7**)

B.2) vector transformations from original reference frames to generic $\boldsymbol{dq_p}$ reference frame:

We can define a generic dq_p reference frame with a $P_p$pole-pair distribution and located at any mechanical position ($\boldsymbol{\theta_{obsp}}$ /$\boldsymbol{p_p}$) from $\boldsymbol{\alpha\beta_p}$, the vector transformation is defined as:

$$\vec{x}^{\alpha\beta_p} = e^{j\theta_{obsp}}\vec{x}^{dq_p} \quad (\mathbf{B\_8})$$

(B_6) & (B_8) $\Rightarrow \vec{\boldsymbol{x}}^{\boldsymbol{\alpha\beta_c}} = \vec{\boldsymbol{x}}^{\boldsymbol{dq_p}{}^*}\boldsymbol{e^{j(\theta_a - \theta_{obsp})}}$ (**B_9**)

(B_4) $\Rightarrow \vec{x}^{\mathrm{xy}_p} = e^{-jP_p(\theta_r+\delta)}\vec{x}^{\alpha\beta_p}$ (**B_10**)

(B_8) in (B_10) $\Rightarrow \vec{\boldsymbol{x}}^{\boldsymbol{xy_p}} = \boldsymbol{e^{j[\theta_{obsp} - P_p(\theta_r+\delta)]}}\vec{\boldsymbol{x}}^{\boldsymbol{dq_p}}$ (**B_11**)

(B_5) $\Rightarrow \vec{x}^{\mathrm{xy}_c} = e^{-jP_c(\theta_r+\delta-\gamma)}\vec{x}^{\alpha\beta_c}$ (**B_12**)

(B_9) In (B_12) $\Rightarrow$ $\boldsymbol{x^{xy_c}} = \boldsymbol{e^{-j[\theta_{obsp} - P_p(\theta_r+\delta)]}}\vec{\boldsymbol{x}}^{*\boldsymbol{dq_p}}$ (**B_13**)

In this way any machine variable can be defined in a generic $\boldsymbol{dq_p}$ reference frame.

B.3) Transformation from dq_p to dq_c

The vector transformation from the original reference system $\boldsymbol{dq_p}$, referred in PW that rotate at the speed of $\boldsymbol{\omega_{obsp}}$, to the original reference system $\boldsymbol{dq_c}$ referred in CW rotating at the speed of $\boldsymbol{\omega_{obsc}}$ is the following:

We know that:

$$\vec{x}^{\alpha\beta_c} = e^{j\theta_{obsc}} \vec{x}^{dq_c} \quad \textbf{(B_14)}$$

From (A_9), (A_14) we get

$$\vec{x}^{dq_c} = \vec{x}^{dq_p}{}^{*} e^{j(\theta_a - \theta_{obsc} - \theta_{obsp})} \quad \textbf{(B_15)}$$

So we can write:

$$\vec{\boldsymbol{x}}^{\boldsymbol{dq_p}} = \vec{\boldsymbol{x}}^{\boldsymbol{dq_p}}{}^{*} \boldsymbol{e}^{-\boldsymbol{j}(\boldsymbol{\theta_{xp}} + \boldsymbol{\theta_{xc}})} \quad \textbf{(B_16)}$$

While:

$$\theta_{xp} = \theta_{obsp} - P_p(\theta_r + \delta) \quad \textbf{(B_17)}$$

$$\theta_{xc} = \theta_{obsc} - P_c(\theta_r + \delta - \gamma) \quad \textbf{(B_18)}$$

APPENDIX C

BDFM ELECTRICAL PARAMETER FOR SIMULATION

	PW	CW	R
Rated voltage	$V_p = 220V$	$V_c = 220V$	
Pole pairs number	$p_p = 1$	$p_c = 3$	
Resistence(Ω)	$R_p = 1.732$	$R_c = 1.079$	$R_r = 0.473$
Self inductance(mH)	$L_p = 714.8$	$L_p = 121.7$	$L_r = 132.6$
Mutuel inductance(mH)	$M_p = 242.1$	$M_c = 59.8$	

Tab.C.1 BDFM Electrical Parameters

APPENDIX D

DIFFERENT ROTORS CONFIGURATION

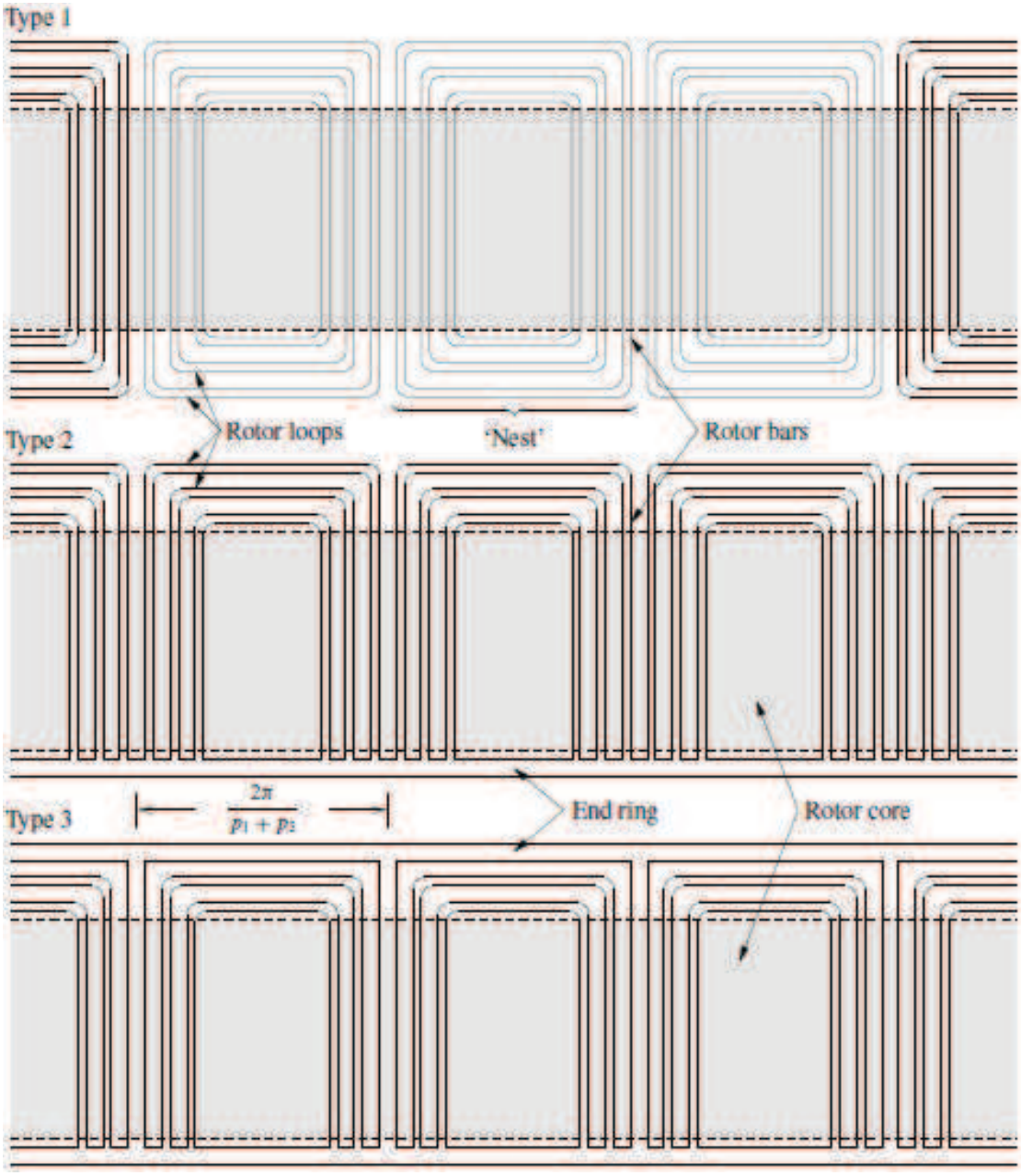

Fig.D.1 Three variant nested loop rotor designs, the difference between the designs are essentially one of ease of fabrication [ROB-05].

REFERENCES

[ZHO-97] D. Zhou, R. Spee, y G. C. Alexander, "Experimental evaluation of a rotor flux oriented control algorithm for brushless doubly-fed machines," IEEE Transactions on Power Electronics, Vol. 12, no. 1, pp. 72-78, 1997.

[ZHO-94] D. Zhou y R. Spee, "Synchronous frame model and decoupled control development for doubly-fed machines," en PESC 1994 Record. 25th Annual IEEE Power Electronics Specialists Conference, Vol. 2, pp. 1229-1236, Taipei, Taiwan, 1994.

[SPE-96] D. Zhou, R. Spee, G. C. Alexander, y A. K. Wallace, "A simplified method for dynamic control of brushless doubly-fed machines," en IECON 1996. 22nd International Conference on Industrial Electronics, Control, and Instrumentation, Vol.2,pp. 946-951,Taipei, Taiwan, 1996.

[SIM-97] M. G. Simoes, B. K. Bose, y R. J. Spiegel, "Design and performance evaluation of a fuzzy-logic-based variable-speed wind generation system," IEEE Transactions on Industry Applications, vol. 33, no. 4, pp.956-965, 1997.

[SHO-02] H. Shoudao, W. Yan, L. Youjie, y W. Yaonan, "Fuzzy-Based Power Factor Control for Brushless Doubly-Fed Machines," en Proceedings of the 4th World Congress on Intelligent Control and Automation, vol. 1, Junio 2002.

[SHI-08] S. Shao, A. Ehsan and M. Richard " Vector Control of the Brushless Doubly-Fed Machine for Wind Power Generation" ICSET 2008pp. 322-327.

[SAR-06] I. Sarasola, J. Poza, E. Oyarbide, y M.A. Rodriguez, "Stability Analysis of a Brushless Doubly-Fed Machine under Closed Loop Scalar Current Control," en IECON 2006. 32nd Annual Conference of the IEEE Industrial Electronics Society, pp. 1527-1532, Paris, Francia, Nov. 2006.

[ROB-04] P. C. Roberts, R. A. McMahon, P. J. Tavner, J. M. Maciejowski, T. J. Flack, y X. Wang, "Performance of rotors in a brushless doubly-fed induction machine (BDFM)," en ICEM 2004. Proceedings 16th International Conference on Electrical Machines. Conference, Cracow, Polonia, 2004.

[ROB-05a] P.C. Roberts, "A Study of Brushless Doubly-Fed (Induction) Machines." PhD thesis, University of Cambridge, 2005.

[ROB-05b] P.C. Roberts, T. J. Flack, J. M. Maciejowski, y R. A. McMahon, P J Tavner "An equivalent circuit for the Brushless Doubly Fed Machine (BDFM) including parameter estimation and experimental verification" Electrical Power Applications,IEE Proceedings, 152(4):933-942, July 2005.

[ROB-02] P. C. Roberts, T. J. Flack, J. M. Maciejowski, y R. A. McMahon, "Two stabilising Control Strategies for the brushless doubly-fed machine (BDFM)" en PEMD 2002. International conference on Power Electronics, Machines and Drives, pp. 341-346, Bath, UK, 2002.

[ROB-06] W. Qi, C. Xiaohu, J. Yanchao, "Fuzzy-based Active and Reactive Control for Brushless Doubly-fed Wind Power Generation System" APCCAS 2006, pp848-851.

[POZ-02] J. Poza, E. Oyarbide, y D. Roye, "New vector control algorithm for brushless doubly-fed machines," en IECON 2002. 28th Annual Conference of the IEEE Industrial Electronics Society, vol.2, pp. 1138-1143, Sevilla, España, 2002.

[POZ-03] J. Poza, "Modélisation, Conception et Commande d'une Machine Asynchrone sans Balais Doublement Alimentée pour la Génération à Vitesse Variable." PhD Dissertation of Mondragón Unibertsitatea e Institut National Polytechnique de Grenoble, 2003.

[Poz-06] J. Poza, E. Oyarbide, D. Roye, M. Rodriguez "Unified reference frame dq model of the brushless doubly-fed machine", IEE Proc Electr Power. Appl. 2006 153 (5),pp.726734

[McM-06] R. A. McMahon, P. C. Roberts, X. Wang, y P. J. Tavner, "Performance of BDFM as generator and motor," IEE Proceedings-Electric Power Applications, vol. 153, no. 2, pp. 289-299, Mar. 2006.

[LI-91b] R. Li, A. K. Wallace, R. Spee, and Y. Wang, "Two-axis model development of cage rotor Brushless Doubly-Fed Machines," IEEE Transactions on Energy Conversion, vol. 6, no. 3 pp. 453-460, 1991.

[FEN-91] L. Feng, X. Longya, y T. A. Lipo, "d-q analysis of a variable speed doubly AC excited reluctance motor," Electric Machines and Power Systems, vol. 19, no. 2, pp. 125-138, Mar. 1991.

[BRA-96] W. R. Brassfield, R. Spee, y T. G. Habetler, "Direct torque control for brushless Doubly fed machines," IEEE Transactions on IndustryApplications, vol. 32, no. 5, pp.1098-1104, 1996.

[BOG-94] M. S. Boger, A. K. Wallace, R. Spee, "Investigation of Appropriate Pole Number Combinations for Brushless Doubly-Fed Machines Applied to Pump Drives"

Department of Electrical and Computer Engineering Oregon State University Corvallis, Oregon 97331 U.S.A IEEE Transactions pp 157-162.

[BOG-95] M. S. Boger, A. K. Wallace, R. Spee, and L. Ruqi, "General pole number model of the Brushless Doubly-Fed Machine," IEEE Transactions on Industry applications, vol. 31 no.5, pp. 1022-1028, Sept. 1995.

[WIL-97.a] S. Williamson, A.C. Ferreira, A.K. Wallace, "Generalised theory of the brushless doubly-fed machine. Part 1: Analysis", IEE Proc.-Electr. Power Appl., Vol.144, No.2,March 1997, pp. 111-122.

[WIL-97b] S. Williamson and A. C. Ferreira, "Generalized Theory of the Brushless Doubly-Fed Machine. Part 2: Model Verification and Performance," IEE Proceedings Electric Power Applications, vol. 144, no. 2,Mar.1997.

[WIE-95] E. Wiedenbrug, M.S. Boger, A.K. Wallace, D. Patterson, "Electromagnetic mechanism of synchronous operation of the brushless doubly-fed machine", IEEE IAS conference, Vol. 1,1995, pp. 774-780.

[MUN-99] A. R. Munoz and T. A. Lipo, "Complex vector model of the squirrel-cage induction machine including instantaneous rotor bar currents," IEEE Transactions on Industry Applications, vol. 35, no. 6, pp. 1332-1340, Nov. 1999.

[MUN -00] A.R. Munoz, T.A. Lipo, "Dual stator winding induction machine drive", IEEE Trans. on Ind. Applications. Vol. 36, No. 5, Sept./Oct. 2000, pp. 1369-1379.

[FAR -08] B. Farhad, O. Hashem, A.Ehsan and M Richard “Derivation of a Vector Model for a Brushless Doubly-Fed Machine with Multiple Loops per Nest” IEEE Transactions pp 606-611.

[AKE-00] L.AKE “The Power Quality Of Wind Turbines” thesis for the degree of doctor of Philosophy Department of Electric Power Engineering CHALMERS UNIVERSITY OF TECHNOLOGY Goteborg, Sweden 2000